AD_____

Award Number: W81XWH-05-1-0233

TITLE: A Proteomic Approach to Identify Phosphorylation-Dependent Targets of BRCT Domains

PRINCIPAL INVESTIGATOR: Zhou Songyang, Ph.D.

CONTRACTING ORGANIZATION: Baylor College of Medicine
Houston, Texas 77030

REPORT DATE: March 2009

TYPE OF REPORT: Final

PREPARED FOR: U.S. Army Medical Research and Materiel Command
Fort Detrick, Maryland 21702-5012

DISTRIBUTION STATEMENT: Approved for Public Release;
Distribution Unlimited

The views, opinions and/or findings contained in this report are those of the author(s) and should not be construed as an official Department of the Army position, policy or decision unless so designated by other documentation.

REPORT DOCUMENTATION PAGE

Form Approved
OMB No. 0704-0188

Public reporting burden for this collection of information is estimated to average 1 hour per response, including the time for reviewing instructions, searching existing data sources, gathering and maintaining the data needed, and completing and reviewing this collection of information. Send comments regarding this burden estimate or any other aspect of this collection of information, including suggestions for reducing this burden to Department of Defense, Washington Headquarters Services, Directorate for Information Operations and Reports (0704-0188), 1215 Jefferson Davis Highway, Suite 1204, Arlington, VA 22202-4302. Respondents should be aware that notwithstanding any other provision of law, no person shall be subject to any penalty for failing to comply with a collection of information if it does not display a currently valid OMB control number. **PLEASE DO NOT RETURN YOUR FORM TO THE ABOVE ADDRESS.**

1. REPORT DATE *(DD-MM-YYYY)*	**2. REPORT TYPE**	**3. DATES COVERED** *(From - To)*
01-03-2009	Final	1 MAR 2005 - 28 FEB 2009

4. TITLE AND SUBTITLE

A Proteomic Approach to Identify Phosphorylation-Dependent Targets of BRCT Domains

5a. CONTRACT NUMBER

5b. GRANT NUMBER
W81XWH-05-1-0233

5c. PROGRAM ELEMENT NUMBER

6. AUTHOR(S)
Zhou Songyang, Ph.D.

E-Mail: songyang@bcm.tmc.edu

5d. PROJECT NUMBER

5e. TASK NUMBER

5f. WORK UNIT NUMBER

7. PERFORMING ORGANIZATION NAME(S) AND ADDRESS(ES)

Baylor College of Medicine
Houston, Texas 77030

8. PERFORMING ORGANIZATION REPORT NUMBER

9. SPONSORING / MONITORING AGENCY NAME(S) AND ADDRESS(ES)
U.S. Army Medical Research and Materiel Command
Fort Detrick, Maryland 21702-5012

10. SPONSOR/MONITOR'S ACRONYM(S)

11. SPONSOR/MONITOR'S REPORT NUMBER(S)

12. DISTRIBUTION / AVAILABILITY STATEMENT
Approved for Public Release; Distribution Unlimited

13. SUPPLEMENTARY NOTES

14. ABSTRACT The importance of protein phosphorylation to breast cancer has been reaffirmed by recent findings that the BRCA1 C-terminal (BRCT) domains are novel phosphopeptide binding modules. Cancer-associated missense and deletion mutations have been found in the BRCT repeat regions of BRCA1, suggesting an essential role of BRCT domains in regulating BRCA1 activity. In addition, BRCT domains are found in many proteins that regulate DNA damage repair, cell cycle, and genome stability, implying a more global role of BRCT domains in genome stability surveillance. These results suggest that the BRCT domain acts as a sensor to protein phosphorylation in response to DNA damage, recruits phosphorylated cellular targets, and mediates signaling complex formation. However, the identities of the in vivo BRCT domain targets are largely unknown. We propose to use several approaches utilizing peptide libraries and peptide arrays to systematically identify phosphoproteins that can interact with BRCT domains. In addition to potential new regulators of genome stability, the approaches can identify phosphorylated sequences on proteins that are important for DNA damage responses and cell cycle. These phosphorylated sites can then used to generate phospho-specific antibodies for breast cancer research as well as diagnostic purposes.

15. SUBJECT TERMS
BRCT domain, peptide library, OPAL, peptide array, proteomics, genome wide, signal transduction pathways, androgen receptor

16. SECURITY CLASSIFICATION OF:			**17. LIMITATION OF ABSTRACT**	**18. NUMBER OF PAGES**	**19a. NAME OF RESPONSIBLE PERSON**
a. REPORT	**b. ABSTRACT**	**c. THIS PAGE**			USAMRMC
U	U	U	UU	43	**19b. TELEPHONE NUMBER** *(include area code)*

Table of Contents

Introduction……5

Body……5

Key Research Accomplishments……12

Reportable Outcomes……13

List of Personnel ……13

Conclusions……14

References……14

Appendices……16

Introduction

Understanding the molecular and cellular mechanisms that trigger breast cancer is essential to the prevention and treatment of this disease. The BRCA1 C-terminal (BRCT) domain was first identified in BRCA1 (2, 4). Cancer associated missense and deletion mutations have been found in the BRCT repeat regions of BRCA1, suggesting an important role of BRCT domains in regulating BRCA1 activity (10, 14). In addition, the BRCT domain is found in many proteins that regulate DNA damage repair, cell cycle, and genome stability, implying a more global role of BRCT domains in genome stability surveillance (2, 4). Consistent with this notion, the BRCT domain has been shown to mediate protein-protein interactions. For example, BRCT domains of BRCA1 associate with helicase BACH1 and CtBP interacting protein CTIP (5, 24). Recently, our lab and others have discovered that BRCT domains are novel phosphopeptide binding modules (13, 16, 23). BRCA1 BRCT domains associate with residue Ser990 on BACH1 in a phosphorylation-dependent manner. Furthermore, we found that several other BRCT domains including those from MDC1 and tumor suppressor BARD1 can bind specific phosphorylated peptides (8, 12, 17). These findings suggest that the BRCT domain recruits phosphorylated cellular targets and mediates signaling complex formation. However, the identities of the *in vivo* BRCT domain targets are largely unknown. In this application, we propose to systematically identify phosphoproteins that can interact with BRCT domains. Through these efforts, we may uncover potential new regulators of genome stability; more importantly, the approach can identify phosphorylated sequences on proteins that are important for DNA damage responses and cell cycle. Such information will help us to understand the mechanism of how protein phosphorylation modulates DNA damage responses and cell cycle in breast epithelial cells. In addition, it should prove invaluable for the development of new screening strategies and treatment for breast cancer.

Body

***Task 1*. Identification of phosphorylated peptide sequences that specifically bind BRCT domains of BRCA1 and BARD1.** We proposed to establish Oriented Peptide Library Arrays (OPAL) for phosphobinding specificities of BRCT domains. And we will carry out genome-wide (human) screens for BRCT domain binding targets using high-density peptide microchips, and confirm that the BRCT binding sites are specific for BRCA1 or BARD1 BRCT domains.

***Task 2*. Biochemical studies of the candidate breast cancer genes and BRCT binding sites identified in Aim1.** We proposed to carry biochemical and cellular experiments to demonstrate the significance of the identified targets.

(1) OPAL strategy for target identification

OPAL was originally synthesized on cellulose paper and worked well with SH2 domains and kinases. We therefore used cellulose paper based OPAL arrays to analyze BRCT domain fusion proteins. However, these arrays tended to generate high background and nonspecific binding when tested against BRCT domains. We reasoned that the non-specific binding most likely arose from interactions between the cellulose surface and BRCT fusion proteins, rather than between phopshopeotides and BRCT fusion proteins.

To solve this problem, we established different approaches to synthesize OPAL. To date, we have experimented with several different synthesis surfaces as well as reaction protocols. And we have synthesized larger arrays as an alternative to circumvent some of the technical problems. For example, one solution was to increase the distance between phsophoserine and the cellulose surface, by adding longer linkers on the cellulose surface. The other was to synthesize soluble

peptide library pools and then spot the peptide libraries on a non-cellulose solid support such as glass. Despite of these improvements and modifications, each method and synthesis surface carries its own limitations that has significantly hindered the progress of OPAL-mediated target screening.

(2) BiFC-mediated target screens

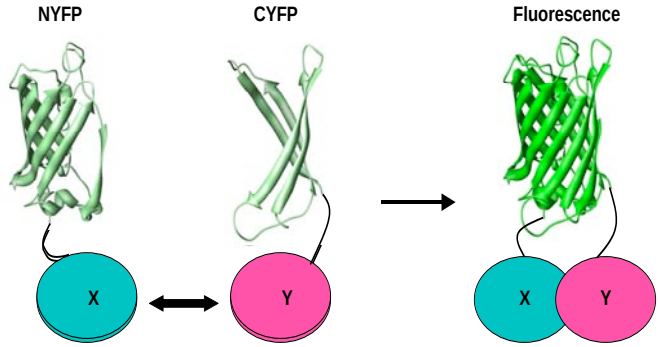

Figure 1. A diagram illustrating the BiFC approach. Interaction between protein X and Y brings fragments of YFP together to form a functional fluorophore.

While we continued to optimize and modify the OPAL arrays, we worked on establishing a novel *in vivo* binding screening strategy that takes advantage of Bi-molecular Fluorescence Complementation (BiFC), to identify binding targets for BRCA1, BARD1, and BRCT domains. Bimolecular fluorescence complementation (BiFC) was originally developed to visualize protein-protein interactions in live cells (9). Two separate proteins are respectively fused to the N- or C-terminal fragment of a fluorescence protein (e.g., YFP). When the two proteins interact, the YFP fragments will be brought to close proximity to form a functional fluorescent complex (Figure 1). BiFC offers several advantages for establishing protein-protein interactions. For example, it enables visualization of interactions in live cells, allows for the examination of the subcellular locations of specific protein-protein interactions, and it is highly amenable to investigating inducible interactions.

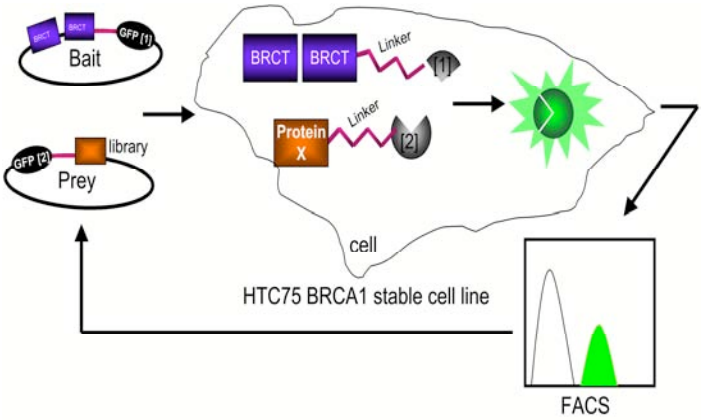

Figure 2. Diagram of the BiFC-hORFeome screen approach.

To develop the BiFC technology for screening for BRCT-BRCA1 interacting proteins in mammalian cells, we constructed expression vectors using the Gateway® cloning system. These vectors were designed to encode either the N- or C-terminal half of YFP (YFPn and YFPc respectively). For the bait, we engineered BRCA1 BRCT domain sequences tagged by YFPn and established stable cell lines expressing YFPn-BRCT.

Next, we generated YFPc-tagged pool cDNA libraries from the Human Open Reading Frame Collection (hORFeome, Openbiosystems). The first hORFeome we obtained contains ~8,000 human individual open reading frames and was used as prey in our studies (Figure 2). Subsequently, we improved upon the BiFC-hORFeome library by constructing a new and more comprehensive hORFeome library that now contains ~12,000 human individual open reading frames. This 1/3 increase in genome coverage has allowed us to more thoroughly screen for BRCT interacting partners.

(2.1) BiFC-hORFeome screens for BRCT domain – the reduction approach

To screen for BRCA1-BRCT interacting proteins using BiFC, we undertook a reduction approach and divided the ~8,000 hORFeome into pools. Each pool was then used to generate high-titer retroviruses for subsequent infection of the YFPn-tagged BRCT-BRCA1 expressing stable cell line. Interaction between YFPn-BRCA1-BRCT and YFPc-tagged prey proteins would bring YFPn and YFPc to close proximity and allow for the assembly of a functional fluorescent complex. The cells can thus be analyzed by fluorescence-activated cell sorting (FACS) to examine the intensity of the fluorescence and by microscopy for the localization (Figure 3).

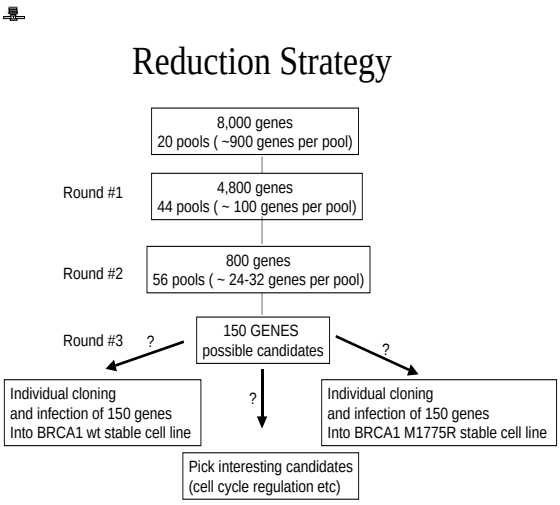

Figure 3. Strategy for Reduction screen.

Indeed, we obtained many cell clones that exhibited either strong or weak fluorescence (Figure 4), indicating that these cells may express potential BRCA1 interacting proteins. These sorted positive cells were further propagated, sorted, and subdivided. Many remained GFP+ after long-term culturing (Figure 5). After three rounds, we were able to narrow down the number of BRCT-BRCA1 candidate binders from ~8,000 genes to ~150 genes. These ~150 candidates are involved in diverse cellular functions including ubiquitination, chromosome maintenance, and cell cycle control. While the reduction pooling screen yielded multiple targets, we encountered many of the limitations of this approach. For example, it biased toward strong protein-protein interactions, because such interactions tend to give rise to higher YFP fluorescence intensity, and are therefore disproportionately enriched in subsequent steps. In addition, the reduction approach took a much longer time to identify the clones that interacted with BRCA1 BRCT domain. We therefore carried out an alternative method.

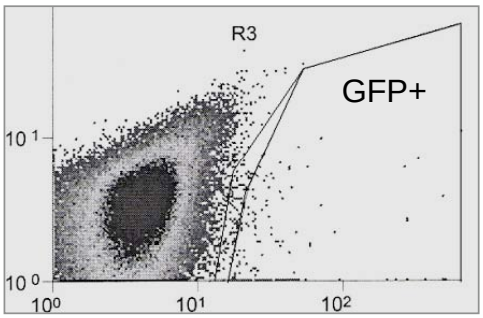

Figure 4. GFP+ cells were FACS sorted into individual clones.

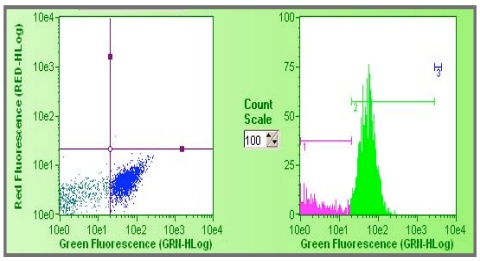

Figure 5. Many of the single clones remain GFP+ after long-term culturing.

(2.2) BiFC-hORFeome screens for BRCT domain – FACS sorting screen

After infecting the YFPn-tagged BRCT-BRCA1 expressing stable cell line using high-titer hORFeome retroviruses, the cells were sorted by FACS. YFP positive cells were sorted individually into 96-well plates. After the cells recovered and expanded, they were further confirmed for whether they remained YFP positive. Genomic DNA was then extracted from the positive clones and used as PCR templates to identify the candidate BRCT-interacting proteins.

Again, we obtained many cell clones that exhibited either strong or weak fluorescence, indicating that these cells may express potential BRCA1 interacting proteins. We then carried out

PCR and sequencing analysis of these isolated clones. Among the genes identified through this approach, several factors were previously unsuspected in DNA damage pathways, for example, NACAP1 and NOL5A (Table 1). Interestingly, some of these proteins were also in the short list of genes identified from our reduction pooling screens, suggesting that these proteins may indeed be true interactors of BRCA1.

	Protein	Putative recog. site	Description
HSA9761	Dimethyladenosine transferase	YQI**S**SPFVF KTL**S**AAFK ILTSTGFSD	Dimethyladenosine transferase (rRNA methylation) [Translation, ribosomal structure and biogenesis]
PKIB	protein kinase (cAMP-dependent, catalytic) inhibitor beta	?	interact with the catalytic subunit of cAMP-dependent protein kinase and act as a competitive inhibitor
CAMKV	hypothetical protein MGC8407	?	Phosphotransferases of the serine or threonine-specific kinase subfamily.
MAMDC2	MAM domain containing 2	VEA**S**CNFEQ PAG**S**CAFEE QNS**S**KKFK	MAM domain. An extracellular domain found in many receptors.
ING5/4	inhibitor of growth family, member 5	KLVRT**S**PEYG GMP**S**VTFGSV KQIE**S**SDYDS	a tumor suppressor protein that can interact with TP53, inhibit cell growth, and induce apoptosis
NACAP1	nascent-polypeptide-associated complex alpha polypeptide	SPA**S**DTYIV	
PTK9L	PTK9L protein tyrosine kinase 9-like (A6-related protein	DPLE**S**VVFIY	Actin depolymerisation factor/cofilin -like domains; these proteins enhance the turnover rate of actin
LOC124220	Similar common salivary protein	GIK**S**IGFEW GQI**S**SAYPS	
DOK3		ALY**S**WPYHF NDLA**S**GLYAS SPTT**S**PIYHN	adapter molecule involved in the negative regulation of imunoreceptor signaling
NOL5A	nucleolar protein 5A	MEDP**S**ISFSK	Putative snoRNA binding domain. This family consists of various Pre RNA processing ribonucleoproteins.

Table 1. A select list of genes identified from BiFC screen.

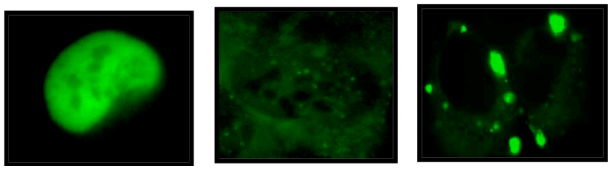

Figure 6. Different patterns of BRCT-target interactions revealed by BiFC.

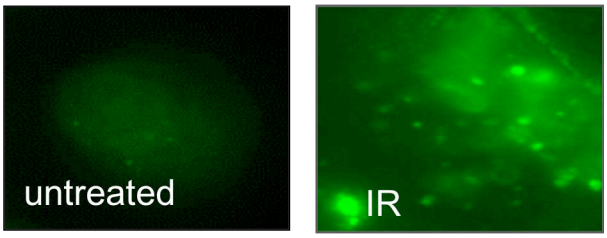

Figure 7. BiFC foci in response to IR DNA

(3) Characterizing the identified interactions

Next, we carried out experiments to further investigate the putative BRCA1 interactors. First, we analyzed the sub-cellular localization of YFP signals in these cells under fluorescence microscopes. We found that the interactions occurred in distinct subcellular compartments amongst different clones (Figure 6). Such findings indicate that (1) the BiFC-hORFeome approach is capable of identifying interactions in different subcellular locations; and (2) the BiFC-hORFeome approach is capable of identifying different types of interactors.

Because BRCA1 mediates DNA damage response, we reasoned that BRCA1-target interactions might be regulated by DNA damage. It has been demonstrated that the BRCT motif is important for BRCA1 nuclear localization (nuclear foci) during S phase and its recruitment to double-stranded break (DSB) foci after irradiation (IR). These foci likely represent sites of DNA damage. We therefore determined whether the localization of the YFP signal (which indicates where the interactions occur) was altered after IR. As shown in Figure 7, we found that some of the putative BRCA1 interacting proteins formed foci after IR treatment, indicating that they may interact with BRCA1 BRCT domain and participate in DNA damage response.

(4) Biochemical and structural studies of BRCT domains and their targets.

(4.1) Surface Plasmon Resonance (SPR) or Fluorescence Polarization (FP) were first used for such studies. When comparing interactions between phosphorylated and unphosphorylated

peptides, an aliquot of the phosphorylated peptides was dephosphorylated with alkaline phosphatase for controls.

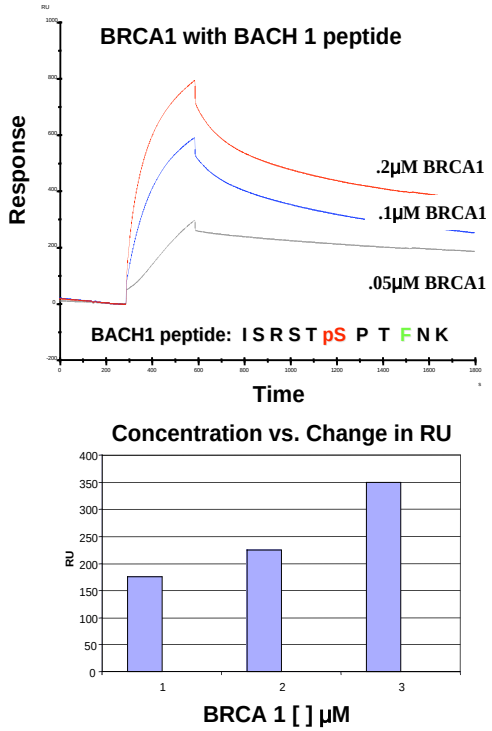

Figure 8. Biacore measurements of BRCA1 BRCT domain and BACH1 peptides.

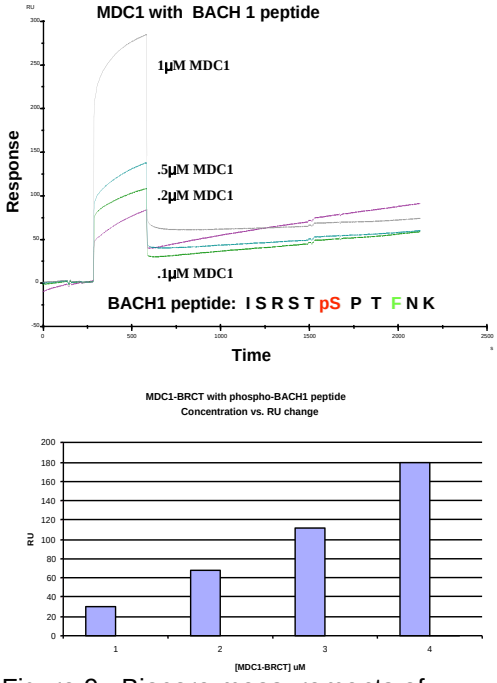

Figure 9. Biacore measurements of MDC1 and BACH1 peptides.

a. SPR is highly sensitive and can measure very low affinities and analyze kinetics data. SPR requires the immobilization of peptides or proteins onto a sensor chip. After trying multiple procedures, we were able to determine the concentration of the peptide as well as the immobilization method that better suits our studies.

First, the biotin-BACH1 peptide was immobilized onto a strepavidin-coated sensor chip. Next, the chip was incubated with different concentrations of BRCA1 GST-BRCT fusion proteins to determine the *on* and *off* rates of the interaction. Based on these preliminary results, wildtype BRCA BRCT clearly discriminates between the phosphorylated vs. the un-phosphorylated peptide (Figure 8). To further confirm the specificity of this interaction, a control MDC1 BRCT domain was used, because it interacts much weaker with the BACH1 sequence (Figure 9). Our results showed the kinetics of BRCA1 BRCT interaction with the phosphorylated BACH1 peptide. These results have validated our system and conditions, and contributed to our understanding of the specificity of the BRCT domains.

b. In general, FP is of very low background, because the interaction occurs in solution without the need to immobilize the protein or peptide. For the FP studies, we examined the BRCT domain of MDC1 histone gamma H2AX (γ-H2AX)(Fig. 10). Briefly, phosphorylated and unphosphorylated forms of FITC-labeled γ-H2AX peptides were incubated with increasing concentrations of MDC1 BRCT domains. The concentration of MDC1-BRCT vs. measurements of fluorescence polarization was plotted and *Kd* values calculated. These studies will allow us to carry out further studies with the various BRCT domains.

(4.2) It remains unclear whether all BRCT domains can mediate phosphorylation-dependent interactions. We decided to use structural analyses to predict BRCT-phosphopeptide interactions. As evidenced by numerous crystal structures of BRCT domains, phosphopeptide recognition is achieved primarily through two key binding pockets formed by the tandem BRCT domains. The phosphoserine recognition pocket is formed by three residues on Lbeta1alpha1 and alpha2 from the first BRCT domain (Figure 11) (3, 7, 18, 20). All the BRCT repeats known to bind phosphopeptides contain a (T/S)G motif and a K/N residue within Lbeta1alpha1 and alpha2

respectively. Based on these observations, we have predicted 5 additional putative phosphopeptide-binding BRCT repeats from human BRCTD1, TOPBP1, ECT2, and XRCC1. These BRCT repeats harbor either the (T/S)G or a closely related (T/S)S motif at the corresponding Lbeta1alpha1 positions (Figure 11). These proteins are involved in cell cycle and DNA damage response. The identification of these putative phospho-binding BRCT motifs provides additional avenues of research into their function in cell cycle control and DNA damage response.

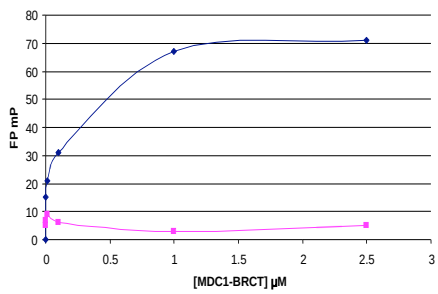

Figure 10. FP measurements of MDC1 and H2AX interaction.

The other key-binding pocket is involved in specificity determination of BRCT-phosphopeptide interaction. As revealed by the structures of phosphopeptides binding to BRCA1 or MDC1 BRCT domains, the P+3 residue (relative to pSer) plays an important role in governing the specificity of BRCT repeats (3, 7, 18, 20). BRCA1 and MDC1 prefer Phe and Tyr respectively at this position (16). Unlike the phosphoserine-binding pocket that is mainly formed by residues from the first BRCT domain, the P+3 pocket is formed by residues from both the first and second BRCT domains (Figure 11). In the BRCA1 BRCT structure, the Phe residue from alpha2, Met residue from Lbeta1'alpha1', and Leu residue from alpha3' contribute to Phe recognition at the pSer+3 position. In comparison, Leu of alpha2, Pro of Lbeta1'alpha1', and Leu of alpha3' help to coordinate the recognition of Tyr at the P+3 position in the MDC1-H2AX peptide structure. Interestingly, MCPH1 contains the same residues as MDC1 in the P+3 pocket and was shown recently to bind the phospho-H2AX peptide (21). These data lend support to utilizing the residues that make up the pSer+3 binding pocket for specificity prediction of BRCT domains. For example, the P+3 pocket residues from PTIP BRCT repeats (residues 560-757) are similar to those of MDC1. Accordingly, PTIP was shown to bind with high affinity peptides with Phe at the P+3 position (13). It is also possible that PTIP BRCT domains may interact with the phosphorylated tail of H2AX (Figure 11). This may explain the finding that PTIP is targeted to phospho-H2AX DNA damage foci (13).

BRCT domains	**pSer pocket**		**P+3 pocket**			**Known Motif or peptides**
	Lβ1α1	α2	Lβ1'α1'	α2	α3'	
BRCA1	SG	K	M	F	L	pSPTF
MDC1	TG	K	P	L	L	pSQEY
MCPH1	SG	N	P	L	L	pSQEY
BARD1	SG	K	H	M	I	pSEDE?
ECT2	TG	K	E	R	W	?
PTIP (560-757)	TG	K	P	L	L	pSQVF pSQEY?
TOPBP1 (22-207)	TS	K	L	L	F	?
TOPBP1 (1177-1401)	SS	K	E	L	A	?
XRCC1	SG	K	E	S	Y	?
BRCTD1	TG	K	K	L	G	?
DNL4	SG	K	T	I	T	pSYYI?

Figure 11. Predicted phosphopeptide-binding pockets for BRCT.

(5) Studies of BARD1 and its funciton

In addition to the above experiments, we also carried out experiments studying the function of BARD1, the tumor suppressor protein that interacts with BRCA1 and contains a BRCT domain that can also bind specific phosphorylated peptides. We generated three retroviral RNAi vectors and obtained two different antibodies for human BARD1. Our pilot studies indicate that these RNAi constructs could significantly knock down BARD1 (>70%). Furthermore, in cells where expression

of BARD1 was inhibited, the cells appeared to accumulate in G2/M. These findings are being further investigated and confirmed. In addition, we are currently carrying out similar BiFC-hORFeome screens for BARD1.

(6) Functiional analysis of the protein complex of the BRCT domain protein RAP1

Although the exact role of telomere maintenance in breast cancer is unclear, telomere dysfunction has been linked to a variety of diseases including cancer (1). Interestingly, one of the core telomere targeted proteins RAP1 also contains a BRCT domain. It has been shown that RAP1 interacts with the double stranded telomere DNA binding protein TRF2. TRF2 itself is a critical regulator of genome integrity, whose inhibition can lead to DNA damage responses at the telomeres. Taken all these observations together, we reasoned that RAP1 and its protein complex merited further studies, the results of which may shed light on novel pathways in breast cancer initiation and progression.

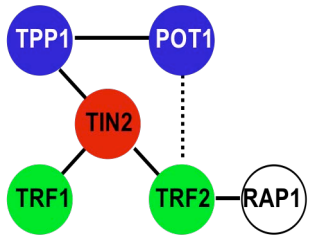

Figure 12. The six protein RAP1 containing complex at the telomeres.

To this end, we performed biochemical and molecular studies of RAP1 and its associated proteins. We found that RAP1 is one of 6 core telomeric proteins that assemble on the telomeres as a molecular platform that protects telomere integrity and maintains telomere length (Figure 12). Within this complex, TPP1 promotes complex formation (15) and interacts directly with the telomerase (19, 22).

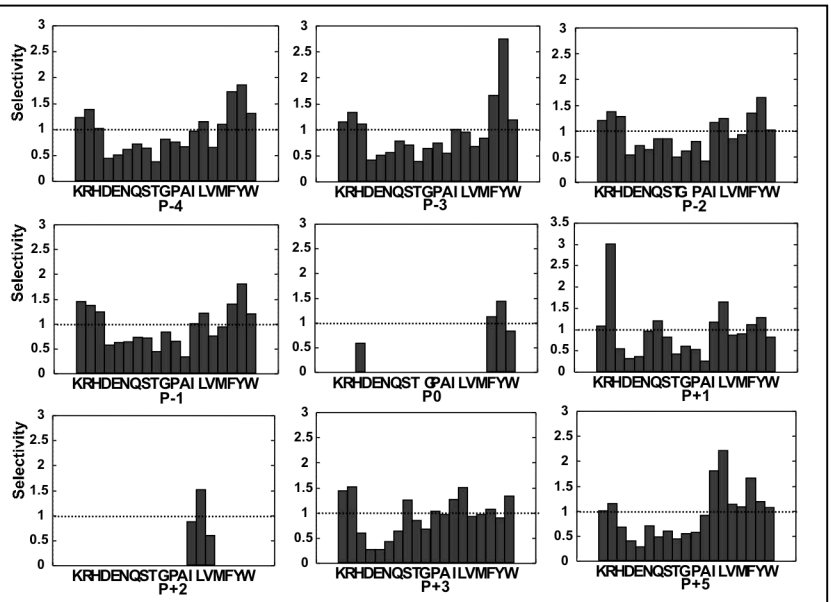

Figure 13. Determination of binding specificity of TRF2 TRFH using oriented libraries.

RAP1 contains a BRCT domain, suggesting that RAP1 complex may interact with the DNA damage and repair pathway. Recent studies indicate that the RAP1 binding partner TRF2 also contains a domain (TRFH) that is capable of recognizing linear peptide sequences found on DNA repair protein Apollo (11). We therefore investigated further such interactions for their biochemical properties and functional significance. We synthesized an oriented library with the sequence: KGXXXX[FYWH]X[ILV]XPXN (X is any amino acids except for Cys).

Because Y504, L506, and P508 of Apollo (which correspond to positions P0, P+2, and P+4) are essential for TRFH interaction with Apollo (6), these positions were partially fixed in this library with a select number of amino acids. Following incubation with GST-TRF2 TRFH fusion proteins, the specifically bound peptide mixtures were isolated and sequenced. As shown in Figure 13, among the four aromatic residues partially fixed

at position P0, TRF2 TRFH preferred Tyr (and Phe to a less extent) for binding. At the P+2 position, Leu (but not Ile or Val) was selected. Additional selections at other positions were also evident, which include Tyr at P-3, Lys at P-1, and Arg at P+1. These observations suggest that a consensus peptide synthesized based on these findings should bind TRF2 TRFH with high affinity. Indeed, our synthesized consensus peptide YRL (KGYYHKYRLSPLN) bound the TRFH domain of TRF2 with high affinity (190 nM). In line with our peptide library data, Ala substitution of the YXL motif in the YRL peptide resulted in its loss of TRF2 interaction, while Ala substitution of P+1 Arg or P+2 Pro reduced its affinity by >10 fold (11). These results indicate that TRF2 TRFH recognizes specific peptide sequences with the core motif of [Y/F]XL. Using this motif, we have identified a list of TRF2/RAP1 interacting proteins that may involve in cancer .

Functional studies further demonstrated the significance of TRF2 TRFH interaction with its targets, the disruption of which leads to DNA damage responses at the telomeres (11). One of the new targets we found to bind the RAP1/TRF2 complex is MCPH1, which in fact a BRCT domain-containing protein. For future studies, we may begin to probe the connection between RAP1-TRF2 interaction and breast cancer, and attempt to elucidate novel pathways involving different BRCT domains.

Key Research Accomplishments

- We have carried out several BiFC *in vivo* interaction studies and obtained a number of novel interaction partners for BRCA1-BRCT domains.
- We have demonstrated that localization of the interaction between BRCA1 and its partner is regulated by DNA damage such as IR in live cells.
- We have performed structural analyses on BRCT domains and found several BRCT domains capable of binding to phosphopetide.
- We have developed a strategy to predict binding specificities of BRCT domains.
- We have investigated into BRCT domain proteins previously unsuspected in breast cancer.
- We have established the functional significance of BRCT binding partners in telomere maintenance.
- We have obtained kinetic data regarding BRCA1 BRCT domain and phosphorylated BACH1 peptide interaction.
- We have shown by both Biacore and FP the interaction between MDC1 BRCT domains and its potential targets.
- We have successfully generated BARD1 knockdown cells and carried out preliminary analysis of these cells.
- We have identified BRCT-domain protein MCHP1 as a key regulator of DNA damage responses at the telomeres

- *Publications*

1. O'Connor MS, Safari A, Xin H, Liu D, **Songyang Z.** (2006) A critical role for TPP1 and TIN2 interaction in high-order telomeric complex assembly. *Proc Natl Acad Sci U S A*. 103:11874-9.

2. Xin H, Liu D, Safari A, Wan M., Sun W, Kim H, O'Connor MW, and **Songyang Z.** (2007) TPP1 is a homologue of ciliate TEBP-beta and interacts with POT1 to recruit telomerase. *Nature*, 45, 559-62.

3. Maria Rodriguez, **Songyang Z**. (2008) BRCT domains: phosphopeptide binding and signaling modules. *Frontiers in Biosciences* 13:5905-15.

4. Kim H, Lee OH, Xin H, Chen LY, Qin J, Chae HK, Lin SY, Safari A, Liu D, **Songyang Z.** (2009) TRF2 functions as a protein hub and regulates telomere maintenance by recognizing specific peptide motifs. *Nat Struct Mol Biol.* [Epub ahead of print] doi:10.1038/nsmb.1575

- Meeting abstracts:

A proteomic approach to identify phosphorylation-dependent targets of BRCT domains. Era of Hope (2008) DOD Breast Cancer Research Program Meeting. Baltimore, MD. June 25, 2008.

Reportable Outcomes

1. Publications

O'Connor MS, Safari A, Xin H, Liu D, **Songyang Z.** (2006) A critical role for TPP1 and TIN2 interaction in high-order telomeric complex assembly. *Proc Natl Acad Sci U S A*. 103:11874-9.

Xin H, Liu D, Safari A, Wan M., Sun W, Kim H, O'Connor MW, and **Songyang Z.** (2007) TPP1 is a homologue of ciliate TEBP-beta and interacts with POT1 to recruit telomerase. *Nature*, 45, 559-62.

Maria Rodriguez, **Songyang Z**. (2008) BRCT domains: phosphopeptide binding and signaling modules. *Frontiers in Biosciences* 13:5905-15.

Kim H, Lee OH, Xin H, Chen LY, Qin J, Chae HK, Lin SY, Safari A, Liu D, Songyang Z. (2009) TRF2 functions as a protein hub and regulates telomere maintenance by recognizing specific peptide motifs. *Nat Struct Mol Biol.* [Epub ahead of print]

2. Meeting abstracts

A proteomic approach to identify phosphorylation-dependent targets of BRCT domains. Era of Hope (2008) DOD Breast Cancer Research Program Meeting. Baltimore, MD. June 25, 2008.

3. Degrees obtained

Maria Rodriguez was a graduate student who initiated many of the experiments outlined here. She demonstrated such productivity and excellence that she was awarded an NIH NRSA predoctoral fellowship and graduated in 2009. Liuh-Yow Chen, a graduate student supported by the grant will be graduating in the summer of 2009, and he will continue with his scientific training as a postdoctoral fellow.

4. Development of cell lines, tissue and serum repositories, and other reagents

OPAL arrays
Oriented peptide libraries
BRCA1 BRCT expressing cell line
Mammalian expression constructs for BiFC screens
Antibodies against various BARD1 complexed proteins
hORFeome pool libraries tagged with various tags
Expression constructs for BRCT domains

List of personnel receiving pay

Zhou Songyang

Liuh-Yow Chen
Ok-Hee Lee
Hyeung Kim

Conclusions

In summary, we have successfully conducted genetic screens of BRCT domain interacting sequences using BiFC. We have obtained and confirmed a number of potential targets for further examination. We have performed structural analyses on BRCT domains and predict BRCT domain-phosphopeptide interactions. The information obtained from our studies should prove especially useful for the development of new and effective screening strategies, drug targets, and treatment for breast cancer.

References

1. **Blackburn, E. H.** 2005. Telomeres and telomerase: their mechanisms of action and the effects of altering their functions. FEBS Lett. **579:**859-62.
2. **Bork, P., K. Hofmann, P. Bucher, A. F. Neuwald, S. F. Altschul, and E. V. Koonin.** 1997. A superfamily of conserved domains in DNA damage-responsive cell cycle checkpoint proteins. Faseb J **11:**68-76.
3. **Botuyan, M. V., Y. Nomine, X. Yu, N. Juranic, S. Macura, J. Chen, and G. Mer.** 2004. Structural basis of BACH1 phosphopeptide recognition by BRCA1 tandem BRCT domains. Structure **12:**1137-46.
4. **Callebaut, I., and J. P. Mornon.** 1997. From BRCA1 to RAP1: a widespread BRCT module closely associated with DNA repair. FEBS Lett **400:**25-30.
5. **Cantor, S. B., D. W. Bell, S. Ganesan, E. M. Kass, R. Drapkin, S. Grossman, D. C. Wahrer, D. C. Sgroi, W. S. Lane, D. A. Haber, and D. M. Livingston.** 2001. BACH1, a novel helicase-like protein, interacts directly with BRCA1 and contributes to its DNA repair function. Cell **105:**149-60.
6. **Chen, Y., Y. Yang, M. van Overbeek, J. R. Donigian, P. Baciu, T. de Lange, and M. Lei.** 2008. A Shared Docking Motif in TRF1 and TRF2 Used for Differential Recruitment of Telomeric Proteins. Science **319:**1092-6.
7. **Clapperton, J. A., I. A. Manke, D. M. Lowery, T. Ho, L. F. Haire, M. B. Yaffe, and S. J. Smerdon.** 2004. Structure and mechanism of BRCA1 BRCT domain recognition of phosphorylated BACH1 with implications for cancer. Nat Struct Mol Biol **11:**512-8.
8. **Goldberg, M., M. Stucki, J. Falck, D. D'Amours, D. Rahman, D. Pappin, J. Bartek, and S. P. Jackson.** 2003. MDC1 is required for the intra-S-phase DNA damage checkpoint. Nature **421:**952-6.
9. **Hu, C. D., and T. K. Kerppola.** 2003. Simultaneous visualization of multiple protein interactions in living cells using multicolor fluorescence complementation analysis. Nat Biotechnol **21:**539-45. Epub 2003 Apr 14.
10. **Huyton, T., P. A. Bates, X. Zhang, M. J. Sternberg, and P. S. Freemont.** 2000. The BRCA1 C-terminal domain: structure and function. Mutat Res **460:**319-32.

11. **Kim, H., O. H. Lee, H. Xin, L. Y. Chen, J. Qin, H. K. Chae, S. Y. Lin, A. Safari, D. Liu, and Z. Songyang.** 2009. TRF2 functions as a protein hub and regulates telomere maintenance by recognizing specific peptide motifs. Nat Struct Mol Biol.
12. **Lou, Z., K. Minter-Dykhouse, X. Wu, and J. Chen.** 2003. MDC1 is coupled to activated CHK2 in mammalian DNA damage response pathways. Nature **421:**957-61.
13. **Manke, I. A., D. M. Lowery, A. Nguyen, and M. B. Yaffe.** 2003. BRCT repeats as phosphopeptide-binding modules involved in protein targeting. Science **302:**636-9.
14. **Nathanson, K. L., R. Wooster, B. L. Weber, and K. N. Nathanson.** 2001. Breast cancer genetics: what we know and what we need. Nat Med **7:**552-6.
15. **O'Connor, M. S., A. Safari, H. Xin, D. Liu, and Z. Songyang.** 2006. A critical role for TPP1 and TIN2 interaction in high-order telomeric complex assembly. Proc Natl Acad Sci U S A **103:**11874-9.
16. **Rodriguez, M., X. Yu, J. Chen, and Z. Songyang.** 2003. Phosphopeptide binding specificities of BRCA1 COOH-terminal (BRCT) domains. J Biol Chem **278:**52914-8.
17. **Stewart, G. S., B. Wang, C. R. Bignell, A. M. Taylor, and S. J. Elledge.** 2003. MDC1 is a mediator of the mammalian DNA damage checkpoint. Nature **421:**961-6.
18. **Varma, A. K., R. S. Brown, G. Birrane, and J. A. Ladias.** 2005. Structural basis for cell cycle checkpoint control by the BRCA1-CtIP complex. Biochemistry **44:**10941-6.
19. **Wang, F., E. R. Podell, A. J. Zaug, Y. Yang, P. Baciu, T. R. Cech, and M. Lei.** 2007. The POT1-TPP1 telomere complex is a telomerase processivity factor. Nature **445:**506-10.
20. **Williams, R. S., M. S. Lee, D. D. Hau, and J. N. Glover.** 2004. Structural basis of phosphopeptide recognition by the BRCT domain of BRCA1. Nat Struct Mol Biol **11:**519-25.
21. **Wood, J. L., N. Singh, G. Mer, and J. Chen.** 2007. MCPH1 Functions in an H2AX-dependent but MDC1-independent Pathway in Response to DNA Damage. J Biol Chem **282:**35416-35423.
22. **Xin, H., D. Liu, M. Wan, A. Safari, H. Kim, W. Sun, M. S. O'Connor, and Z. Songyang.** 2007. TPP1 is a homologue of ciliate TEBP-beta and interacts with POT1 to recruit telomerase. Nature **445:**559-62.
23. **Yu, X., C. C. Chini, M. He, G. Mer, and J. Chen.** 2003. The BRCT domain is a phospho-protein binding domain. Science **302:**639-42.
24. **Yu, X., L. C. Wu, A. M. Bowcock, A. Aronheim, and R. Baer.** 1998. The C-terminal (BRCT) domains of BRCA1 interact in vivo with CtIP, a protein implicated in the CtBP pathway of transcriptional repression. J Biol Chem **273:**25388-92.

A critical role for TPP1 and TIN2 interaction in high-order telomeric complex assembly

Matthew S. O'Connor, Amin Safari, Huawei Xin, Dan Liu*, and Zhou Songyang*

Verna and Marrs McLean Department of Biochemistry and Molecular Biology, Baylor College of Medicine, One Baylor Plaza, Houston, TX 77030

Communicated by Salih J. Wakil, Baylor College of Medicine, Houston, TX, June 26, 2006 (received for review March 8, 2006)

Mammalian telomeric proteins function through dynamic interactions with each other and telomere DNA. We previously reported the formation of a high-molecular-mass telomeric complex (the mammalian telosome) that contains the six core proteins TRF1, TRF2, RAP1, TIN2, POT1, and TPP1 (formerly named PTOP/PIP1/TINT1) and mediates telomere end-capping and length control. In this report, we sought to elucidate the mechanism of six-protein complex (or shelterin) formation and the function of this complex. Through reconstitution experiments, we demonstrate here that TIN2 and TPP1 are key components in mediating the six-protein complex assembly. We demonstrate that not only TIN2 but also TPP1 are required to bridge the TRF1 and TRF2 subcomplexes. Specifically, TPP1 helps to stabilize the TRF1–TIN2–TRF2 interaction and promote six-protein complex formation. Consistent with this model, overexpression of TPP1 enhanced TIN2–TRF2 association. Conversely, knocking down TPP1 reduced the ability of endogenous TRF1 to associate with the TRF2 complex. Our results suggest that coordinated interactions among TPP1, TIN2, TRF1, and TRF2 may ensure robust assembly of the telosome, telomere targeting of its subunits, and, ultimately, regulated telomere maintenance.

protein complex | telomere | telosome

Mammalian telomeres are regulated by the telomerase and telomeric proteins (1–6). Among the telomere-associated proteins important for mammalian telomere homeostasis, POT1 is likely the major regulator of telomere length control (7–9). POT1 binds the 3′ G-rich telomere overhangs through its oligonucleotide-binding folds (7, 10, 11) and may regulate telomerase access (12–14). The telomere recruitment of POT1 thus constitutes an important step in telomere end-capping and length control. Recently, a new telomeric protein TPP1 (previously PTOP/PIP1/TINT1) was identified as a regulator of POT1 (9, 15, 16). The telomeric targeting of POT1 depends on its interaction with TPP1 (9). It remains to be determined how TPP1 interacts with other telomeric proteins and whether TPP1 has any function other than targeting POT1.

In contrast to POT1, TRF1 and TRF2 directly bind double-stranded telomere DNA and interact with a number of proteins to maintain telomere structure and length (1–5). It has been shown that TRF1 counts and controls the length of telomere repeats, probably through its interaction with TIN2, Tankyrase, PINX1, TPP1, and POT1 (7, 9, 12, 15, 17–24). In comparison, TRF2 has an essential role in end protection and the telomeric recruitment of several proteins, including the BRCA1 C-terminal domain-containing protein RAP1, the nucleotide excision repair protein ERCC1/XPF, BLM, and the DNA repair MRN complex (24–31). Because of their abilities to interact with multiple proteins, TRF1 and TRF2 are by definition hubs of protein–protein interaction at the telomeres (32). Recent studies have established multiple pairwise interactions among the six telomeric proteins (TRF1, TRF2, RAP1, TIN2, POT1, and TPP1), including the association of TIN2 with both TRF1 and TRF2 (16, 33–35). In fact, the six proteins could be copurified in mammalian cells in a large-molecular-mass complex referred to as the mammalian telosome/shelterin (16, 32–36)

The physical link between TRF1 and TRF2 suggests coordinated and integrated signals in telomere maintenance. The connectivity between TRF1 and TRF2 appeared vital for telomere maintenance, because reducing TRF1 levels also resulted in decreased TRF2 telomere localization (37). Moreover, POT1 is most likely one of the initiators of telomere maintenance activity mediated by the telosome. Information regarding the state and length of the telomere ends can be transmitted from TRF1 and TRF2 to POT1 through their interaction within the complex. The assembly and function of the mammalian telosome, and, in particular, the roles and contribution of individual core proteins remain largely unknown. Here we investigated the mechanism of telosome assembly through reconstitution and fractionation experiments. Our findings indicate that the six telomeric proteins are sufficient to form a large complex. Both TPP1 and TIN2 are essential mediators of this process. In addition, the TPP1–TIN2 interaction regulates the bridging between TRF1 and TRF2 and promotes and stabilizes the assembly of high-order telomeric complexes.

Results

TIN2 and TPP1 Are Key Components that Mediate the Six-Protein Complex Assembly. Among the six telomeric proteins, multiple pairwise interactions have been demonstrated (summarized in Fig. 1*a*). What is the contribution and significance of each interaction to telosome assembly?

To address this question, we assessed the individual contribution of the six proteins in a reconstitution experiment by transiently expressing epitope-tagged telomere proteins in 293T cells. In this system, transiently expressed exogenous proteins were in vast excess (10- to 100-fold) compared with endogenous proteins (data not shown). As a result, the protein–protein interactions assayed occurred primarily between exogenously expressed proteins.

Consistent with the six-protein complex model, immunoprecipitation of V5-RAP1 brought down FLAG-tagged POT1, TRF1, TRF2, TIN2, and GFP-tagged TPP1 (Fig. 1*b*, lane 1). With RAP1 as the anchor, we then assayed how the six-protein complex assembly might be affected when the remaining components were individually removed. As expected, in the absence of TRF2, the association of RAP1 with the other four telomeric proteins was disrupted (Fig. 1*b*, lane 3). Furthermore, POT1 appeared dispensable for the formation of the TRF2, RAP1, TIN2, TPP1, and TRF1 complex (lane 6). Similar results were also obtained for TRF1, because the remaining five proteins were able to complex without TRF1 (lane 2).

The most striking results were obtained when either TPP1 or TIN2 was omitted from the reaction. The complex completely failed to form when TIN2 was excluded (which added further proof that endogenous proteins were not affecting this assay) (Fig. 1*b*, lane 4). When TPP1 was absent (Fig. 1*b*, lane 5), TRF1

Conflict of interest statement: No conflicts declared.

*To whom correspondence may be addressed. E-mail: songyang@bcm.tmc.edu or danl@bcm.tmc.edu.

© 2006 by The National Academy of Sciences of the USA

www.pnas.org/cgi/doi/10.1073/pnas.0605303103

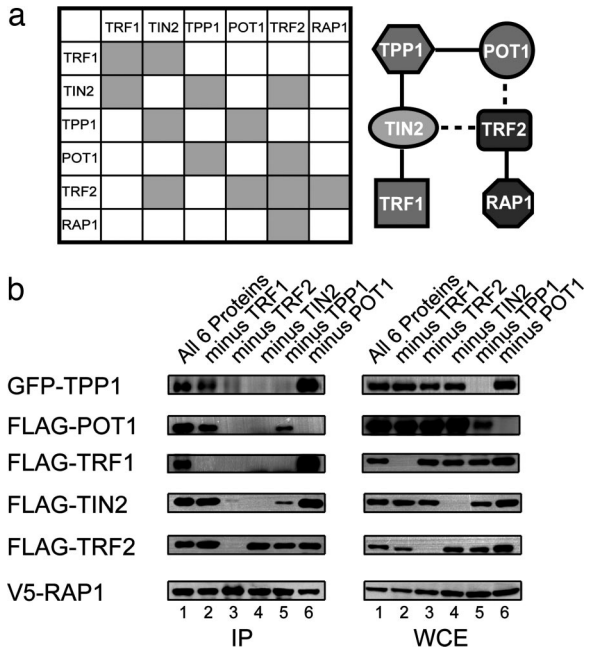

Fig. 1. TPP1 and TIN2 are key components that mediate six-protein complex formation. (*a*) A schematic representation of known pairwise interactions between known mammalian telomere proteins (*Left*) and a possible model of interactions in the six-protein complex (*Right*). Known pairwise interactions: TRF1–TRF1 (44), TRF1–TIN2 (18), TIN2–TPP1 (9, 16), POT1–TPP1 (9, 15), TRF2–TIN2 (16, 33–35), TRF2–TRF2 (45), TRF2–RAP1 (25), and POT1–TRF2 (46). Dashed lines indicate weak interactions. (*b*) TPP1 and TIN2 regulate six-protein complex assembly. Expression constructs encoding V5-RAP1 were cotransfected into 293T cells with either all five expression vectors encoding FLAG-POT1, FLAG-TIN2, FLAG-TRF1, FLAG-TRF2, and GFP-TPP1 or any four of the five vectors. Approximately 3 μg of DNA was transfected for each construct. Two days after transfection, whole-cell extracts were prepared and immunoprecipitated (IP) with anti-V5 antibodies. Coimmunoprecipitated proteins were detected by Western blotting by using anti-TPP1 antibodies (for GFP–TPP1) and the appropriate anti-epitope tag antibodies (FLAG and V5).

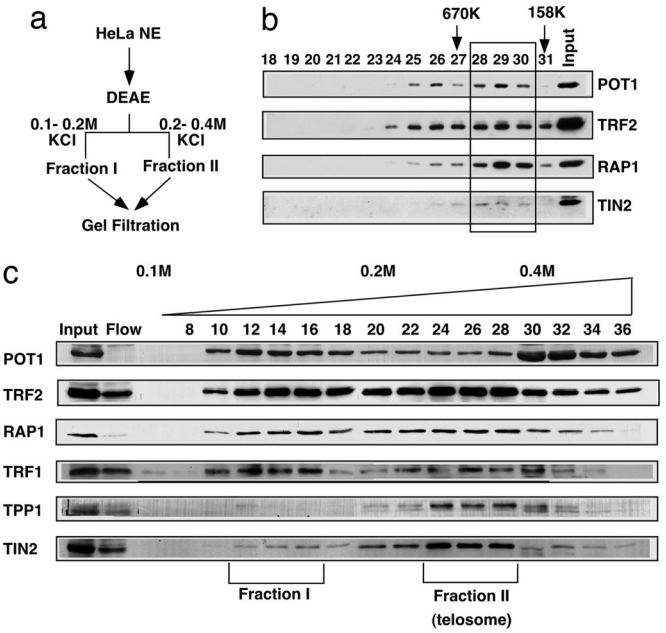

Fig. 2. Two distinct POT1-containing protein complexes exist in human cells. (*a*) HeLa cell nuclear extracts (HeLa NE) were fractionated on a DEAE ion-exchange column. The bound proteins were eluted with increasing concentrations of KCl. The two main fractions (I and II) that contained telomeric proteins were then further fractionated on a gel filtration column. (*b*) Fractions from the DEAE column were collected and resolved by SDS/PAGE. Telomeric proteins were detected through Western blotting by using various antibodies as indicated. ''Flow'' indicates flow through. (*c*) Fraction I from the DEAE column was fractionated on a gel filtration column. Telomeric proteins at individual fractions (fractions 18–31) were detected through Western blotting with different antibodies as indicated. The majority of telomeric proteins were coeluted at ≈500 kDa (indicated by the box). Molecular masses of the gel-filtration standards are indicated.

no longer coimmunoprecipitated with TRF2, and the levels of TIN2 and POT1 that associated with TRF2 were greatly reduced. The importance of TPP1 and TIN2 in six-protein complex formation was further confirmed by using V5-TRF2 as an alternative anchor (data not shown). We did observe a reduction of POT1 levels in the absence of TPP1. However, this lower level of POT1 could not account for the loss of TRF1 and decrease of TIN2 in the RAP1 complex, because the absence of POT1 did not disrupt high-order complex formation (Fig. 1*b*, lane 6). The above findings support the notion that TPP1 and TIN2 are critical for six-protein complex assembly and that the bridging between the TRF1 and TRF2 subcomplexes may be impaired in the absence of either TPP1 or TIN2.

Identification of Two Distinct POT1-Containing Complexes. POT1 recruitment to the telomeres depends on TPP1 (9). When TPP1 was removed in the reconstitution experiments, interactions between POT1 and other components of the six-protein complex were indeed severely affected (Fig. 1*b*, lane 5). However, a small amount of POT1 was able to complex with RAP1, TRF2, and TIN2. To further investigate the physiological relevance of this finding, we analyzed endogenous POT1 protein complexes using HeLa cell nuclear extracts. Consistent with our reconstitution experiments, endogenous POT1 could be found in two major fractions on the DEAE ion-exchange column (Fig. 2 *a* and *b*). The 0.2–0.4 M KCl fraction II contains POT1, TRF1, TRF2, TIN2, RAP1, and TPP1 (Fig. 2*b*). The majority of TIN2 and TPP1 were eluted in this fraction. Through gel filtration, we confirmed that fraction II corresponds to the high-molecular-mass mammalian telosome (≈1 MDa) described previously (9). Interestingly, fraction I (which eluted at 0.1–0.2 M KCl) contained barely detectable amounts of TPP1 (Fig. 2*b*), suggesting that this is a distinct POT1-containing complex. Indeed, upon further fractionation of fraction I on a gel filtration column, POT1 was found to elute in a smaller complex (≈500 kDa) (Fig. 2*c*). Notably, TRF2, RAP1, and a small amount of TIN2 were also coeluted with POT1 in this fraction, indicating that POT1, RAP1, TRF2, and TIN2 can indeed form a complex. Importantly, this POT1 complex found in fraction I of the DEAE column mirrors the four-protein complex formed in the 293T reconstitution experiments (Fig. 1*b*, lane 5). These findings indicate the existence of two POT1 complexes in mammalian cells: one that contains all six telomeric proteins and one that does not contain TPP1. Our results so far point to an essential role for TPP1 in the formation and function of higher-molecular-mass telomeric complexes. The possible functional differences of the complex without TPP1 and the six-protein complex are quite intriguing and merit further investigation.

TPP1 Promotes Higher-Order Complex Formation Through TIN2. Within the six telomeric proteins, TIN2–TRF2 association establishes the TRF1–TIN2–TRF2 link and connects TRF1 to the TRF2 subcomplex (16, 33–35). Interestingly, in the absence of TPP1, TRF2 could no longer coimmunoprecipitate with TRF1, and its ability to coimmunoprecipitate with TIN2 (but not other telomere proteins) decreased by ≈70% (Fig. 1*b*). These findings imply that TIN2–TRF2 or TIN2–TRF1 interaction alone is

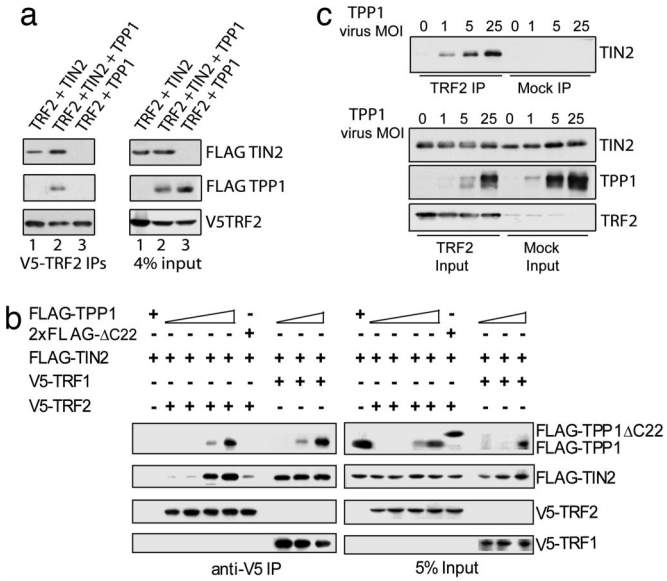

Fig. 3. TPP1 promotes the interaction between TIN2 and TRF2. (*a*) TPP1 directly binds TIN2 but not TRF2. Expression vectors encoding V5-TRF2 were cotransfected into 293T cells, with expression vectors encoding FLAG-TIN2 (lane 1), both FLAG-TPP1 and FLAG-TIN2 (lane 2), or FLAG-TPP1 (lane 3). Approximately 3 μg of DNA was transfected for each construct. Whole-cell extracts were immunoprecipitated with anti-V5 antibodies and blotted with anti-FLAG-HRP antibodies. (*b*) TPP1 promotes interaction between TIN2 and TRF2. 293T cells were transiently transfected with expression vectors for V5-TRF2 (3.3 μg) or V5-TRF1 (4.5 μg) in combination with FLAG-TIN2 (1.5 μg) and increasing amounts of C-terminally tagged FLAG-TPP1 (0, 0.7, 2.4, and 5.6 μg for TRF2, and 0, 0.7, and 2.4 μg for TRF1). The TPP1 deletion mutant TPP1ΔC22 (2xFLAG-tagged at both termini) (5 μg) was also used as a control for TPP1. 2×FLAG-TPP1 and FLAG-TPP1 behaved similarly in these experiments (data not shown). Anti-V5 immunoprecipitates from lysates of these cells were resolved by SDS/PAGE and Western-blotted with anti-FLAG-HRP or anti-V5-HRP antibodies. (*c*) TPP1 promotes TIN2–TRF2 interaction in insect cells. Sf9 cells were coinfected with His-TRF2 and His-TIN2 baculoviruses along with increasing amounts of His-TPP1 viruses. Three days after infection, His-TRF2 was pulled down from insect cell extracts with anti-TRF2 antibodies. Extracts expressing TIN2 and TPP1 without His-TRF2 were used as controls (Mock IP). In the input whole-cell extracts there is a TRF2 antibody cross-reactive band. His-TIN2 or TPP1 proteins were detected with anti-TIN2 or anti-TPP1 antibodies. MOI, multiplicity of infection.

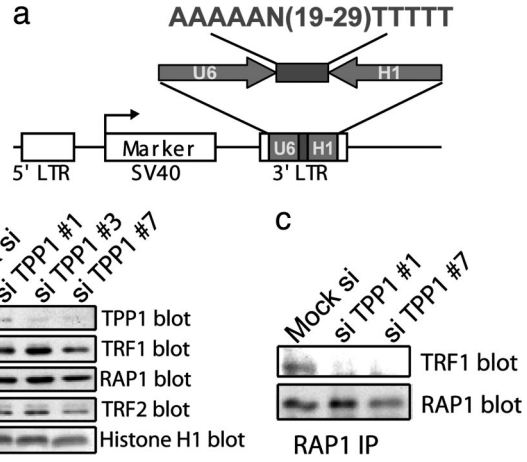

Fig. 4. TPP1 regulates TRF1 association with the TRF2/RAP1 complex *in vivo*. (*a*) Design of the pRetro-dual RNAi vector for TPP1 knockdown. TPP1 RNAi oligos were cloned between the head-to-head-positioned U6 and H1 promoters. (*b*) Reducing endogenous TPP1 levels by RNAi decreases TRF1 recruitment to the TRF2/RAP1 complex. (*Left*) Nuclear extracts (420 mM KCl extracted) were prepared from HT1080 cells that were transfected with pRetro-dual control and TPP1 RNAi vectors. The extracts were resolved by SDS/PAGE and Western-blotted with the indicated antibodies. The anti-Histone H1 antibody was used as a loading control (note that the siTPP1 #7 lane was slightly underloaded). (*Right*) Nuclear extracts from HT1080 cells expressing pRetro-dual siTPP1 #1 and siTPP1 #7 were immunoprecipitated with anti-RAP1 antibodies, and Western-blotted with anti-RAP1 and anti-TRF1 antibodies.

insufficient to trigger six-protein complex formation. We therefore speculated that TPP1 might promote TIN2–TRF2 and TRF1–TIN2–TRF2 association, leading to proper high-order telomeric complex assembly.

First, we investigated the function of TIN2 and TPP1 by examining the interactions of TRF2, TIN2, and TPP1 in transient transfection experiments. Consistent with our hypothesis, we could not detect direct interaction between TRF2 and TPP1 (Fig. 3*a*), but TPP1 coimmunoprecipitated together with TIN2 and TRF2, indicating the formation of a TPP1–TIN2–TRF2 complex. With increasing amounts of TPP1 (although the total amounts of TIN2 and TRF2 remained constant), the amount of TIN2 that associated with TRF2 increased as well (Fig. 3*b*). In contrast, when TRF2 was replaced with TRF1, binding of TRF1 to TIN2 was unaltered by changes in the amount of TPP1, confirming the specific role of TPP1 in promoting TRF2–TIN2 association (Fig. 3*b*). Furthermore, we demonstrated that TPP1 could promote TIN2–TRF2 binding by using recombinant TRF2, TIN2, and TPP1 proteins from insect cells. As shown in Fig. 3*c*, enhanced association of His-tagged TRF2 with TIN2 was observed with increased coexpression of TPP1, consistent with the notion that TPP1 directly regulates TIN2–TRF2 interaction. These data also ruled out the possible involvement of endogenous proteins in our experiments using 293T cells. In the absence of TPP1, we found little or no incorporation of TRF1 into the RAP1–TRF2 complex (Fig. 1*b*, lane 5), suggesting that TPP1 may stabilize the TRF1–TIN2–TRF2 three-protein complex through its regulation of TIN2–TRF2 interaction.

Our data so far support the model that TPP1 acts as an essential component of the six-protein complex by regulating TIN2–TRF2 interaction and the connectivity of TRF1 and TRF2 subcomplexes. Without TPP1, the formation of the TRF1–TIN2–TRF2 complex may be impaired. We previously showed altered telomeric localization of POT1 in TPP1 knockdown cells (9). However, the siRNA oligonucleotides (oligos) used previously only led to significant TPP1 knockdown in ≈50% of the cells, preventing us from performing biochemical analyses of TPP1 function in six-protein complex assembly. To achieve this goal, we generated and optimized a dual-promoter RNAi vector for screening oligos against TPP1 (Fig. 4*a*) (see *Materials and Methods*).

We found three RNAi vectors to substantially (70–90%) knockdown TPP1 after their transfection into HT1080 cells (Fig. 4*b*). The TPP1 RNAi cells grew more slowly than did control cells (data not shown). The phenotypes of these cells with regard to cell cycle and telomere end capping currently require additional investigation. Interestingly, the level of RAP1-assocaited TRF1 was reduced by ≈80% in TPP1 knockdown cells (Fig. 4*c*), suggesting a key role of TPP1 in six-protein complex assembly and in regulating the connectivity between the TRF1 and TRF2 complexes *in vivo*.

TPP1 Promotes Six-Protein Complex Formation Through Its Interaction with TIN2. The data thus far indicate that both TPP1 and TIN2 are necessary for six-protein complex formation. Because TPP1 interacts with TIN2 directly (16, 33–35), the TPP1–TIN2 association may be coupled to six-protein complex assembly. Our deletional analyses in yeast indicated that the C-terminal half of TPP1 mediated its interaction with TIN2 (9). In fact, deletion of either the C terminus (TPP1ΔC) or just the last 22 residues of

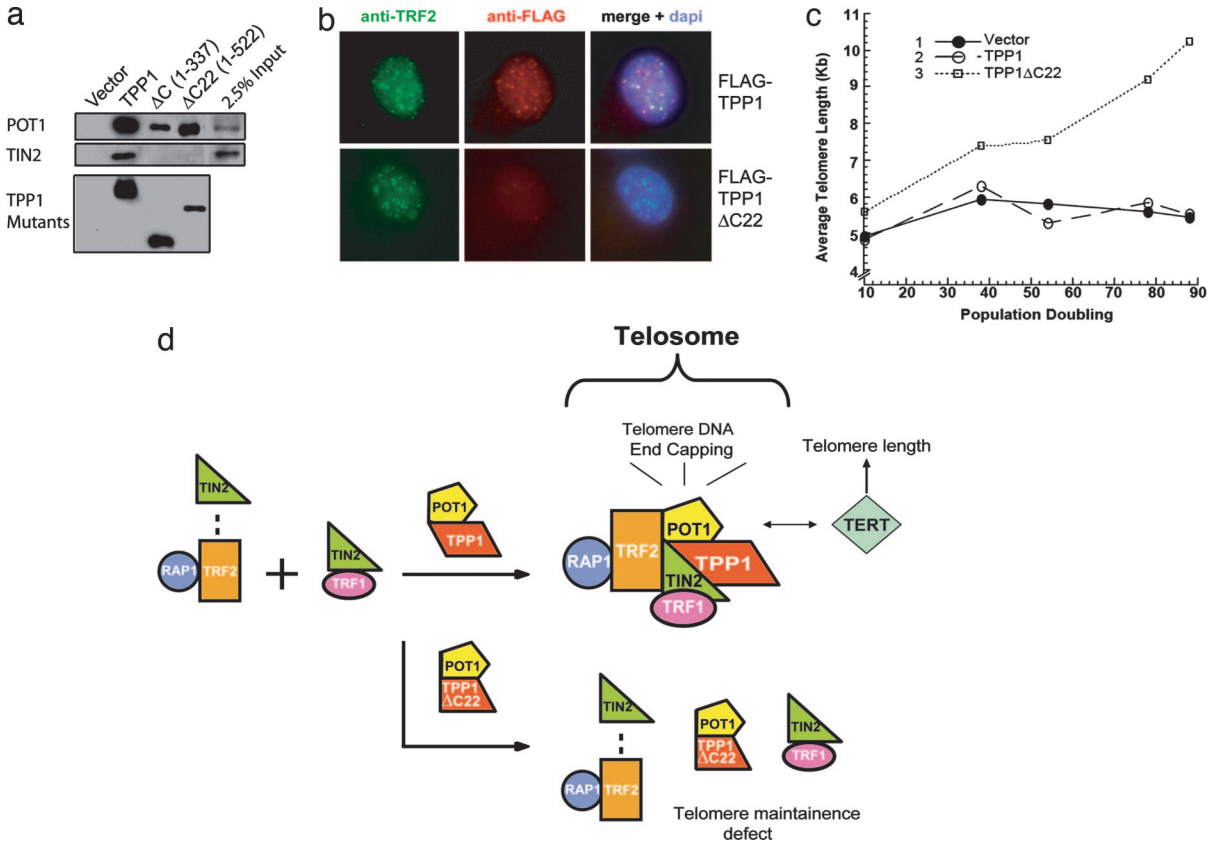

Fig. 5. The extreme C terminus of TPP1 is required for direct TPP1–TIN2 interaction and enhanced TIN2–TRF2 association. (*a*) The last 22 aa of TPP1 are required for TPP1–TIN2 interaction in human cells. Whole-cell extracts from HT1080 cells expressing various FLAG-tagged TPP1 and TPP1 mutants (TPP1ΔC and ΔC22) were immunoprecipitated with anti-FLAG M2 antibodies. Endogenous POT1 or TIN2 was detected by Western blotting with anti-POT1 or anti-TIN2 antibodies. (*b*) TPP1ΔC22 no longer localizes to the telomeres. The telomere localization of FLAG-tagged wild-type or mutant TPP1 was analyzed by indirect immunofluorescence. The cells were doubly permeabilized and costained with anti-FLAG and anti-TRF2 antibodies. (*c*) TPP1–TIN2 mediated six-protein complex assembly is necessary for telomere length maintenance. Expression of TPP1ΔC22 but not TPP1 in HT1080 cells resulted in telomere elongation. Mean telomere restriction fragment length in control (vector alone) HT1080 cells and those expressing TPP1 or TPP1ΔC22 were plotted against population doublings. (*d*) A schematic representation of the six-protein complex assembly model. Overexpression of TPP1ΔC22 disrupts telosome assembly and favors the formation of subcomplexes containing TIN2–TRF2–RAP1, POT1–TPP1ΔC22, or TIN2–TRF1.

TPP1 (TPP1ΔC22) was sufficient to eliminate TIN2-binding (but not POT1-binding) in yeast (data not shown) (7–9) and in mammalian cells (Fig. 5*a*). Furthermore, TPP1ΔC22 no longer localized to telomeres (Fig. 5*b*), consistent with previous observations that demonstrated that TIN2 mediated the telomere targeting of TPP1 (16),

How does the disruption of TPP1-mediated six-protein complex formation affect telomere maintenance? We reasoned that the inability of TPP1ΔC22 to promote six-protein complex assembly might affect telomere length control. To examine this possibility, we determined the average telomere length in HT1080 cells expressing TPP1 and TPP1ΔC22. As shown in Fig. 5*c*, expression of TPP1ΔC22 but not TPP1 resulted in elongated telomeres. These data indicate that TPP1–TIN2 interaction regulates the formation of the six-protein complex necessary for telomere length control.

Collectively, our findings suggest possible cooperativity in TRF1–TIN2–TRF2–TPP1 complex formation and imply that the interaction between the TRF1 and TRF2 protein hubs, a key connection in the assembly and chromatin targeting of high-order telomeric complexes, may be stimulated by the heterodimerization of TIN2 and TPP1.

Discussion

Recent advances in elucidating the interaction and function of key telomeric proteins have allowed a better understanding of the intricacies of the mammalian telosome/shelterin that regulates telomere maintenance. At its core is the six-protein complex made up of TIN2, TRF1, TRF2, RAP1, TPP1, and POT1. Because of its ability to bind both TRF1 and TRF2, TIN2 is emerging as a key player in telomere chromatin formation (16, 33–35). Removal of TIN2, as done in our reconstitution experiments (Fig. 1), leads to the elimination of the bridge between the TRF1 and TRF2 subcomplexes. Surprisingly, TIN2–TRF2 interaction alone appeared to be insufficient to initiate TRF1 recruitment and six-protein complex formation. Given that TIN2 can bind either TRF1 or TRF2, TIN2–TRF1 and TIN2—TRF2 may in fact exist in separate subcomplexes. Our study has revealed that TPP1 also is a critical regulator of telomeric protein–protein interactions. By virtue of its interaction with TIN2, TPP1 stabilizes the TIN2–TRF2 and TRF1–TIN2–TRF2 interactions, stimulates the connection between the TRF1 and TRF2 subcomplexes, and promotes telosome assembly.

In budding yeast, telomeric proteins are packed into nuclease-resistant telosome structures (38). Whether the mammalian telomeric proteins and telomere DNA complex also can form into nuclease-resistant structures remains to be elucidated. The exact identities of the subunits of the mammalian telosome probably differ from the yeast telosome, because homologues of several mammalian telomeric proteins have yet to be found in budding yeast. Mammalian telosomes may very well act as key

molecular machineries that regulate mammalian telomeres in a coordinated fashion. Our experiments here have highlighted the importance of TPP1–TIN2 interaction in six-protein complex function and represent a noteworthy step toward the understanding of this dynamic and complicated process.

How does TPP1–TIN2 interaction regulate TIN2–TRF2 binding? Our data are consistent with a direct role for TPP1 in regulating telosome stability. We speculate that the answer may at least partly lie in the structure of TIN2. The N-terminal half of TIN2 is predicted to have high helical contents and conserved throughout evolution (data not shown). This region interacts with TPP1 (D.L. and Z.S., unpublished data) and TRF2 (16, 33). C-terminal to this TIN2 region is the TRF1-binding domain (18). It is possible that TPP1 binding of TIN2 may stabilize or alter the conformation of TIN2, which in turn enhances TIN2–TRF2 interaction and enables TIN2 to simultaneously interact with both TRF2 and TRF1 (Fig. 5*d*).

What are the consequences of a stabilized link between TRF1 and TRF2? We think that the structural unit that contains TPP1, TIN2, TRF1, and TRF2 may have increased affinity for telomeric DNA, as observed for TRF1 (39). Several lines of evidence support this notion. First, multivalent interactions are known to enhance affinity, and in this case both TRF1 and TRF2 can bind telomeres. Second, recent studies suggest that the interaction of TRF1 and TRF2 with the telomere is in fact extremely dynamic. For example, Mattern *et al.* (40) demonstrated via fluorescence recovery after photobleaching that one fraction of GFP–TRF2 is bound more tightly to the telomeres, whereas GFP–TRF1 and the majority of GFP–TRF2 exhibited fast-off kinetics ($<$10 s) in live cells (40), a surprising result given the prevailing notion that TRF1 and TRF2 tightly bind to telomeres. This tightly bound TRF2 fraction may represent the six-protein complex, which may be stabilized by TPP1–TIN2 interaction. Finally, in TRF1-knockout mouse ES cells, TRF2 telomere localization was also impaired (37). This observation suggests that TRF2 requires TRF1 for stable telomere association and supports the model that the six-protein complex is one of the functional complexes that regulate telomere localization of multiple telomeric proteins.

What is the functional significance of TPP1–TIN2-mediated six-protein complex assembly? We would like to propose the following model (Fig. 5*d*). TRF2 and RAP1 form a stable subcomplex that weakly associates with TIN2. TRF1 and TIN2 are in a different stable subcomplex that does not interact with TRF2. Through direct interaction with TIN2, TPP1 promotes TIN2–TRF2 binding and stimulates TRF1–TIN2–TRF2 connectivity. This network of interactions ensures proper targeting of the business end of the six-protein complex, POT1, and allows the regulation of telomere length and end-capping. TPP1 may have additional function, such as modulating the stability of TRF2. It is clear, however, that the ability of TPP1 to bind TIN2 and promote TRF1–TIN2–TRF2 complex formation is an essential function of TPP1. The TPP1–TIN2 interaction has a two-pronged effect: telomeric targeting of POT1 and signaling for high-order telomeric complex assembly. This model predicts that perturbations in the six-protein complex and its components would result in the disruption of telomere maintenance. Indeed, knockdown or inactivation of any of the six telomeric proteins, including TPP1 (15, 30, 34, 41), led to misregulated telomere length and/or telomere end protection. The six-protein complex thus forms the basic platform on which layers of telomere signaling networks can be assembled into the telomere interactome (32) for the proper protection and maintenance of mammalian telomeres.

Materials and Methods

Expression Constructs and Antibodies. For generating stable cell lines, singly or doubly FLAG-tagged full-length human TPP1 and its deletion mutants TPP1ΔC22 (residues 1–522) and TPP1ΔC (residues 1–337) were cloned into a pBabe-based retroviral vector. For expression in 293T cells, full-length POT1, TPP1, RAP1, TIN2, TRF1, or TRF2 were either cloned into the pCL vector (FLAG-tagged) or TOPO-cloned into pcDNA3.1 or pcDNA3.1-C-GFP (Invitrogen, Carlsbad, CA) to generate V5- or GFP-tagged fusion proteins. For insect cell expression, His-TPP1, His-TIN2, or His-TRF2 baculoviruses were produced by using the Blue-Bac baculovirus kit (Invitrogen).

The following antibodies were used: anti-V5 and anti-GFP (ChemiCON, Temecula, CA); anti-histone H1 (a generous gift from Estela Medrano, Baylor College of Medicine, Houston, TX); anti-FLAG M2 (Sigma, Lenexa, KS); anti-TRF2 (CalBiochem, San Diego, CA); anti-hRAP1 (30); anti-TIN2 and anti-TPP1 (9); goat anti-TRF1 (Bethyl Laboratories, Montgomery, TX); and anti-TRF1 (17) and POT1 (12) (gifts from Titia de Lange, The Rockefeller University, New York, NY). Anti-FLAG M2 antibody agarose beads (Sigma) and HRP-conjugated anti-V5 antibody (Bethyl Laboratories) also was used for immunoprecipitation and Western blotting, respectively.

Immunoprecipitation, Western Blot, and Immunofluorescence. For six-protein complex reconstitution and interaction studies, 293T or HT1080 cells were cotransfected with plasmids encoding various telomeric proteins in different combinations. At 48 h after transfection, the cells were harvested and extracted with a high-salt-concentration buffer (20 mM Hepes, pH 7.9/420 mM KCl/0.1 mM EDTA/5 mM $MgCl_2$/0.2%Nonidet P-40/1 mM DTT/0.2 mM PMSF/25% glycerol) (12). The extracts were then dialyzed in a low-concentration salt buffer (20 mM Hepes, pH 7.9/100 mM KCl/0.1 mM EDTA/1 mM DTT/0.5 mM PMSF/25% glycerol) (12). Subsequent immunoprecipitation and Western blotting with appropriate antibodies were carried out as previously described (9).

Indirect immunofluorescence was performed as described previously (30). FLAG-tagged proteins and endogenous TRF2 (an indicator of telomere localization) were detected with anti-FLAG and anti-TRF2 antibodies followed by secondary antibodies. Fluorescence microscopy was performed on a Nikon (Melville, NY) TE200 microscope equipped with a Coolsnap-fx charge-coupled device camera.

Fractionation of Telomere-Associated Complexes. Chromatographic experiments were performed as previously described (9). Briefly, HeLa cell nuclear extracts were fractionated on an AKTA DEAE-Sepharose ion-exchange column (Amersham Pharmacia, Pittsburgh, PA) equilibrated with buffer A (50 mM Hepes, pH 7.5/0.2 mM EDTA/0.5 mM DTT/0.2 mM PMSF/5% glycerol) containing 100 mM KCl. Bound proteins were step-eluted with increasing concentrations of KCl (200–1,000 mM) in buffer A. The fractions from this column were then loaded on a Superose 6 HR 10/30 gel filtration column. The resulting fractions from the DEAE or gel filtration column were resolved by SDS/PAGE and probed with various antibodies as appropriate.

Binding Assays Using Insect Cell Expression Systems. Sf9 cells ($\approx 5 \times 10^6$) were coinfected with His-TRF2, His-TIN2, and increasing amounts of His-TPP1 baculoviruses. At 3 days after infection, the cells were collected, lysed in 1× NETN buffer (20 mM Tris, pH 8/1 mM EDTA/90 mM NaCl/0.5% NP-40), and incubated with anti-TRF2 antibody (ChemiCON) (3.5 μg) followed by protein G agarose beads (Santa Cruz Biotechnology, Santa Cruz, CA) for 2 h at 4°C. Cells not infected with His-TRF2 were used controls. The eluted proteins were resolved by SDS/PAGE and blotted with anti-TIN2 antibodies.

RNAi Knockdown of TPP1. To analyze the effects of TPP1 knockdown, we designed a vector system (pRetro-dual) based on the dual-promoter RNAi approach (42). Briefly, TPP1-specific RNAi oligos were cloned between the head-to-head positioned U6 and H1 promoters. This dual promoter RNAi cassette is then cloned into the 3′ ΔLTR (with the enhancer deleted) of the retroviral vector. After retroviral infection, two copies of the RNAi cassette will be integrated into the target genome, resulting in more efficient RNAi. The vector also contains a puromycin-resistance marker for the establishment of stable cells. These RNAi vectors also are suitable for transient transfection experiments.

The pRetro-dual vectors require shorter and fewer DNA oligo sequences. To identify the optimal knockdown sequences for TPP1, several vectors that cover different regions of the target gene were constructed. Of these constructs, we found three vectors (oligo 1, 5′-GACGTCAAAAACCAAGACTTAGATGTTCAGAATTTTTAGATCT-3′; oligo 3, 5′-GACGTCAAAAACTCTGAGAATGACCAGCTAATTTTTTAGATCT-3′, and oligo 7, 5′-AAAAAGTGGTACCAGCATCAGCCTTTTTTTTAGATCT-3′) that significantly reduced TPP1 expression. HT1080 cells were transfected with the various siTPP1 constructs and assayed in immunoprecipitation experiments 72 h after transfection.

Telomere Restriction Fragment Assay. HT1080 cells were infected with retroviruses encoding various TPP1 proteins. Puromycin was added to the culture media for 3 days. The surviving cells were subsequently maintained as a pool without clonal selection (at which point designated as P0), passaged, and collected at various time points. The telomere restriction fragment assay was performed as previously described (17). The data were then analyzed by using a PhosphorImager (Amersham Pharmacia) and the Telorun analysis tool (43).

We thank Dr. Doug Chan and Hunter Richards, Andrew Laegeler, and Yiying Xie for technical help. This work was supported by the National Institutes of Health (Z.S.), the Department of Defense, the American Cancer Society, and the Welch Foundation.

1. Blackburn, E. H. (2001) *Cell* **106,** 661–673.
2. Wright, W. E. & Shay, J. W. (2001) *Curr. Opin. Genet. Dev.* **11,** 98–103.
3. de Lange, T. (2002) *Oncogene* **21,** 532–540.
4. Kim, S. H., Kaminker, P. & Campisi, J. (2002) *Oncogene* **21,** 503–511.
5. Maser, R. S. & DePinho, R. A. (2002) *Science* **297,** 565–569.
6. Wong, J. M. & Collins, K. (2003) *Lancet* **362,** 983–988.
7. Baumann, P. & Cech, T. R. (2001) *Science* **292,** 1171–1175.
8. Loayza, D., Parsons, H., Donigian, J., Hoke, K. & de Lange, T. (2004) *J. Biol. Chem.* **279,** 13241–13248.
9. Liu, D., Safari, A., O'Connor, M. S., Chan, D. W., Laegeler, A., Qin, J. & Songyang, Z. (2004) *Nat. Cell Biol.* **6,** 673–680.
10. Lei, M., Baumann, P. & Cech, T. R. (2002) *Biochemistry* **41,** 14560–14568.
11. Lei, M., Podell, E. R. & Cech, T. R. (2004) *Nat. Struct. Mol. Biol.* **11,** 1223–1229.
12. Loayza, D. & de Lange, T. (2003) *Nature* **424,** 1013–1018.
13. Colgin, L. M., Baran, K., Baumann, P., Cech, T. R. & Reddel, R. R. (2003) *Curr. Biol.* **13,** 942–946.
14. Kelleher, C., Kurth, I. & Lingner, J. (2005) *Mol. Cell. Biol.* **25,** 808–818.
15. Ye, J. Z., Hockemeyer, D., Krutchinsky, A. N., Loayza, D., Hooper, S. M., Chait, B. T. & de Lange, T. (2004) *Genes Dev.* **18,** 1649–1654.
16. Houghtaling, B. R., Cuttonaro, L., Chang, W. & Smith, S. (2004) *Curr. Biol.* **14,** 1621–1631.
17. van Steensel, B. & de Lange, T. (1997) *Nature* **385,** 740–743.
18. Kim, S. H., Kaminker, P. & Campisi, J. (1999) *Nat. Genet.* **23,** 405–412.
19. Smith, S. & de Lange, T. (2000) *Curr. Biol.* **10,** 1299–1302.
20. Smogorzewska, A., van Steensel, B., Bianchi, A., Oelmann, S., Schaefer, M. R., Schnapp, G. & de Lange, T. (2000) *Mol. Cell. Biol.* **20,** 1659–1668.
21. Smith, S., Giriat, I., Schmitt, A. & de Lange, T. (1998) *Science* **282,** 1484–1487.
22. Zhou, X. Z. & Lu, K. P. (2001) *Cell* **107,** 347–359.
23. Cong, Y. S., Wright, W. E. & Shay, J. W. (2002) *Microbiol. Mol. Biol. Rev.* **66,** 407–425.
24. Lillard-Wetherell, K., Machwe, A., Langland, G. T., Combs, K. A., Behbehani, G. K., Schonberg, S. A., German, J., Turchi, J. J., Orren, D. K. & Groden, J. (2004) *Hum. Mol. Genet.* **13,** 1919–1932.
25. Li, B., Oestreich, S. & de Lange, T. (2000) *Cell* **101,** 471–483.
26. Zhu, X. D., Kuster, B., Mann, M., Petrini, J. H. & de Lange, T. (2000) *Nat. Genet.* **25,** 347–352.
27. Stavropoulos, D. J., Bradshaw, P. S., Li, X., Pasic, I., Truong, K., Ikura, M., Ungrin, M. & Meyn, M. S. (2002) *Hum. Mol. Genet.* **11,** 3135–3144.
28. Opresko, P. L., von Kobbe, C., Laine, J. P., Harrigan, J., Hickson, I. D. & Bohr, V. A. (2002) *J. Biol. Chem.* **277,** 41110–41119.
29. Zhu, X. D., Niedernhofer, L., Kuster, B., Mann, M., Hoeijmakers, J. H. & de Lange, T. (2003) *Mol. Cell.* **12,** 1489–1498.
30. O'Connor, M. S., Safari, A., Liu, D., Qin, J. & Songyang, Z. (2004) *J. Biol. Chem.* **279,** 28585–28591.
31. Opresko, P. L., Otterlei, M., Graakjaer, J., Bruheim, P., Dawut, L., Kolvraa, S., May, A., Seidman, M. M. & Bohr, V. A. (2004) *Mol. Cell* **14,** 763–774.
32. Songyang, Z. & Liu, D. (2006) *Crit. Rev. Eukaryotic Gene Expression* **16,** 103–118.
33. Kim, S. H., Beausejour, C., Davalos, A. R., Kaminker, P., Heo, S. J. & Campisi, J. (2004) *J. Biol. Chem.* **279,** 43799–43804.
34. Ye, J. Z., Donigian, J. R., Van Overbeek, M., Loayza, D., Luo, Y., Krutchinsky, A. N., Chait, B. T. & De Lange, T. (2004) *J. Biol. Chem.* **279,** 47264–47271.
35. Liu, D., O'Connor, M. S., Qin, J. & Songyang, Z. (2004) *J. Biol. Chem.* **279,** 51338–51342.
36. de Lange, T. (2005) *Genes Dev.* **19,** 2100–2110.
37. Iwano, T., Tachibana, M., Reth, M. & Shinkai, Y. (2003) *J. Biol. Chem.* **14,** 14.
38. Wright, J. H., Gottschling, D. E. & Zakian, V. A. (1992) *Genes Dev.* **6,** 197–210.
39. Kim, S. H., Han, S., You, Y. H., Chen, D. J. & Campisi, J. (2003) *EMBO Rep* **4,** 685–691.
40. Mattern, K. A., Swiggers, S. J., Nigg, A. L., Lowenberg, B., Houtsmuller, A. B. & Zijlmans, J. M. (2004) *Mol. Cell. Biol.* **24,** 5587–5594.
41. Ye, J. Z. & de Lange, T. (2004) *Nat. Genet.* **36,** 618–623.
42. Zheng, L., Liu, J., Batalov, S., Zhou, D., Orth, A., Ding, S. & Schultz, P. G. (2004) *Proc. Natl. Acad. Sci. USA* **101,** 135–140.
43. Ouellette, M. M., Liao, M., Herbert, B. S., Johnson, M., Holt, S. E., Liss, H. S., Shay, J. W. & Wright, W. E. (2000) *J. Biol. Chem.* **275,** 10072–10076.
44. Bianchi, A., Smith, S., Chong, L., Elias, P. & de Lange, T. (1997) *EMBO J.* **16,** 1785–1794.
45. Broccoli, D., Smogorzewska, A., Chong, L. & de Lange, T. (1997) *Nat. Genet.* **17,** 231–235.
46. Yang, Q., Zheng, Y. L. & Harris, C. C. (2005) *Mol. Cell. Biol.* **25,** 1070–1080.

LETTERS

TPP1 is a homologue of ciliate TEBP-β and interacts with POT1 to recruit telomerase

Huawei Xin[1], Dan Liu[1], Ma Wan[1], Amin Safari[1], Hyeung Kim[1], Wen Sun[1], Matthew S. O'Connor[1] & Zhou Songyang[1]

Telomere dysfunction may result in chromosomal abnormalities, DNA damage responses, and even cancer[1]. Early studies in lower organisms have helped to establish the crucial role of telomerase and telomeric proteins in maintaining telomere length and protecting telomere ends[2–7]. In *Oxytricha nova*, telomere G-overhangs are protected by the TEBP-α/β heterodimer[3,4]. Human telomeres contain duplex telomeric repeats with 3′ single-stranded G-overhangs, and may fold into a t-loop structure that helps to shield them from being recognized as DNA breaks[8,9]. Additionally, the TEBP-α homologue, POT1, which binds telomeric single-stranded DNA (ssDNA)[10], associates with multiple telomeric proteins (for example, TPP1, TIN2, TRF1, TRF2 and RAP1) to form the six-protein telosome/shelterin[11,12] and other subcomplexes. These telomeric protein complexes in turn interact with diverse pathways to form the telomere interactome[13] for telomere maintenance. However, the mechanisms by which the POT1-containing telosome communicates with telomerase to regulate telomeres remain to be elucidated. Here we demonstrate that TPP1 is a putative mammalian homologue of TEBP-β and contains a predicted amino-terminal oligonucleotide/oligosaccharide binding (OB) fold. TPP1–POT1 association enhanced POT1 affinity for telomeric ssDNA. In addition, the TPP1 OB fold, as well as POT1–TPP1 binding, seemed critical for POT1-mediated telomere-length control and telomere-end protection in human cells. Disruption of POT1–TPP1 interaction by dominant negative TPP1 expression or RNA interference (RNAi) resulted in telomere-length alteration and DNA damage responses. Furthermore, we offer evidence that TPP1 associates with the telomerase in a TPP1-OB-fold-dependent manner, providing a physical link between telomerase and the telosome/shelterin complex. Our findings highlight the critical role of TPP1 in telomere maintenance, and support a yin–yang model in which TPP1 and POT1 function as a unit to protect human telomeres, by both positively and negatively regulating telomerase access to telomere DNA.

It is unknown whether heterodimers that are similar to ciliate TEBP-α/β are used in other species for telomere-end maintenance. TEBP-α homologues include mammalian POT1 and *Saccharomyces cerevisiae* Cdc13, which contain OB folds and function in telomere-capping control by directly binding to telomeric ssDNA[4,10,14]. However, no mammalian TEBP-β homologues have been identified. We recently cloned the human telomeric protein TPP1 and showed direct interactions between human TPP1 and human POT1 (refs 15, 16). Given that POT1 is a TEBP-α homologue, we predicted that TPP1 might function as the mammalian homologue of TEBP-β. Secondary-structure analyses suggest the presence of a potential OB fold within TPP1 (residues 87–240; Fig. 1a; Supplementary Fig. 2a). In addition, three-dimensional position-specific scoring matrix threading analysis predicted that the TPP1 N terminus (residues 87–316) is most similar to the N-terminal core domain of TEBP-β

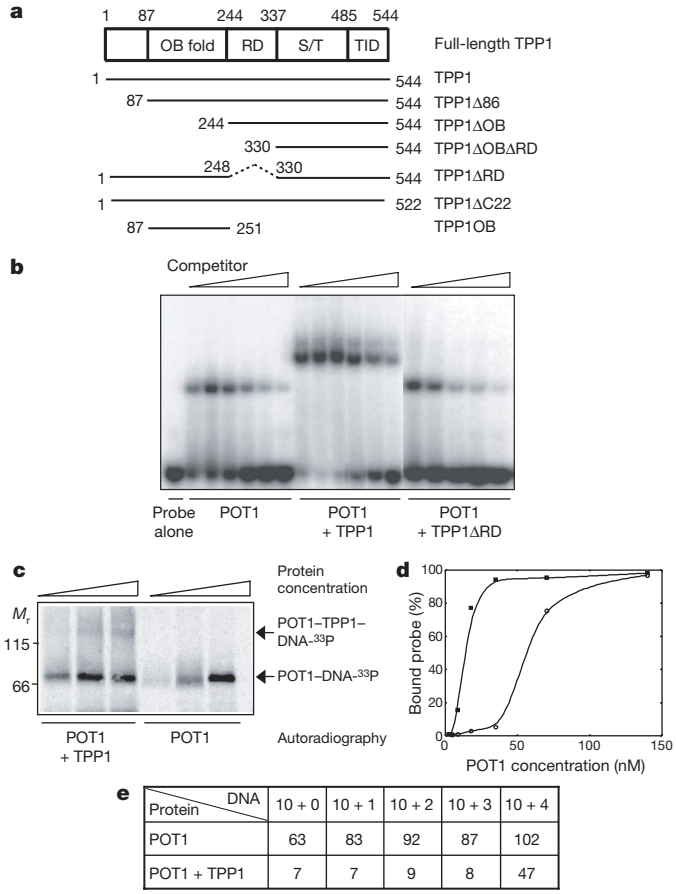

e

Protein \ DNA	10 + 0	10 + 1	10 + 2	10 + 3	10 + 4
POT1	63	83	92	87	102
POT1 + TPP1	7	7	9	8	47

Figure 1 | TPP1 is a homologue of ciliate TEBP-β that interacts with POT1 to bind ssDNA. a, TPP1 domain organization and TPP1-deletion mutants. RD, POT1-recruitment domain. S/T, Ser-rich region. TID, TIN2-interacting domain. **b**, Flag-tagged POT1 alone, or co-purified with wild-type TPP1 or TPP1ΔRD from 293T cells, were tested for their binding to the radiolabelled probe 49T3. Increasing amounts of non-radiolabelled 49T3 competitors (0, 30, 60, 120, 240 and 480 nM) were also added. **c**, POT1, TPP1 and telomere DNA form a ternary complex. Increasing amounts of insect-cell-purified POT1 (35, 70 and 140 nM), or TPP1 plus POT1 (17.5, 35 and 70 nM) were incubated with the ^{33}P-labelled oligonucleotide 10 + 0 (TTACGGTTAGGGTTAG). The reactions were then treated with UV and glutaraldehyde to cross-link DNA to proteins, followed by SDS–PAGE and autoradiography. **d**, TPP1 enhances POT1 DNA-binding affinity. EMSA was performed using the radiolabelled oligonucleotide 10 + 0 (15 nM) and 2-fold dilutions (from 140 nM) of POT1 (open circles) or POT1 plus TPP1 (filled squares). **e**, Estimated K_d (nM) of POT1 and POT1–TPP1 to G-strand oligonucleotides with different 3′-end nucleotides.

[1]Verna and Marrs McLean Department of Biochemistry and Molecular Biology, Baylor College of Medicine, One Baylor Plaza, Houston, Texas 77030, USA.

©2007 Nature Publishing Group

(ref. 17; Supplementary Fig. 2b). TEBP-α contains three OB folds, the first two are involved in ssDNA recognition whereas the third one interacts with TEBP-β (ref. 17). Interestingly, we found that POT1 probably harbours a third OB fold as well (in its PTOP/TPP1-binding region—PBR—domain, which associates with TPP1; data not shown). These observations suggest evolutionarily conserved interaction motifs between TEBP-α/β and POT1–TPP1, and that TPP1 is a putative homologue of TEBP-β.

Next, we tested whether TPP1, similar to TEBP-β (ref. 4), could cooperate with POT1 in recognizing telomeric ssDNA. Although TPP1 exhibited little or no telomere ssDNA-binding activities in gel-shift experiments (Supplementary Fig. 2c) as was reported for TEBP-β (ref. 4), the addition of TPP1 to POT1 oligonucleotide-binding reactions resulted in super-shifted probes compared with POT1 alone, implying the formation of a POT1–TPP1–DNA complex (Fig. 1b). Deletion of the POT1-binding recruitment domain (RD) of TPP1 (TPP1ΔRD) abolished the super-shift, suggesting that direct POT1–TPP1 interaction is required for POT1–TPP1–DNA complex formation. Further support for the ternary complex came from antibody super-shift experiments (Supplementary Fig. 2c), and from cross-linking experiments in which radio-labelled telomere ssDNA could be cross-linked with insect-cell-purified POT1 and TPP1 (Fig. 1c).

Compared with POT1 alone, POT1–TPP1 together exhibited a ~9-fold increase in affinity (7 nM versus 63 nM) for the oligonucleotide that contains the decamer core recognized by POT1 (TTACGGTTAGGGTTAG, 10 + 0) (Fig. 1d, e; Supplementary Fig. 2d, e). Notably, POT1–TPP1 also had much higher affinity (compared with POT1 alone) towards core telomere repeats containing 3′ nucleotide extensions (for example, TTAGGGTTAGGG, 10 + 2) (Fig. 1e)[18]. In fact, TPP1 enhanced the affinity of POT1 to a number of the telomere oligonucleotides tested (Fig. 1e), emphasizing the biochemical and structural similarities between TEBP-α/β and POT1–TPP1, and indicating that TPP1 is indeed a TEBP-β homologue.

TPP1 binds and targets POT1 to telomeres through the TPP1 RD domain and the POT1 PBR domain[15]. POT1 may also be recruited to telomeres through its interaction with TRF2 (ref. 19), or through its two N-terminal OB folds[18]. To examine the role of POT1 N-terminal

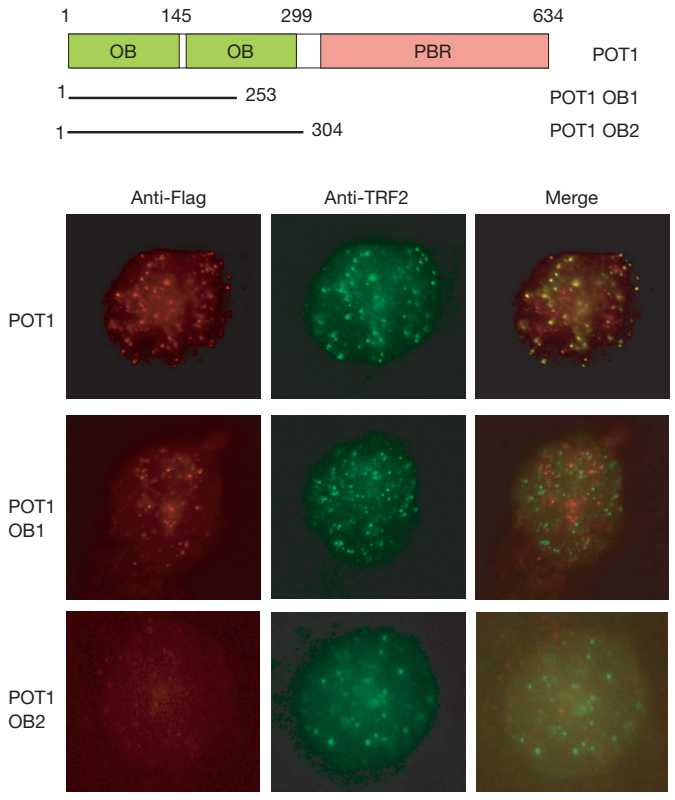

Figure 2 | POT1 telomeric targeting depends on POT1–TPP1 interaction. Immunostaining analysis of Flag-tagged POT1, POT1 OB1, or POT1 OB2 using polyclonal anti-Flag (red) and anti-TRF2 antibodies (green). PBR, TPP1-binding region.

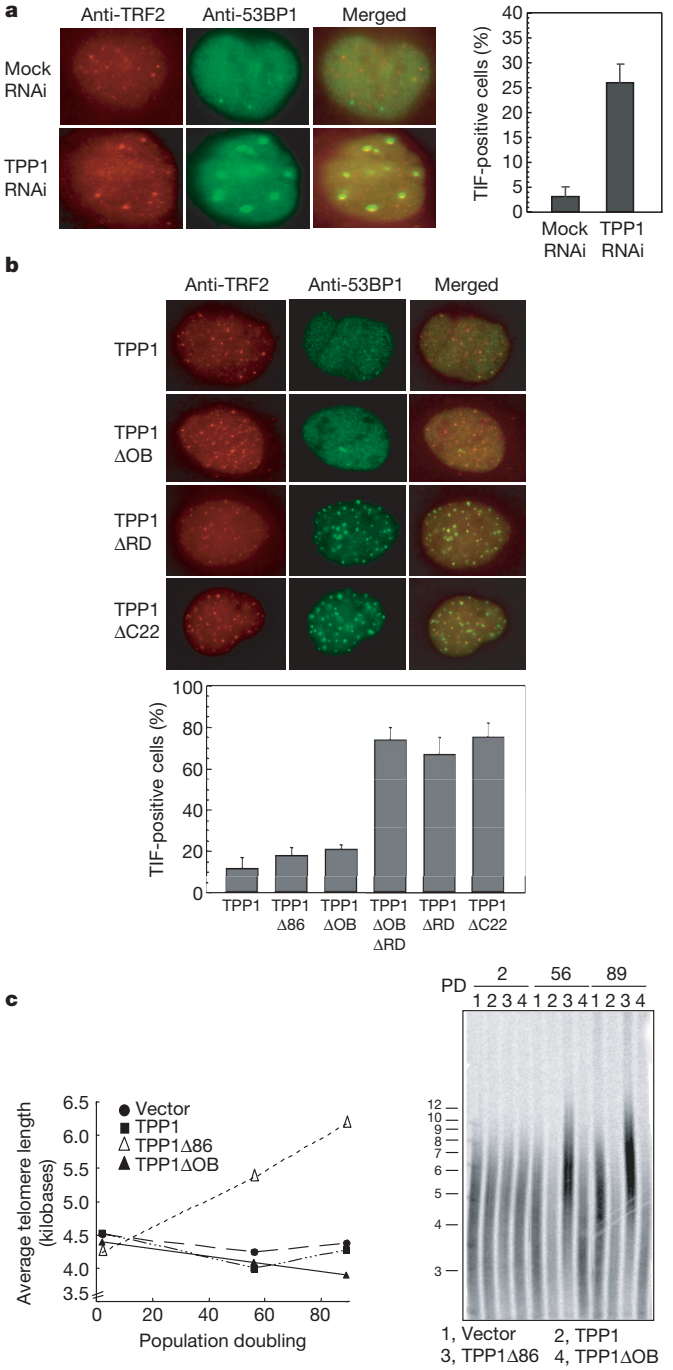

Figure 3 | The TPP1 OB fold and TPP1–POT1 interaction are important for telomere-end protection and -length control. a, TPP1 knockdown results in TIF. HTC75 cells stably expressing TPP1 shRNA sequences were immunostained (left panel) with anti-53BP1 (green) and TRF2 (red) antibodies and quantified (right panel). Error bars indicate s.e.m. ($n > 4$). **b**, TIF analysis of HTC75 cells expressing full-length or truncated TPP1 (top panel) and quantification (bottom panel). Error bars indicate s.e.m. ($n \geq 4$). **c**, HTC75 cells expressing full-length or N-terminally truncated TPP1 were subjected to Telomere Restriction Fragment analysis as previously described[15] (left panel). Right panel, Southern hybridization blot showing telomere length. PD, population doubling.

©2007 Nature Publishing Group

OB folds in telomere targeting, we analysed the localization of POT1 PBR-deletion mutants that contained only the first (POT1 OB1) or both (POT1 OB2) OB folds. Both POT1 mutants were defective in telomere localization as determined by indirect immunofluorescence (Fig. 2), and the ability of POT1 OB2 to chromatin-immunoprecipitate telomeric DNA was greatly reduced (>10-fold; Supplementary Fig. 3a), supporting the notion that the OB folds alone are insufficient for POT1 telomeric targeting. Furthermore, RNAi knockdown of TPP1 led to reduced telomere localization of endogenous POT1 (Supplementary Fig. 3c). Taken together, these data indicate that POT1 telomere targeting depends largely on its interaction with TPP1, and underlines the critical role of the POT1–TPP1 complex in telomere maintenance.

Disruption of the POT1–TPP1 interaction may lead to deprotected telomere ends and Telomere Dysfunction Induced Foci (TIF; for example, 53BP1 telomeric foci)[20–23]. Indeed, RNAi knockdown of TPP1 resulted in a ~20% increase in TIF-positive cells (Fig. 3a). Furthermore, in cells expressing TPP1ΔRD or TPP1ΔC22 (a TIN2-interacting domain (TID) mutant that should compromise the telomeric association of endogenous POT1–TPP1)[24], TIFs were readily detectable in >70% of the cells (Fig. 3b), whereas TPP1Δ86 and TPP1ΔOB expressing cells were similar to TPP1 cells (Fig. 3b; Supplementary Fig. 4). Given that both TPP1Δ86 and TPP1ΔOB contain intact RD and TID domains (Fig. 1a), these observations imply that the TPP1 RD domain may be more critical than the OB fold in POT1 telomere targeting and POT1-mediated end protection *in vivo*. For POT1-mediated length control, we have shown previously that the PBR-only mutant of POT1 (POT1 PBR) can act as a dominant negative form to elongate telomeres[15]. The interaction of POT1 PBR with TPP1 seems necessary for its telomere elongation phenotype, because mutations in the PBR region that disrupted the TPP1–POT1 PBR interaction[15] resulted in a failure of these mutants to extend telomeres (Supplementary Fig. 5). These results reaffirm the notion that TPP1 binding is required for POT1-mediated telomere-length control. Taken together, our data establish that the interaction between POT1 and TPP1 serves to modulate POT1 function at the telomeres, and that POT1 and TPP1 together function as a unit in end protection and length control of telomeres.

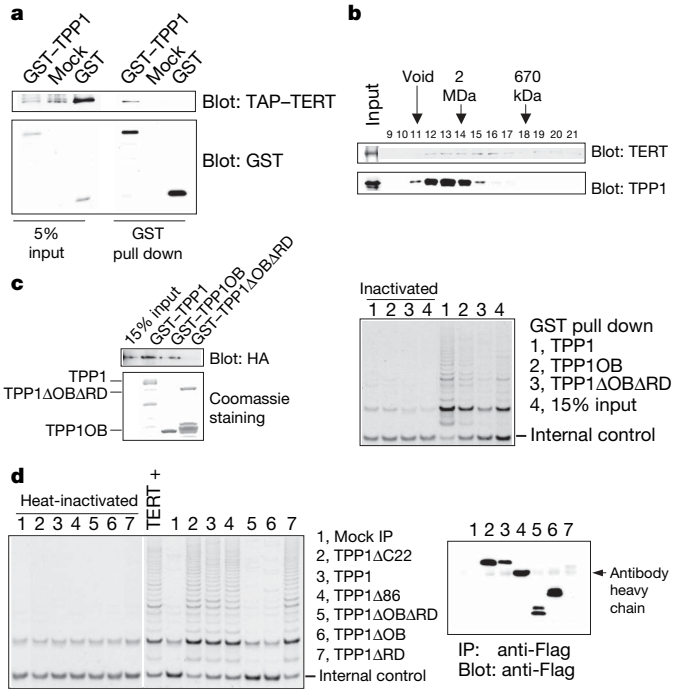

Figure 4 | The TPP1 OB fold is important for recruitment of telomerase activity. a, 293T cells transiently expressing TAP–TERT alone (mock), with GST, or with GST–TPP1 were harvested, lysed and incubated with glutathione beads. The precipitates were resolved by SDS–PAGE and blotted with peroxidase-anti-peroxidase (PAP; for protein A on the TAP-tag) or anti-GST–HRP. **b**, Nuclear extracts from HeLa cells expressing TAP–TERT were fractionated, resolved by SDS–PAGE and probed with PAP and anti-TPP1 antibody[15]. **c**, TPP1 interacts with telomerase *in vitro*. *In vitro*-translated HA–TERT/TR was immunoprecipitated with anti-HA agarose beads and eluted with HA peptides (Sigma)[30]. GST-tagged TPP1, TPP1OB and TPP1ΔOBΔRD, were then used to pull down HA–TERT/TR, followed by SDS–PAGE and blotting with anti-HA antibodies (left panel) or TRAP assays (right panel). Samples were also heat-inactivated for negative controls. **d**, Anti-Flag immunoprecipitates from HTC75 cells expressing Flag-tagged TPP1 mutants were eluted with Flag peptides for TRAP assays (left panel), or probed with anti-Flag antibodies (right panel). Samples were also heat-inactivated for negative controls. On the basis of serial dilutions and comparisons with the positive control (TERT +; ≈500 cells), we estimated TPP1 to bring down ~20% telomerase activity.

How does the POT1–TPP1 complex regulate telomere length? Both the RD and TID domains of TPP1 (Fig. 1a) are probably critical for this function because they are required for TPP1 and POT1 targeting[15,24,25]. Indeed, overexpression of the dominant negative mutant TPP1ΔRD led to dramatically extended telomeres (data not shown), as is the case for TPP1ΔC22 (ref. 24). These observations are consistent with the model where the six-protein complex may negatively regulate telomerase access by sequestering telomere ends[11,12]. Consequently, displacement of POT1 from telomeric ssDNA makes telomeres more accessible to the telomerase[26]. To determine whether the TPP1 OB fold has any role in telomere-length control, we examined HTC75 cells expressing TPP1 mutants with N-terminal deletions. All the TPP1 mutants examined in this study (except for TPP1ΔC22) were targeted to the telomeres (data not shown). As previously reported[15,16,25], full-length TPP1 expression had little effect on telomere length (Fig. 3c). Deletion of the first 86 amino acids (TPP1Δ86 with an intact OB fold) resulted in telomere lengthening, indicating a possible regulatory role for the first 86 amino acids (Fig. 3c). Interestingly, further deletion into the OB fold (TPP1ΔOB) abrogated the telomere elongation effect, indicating that the TPP1 OB fold may positively regulate telomere length by directly participating in telomerase recruitment.

We went on to test this hypothesis by investigating whether TPP1 could interact with the telomerase. In precipitation experiments using extracts from human cells expressing tandom affinity purification tag (TAP)–human Telomerase Reverse Transcriptase (TERT) and glutathione *S*-transferase (GST)–TPP1, we found TAP–TERT associated with GST–TPP1 (Fig. 4a). In addition, both TAP–TERT and endogenous TPP1 were eluted as a ~2 MDa complex by gel filtration (Fig. 4b). Furthermore, both full-length TPP1 and TPP1 OB fold (Fig. 1a), but not TPP1 ΔOBΔRD, were able to pull down *in vitro* translated haemagglutinin (HA)–TERT proteins as well as telomerase activity (Fig. 4c). These observations indicate that the putative TPP1 OB fold may be required for regulating telomerase recruitment. Consistent with this idea, whereas robust telomerase activity was detected in Flag–TPP1 immunoprecipitates from HT1080 cells, deletion of the putative TPP1 OB fold (TPP1ΔOB and TPP1ΔOBΔRD) led to a reduction (>5-fold) in associated telomerase activity (Fig. 4d). In contrast, the POT1-binding mutant TPP1ΔRD still retained the ability to associate with telomerase activity (Fig. 4d), suggesting that the TPP1 OB fold, but not POT1, participates in recruiting telomerase. Because TPP1 alone does not bind ssDNA, POT1 and TPP1 (as integral components of the telosome/shelterin) probably function together to positively recruit telomerase to telomeric ssDNA through the TPP1 OB fold, in addition to protecting telomere ends and negatively regulating telomerase access.

Our results underlined the evolutionarily conserved mechanism in telomere-end capping, where OB-fold-containing TEBP homologues work in concert to protect telomere overhangs. This mode of end protection is probably more widely used than previously thought, because TPP1 homologues are found in many of the vertebrate species examined. It is interesting to note that, unlike

©2007 Nature Publishing Group

TEBP-β (ref. 27), TPP1 does not seem to promote G-quadruplex formation *in vitro* (data not shown), suggesting a functional divergence in this respect. Most importantly, our findings suggest dual roles of the POT1–TPP1 complex in regulating telomerase access. The binding of the POT1–TPP1 complex to telomeric ssDNA serves to cap telomere ends and prevent telomerase access to the ssDNA template. Indeed, previous studies have demonstrated that expression of POT1-OB-fold-deletion mutants or the TPP1 RD domain alone extends telomeres[15,26]. However, POT1–TPP1 can also physically recruit the telomerase complex, perhaps to facilitate rapid telomere repair/extension during the cell cycle or in response to local telomere damage on POT1 disassociation (Supplementary Fig. 1)[28]. Notably, the TPP1 OB fold is at the centre of both processes. The yin–yang model of POT1–TPP1 function highlights the dynamic nature of telomere regulation, and the complexity of telomere maintenance pathways mediated by the telomerase together with telomere protein complexes within the telomere interactome.

METHODS

Oligonucleotides and vectors. Oligonucleotides used were: 49T3, AAGGATATGGCCACGGTGCGGACGGCACTG(TTAGGG)$_3$; 10 + 0, TTACGGTTAGGGTTAG; and 10 + 1 through 10 + 4 with increasing 3′ extensions of 10 + 0 (G, GG, GGT and GGTT).

Various TPP1, POT1, and TAP–TERT constructs were cloned into pcDNA3 or a Flag-tagged pBabe-based vector for transient or stable expression. POT1, TPP1 and TPP1 mutants were cloned into pGEX or the pFAST baculovirus vector system (Invitrogen) for insect cell or *Escherichia coli* expression. HA–TERT and TR plasmids are gifts from J. L. Chen (Arizona State University). For RNAi, a pRetro-dual vector or a retroviral shRNA vector expressing sequences from TPP1 siRNA Oligo 1 was used[24].

Protein expression and purification. Flag-tagged TPP1, POT1, TPP1 or TPP1ΔRD were expressed alone or together in 293T cells and purified using anti-Flag agarose beads (Sigma). GST–TPP1, GST–POT1, Flag–POT1 or GST–TPP1ΔOB were expressed alone or together in a baculovirus insect cell system (Invitrogen), purified using glutathione beads, and eluted with glutathione or cleaved from the N-terminal GST tag by the ProScission Protease (Amersham).

Electrophoretic Mobility Shift Assay (EMSA), antibody supershift and cross-linking. EMSA was performed as described previously[18]. For antibody supershift, the purified proteins were incubated first with either anti-GST or anti-Flag M2 antibodies followed by addition of radiolabelled DNA probes. For cross-linking, radiolabelled DNA and protein mixtures were cross-linked by ultraviolet (UV) radiation and then incubated with 0.004% glutaraldehyde for 60 min at room temperature[29].

Telomere Repeat Amplification Protocol (TRAP). Anti-Flag immunoprecipitates from wild-type- and mutant-TPP1-expressing HTC75 cells were eluted with Flag peptides (Sigma), diluted, and used for TRAP assays using a telomerase detection kit (Chemicon). *In vitro*, TPP1-associated telomerase activities were similarly assayed.

Chromatographic fractionation of telomere-associated complexes. Gel filtration experiments were performed as previously described[11] using nuclear extracts from TAP–TERT expressing HeLa cells, followed by SDS–polyacrylamide gel electrophoresis and western blotting. More detailed methodology and reagent information can be found in Supplementary Methods.

Received 24 August; accepted 20 November 2006.
Published online 21 January 2007.

1. Chadwick, D. J. & Cardew. G. (eds) *Telomeres and Telomerase* (John Wiley & Sons, Chichester, UK, 1997).
2. Gottschling, D. E. & Zakian, V. A. Telomere proteins: specific recognition and protection of the natural termini of *Oxytricha* macronuclear DNA. *Cell* **47,** 195–205 (1986).
3. Greider, C. W. & Blackburn, E. H. The telomere terminal transferase of *Tetrahymena* is a ribonucleoprotein enzyme with two kinds of primer specificity. *Cell* **51,** 887–898 (1987).
4. Gray, J. T., Celander, D. W., Price, C. M. & Cech, T. R. Cloning and expression of genes for the *Oxytricha* telomere-binding protein: specific subunit interactions in the telomeric complex. *Cell* **67,** 807–814 (1991).
5. Lingner, J. & Cech, T. R. Telomerase and chromosome end maintenance. *Curr. Opin. Genet. Dev.* **8,** 226–232 (1998).
6. Shore, D. Telomere length regulation: getting the measure of chromosome ends. *Biol. Chem.* **378,** 591–597 (1997).
7. Bertuch, A. A. & Lundblad, V. The maintenance and masking of chromosome termini. *Curr. Opin. Cell Biol.* **18,** 247–253 (2006).
8. Henderson, E., Hardin, C. C., Walk, S. K., Tinoco, I. Jr & Blackburn, E. H. Telomeric DNA oligonucleotides form novel intramolecular structures containing guanine–guanine base pairs. *Cell* **51,** 899–908 (1987).
9. Griffith, J. D. *et al.* Mammalian telomeres end in a large duplex loop. *Cell* **97,** 503–514 (1999).
10. Baumann, P. & Cech, T. R. Pot1, the putative telomere end-binding protein in fission yeast and humans. *Science* **292,** 1171–1175 (2001).
11. Liu, D., O'Connor, M. S., Qin, J. & Songyang, Z. Telosome, a mammalian telomere-associated complex formed by multiple telomeric proteins. *J. Biol. Chem.* **279,** 51338–51342 (2004); published online 20 September 2004.
12. de Lange, T. Shelterin: the protein complex that shapes and safeguards human telomeres. *Genes Dev.* **19,** 2100–2110 (2005).
13. Songyang, Z. & Liu, D. Inside the mammalian telomere interactome: regulation and regulatory activities of telomeres. *Crit. Rev. Eukaryot. Gene Expr.* **16,** 103–118 (2006).
14. Nugent, C. I., Hughes, T. R., Lue, N. F. & Lundblad, V. Cdc13p: a single-strand telomeric DNA-binding protein with a dual role in yeast telomere maintenance. *Science* **274,** 249–252 (1996).
15. Liu, D. *et al.* PTOP interacts with POT1 and regulates its localization to telomeres. *Nature Cell Biol.* **6,** 673–680 (2004); published online 6 June 2004.
16. Ye, J. Z. *et al.* POT1-interacting protein PIP1: a telomere length regulator that recruits POT1 to the TIN2/TRF1 complex. *Genes Dev.* **18,** 1649–1654 (2004); published online 1 July 2004.
17. Horvath, M. P., Schweiker, V. L., Bevilacqua, J. M., Ruggles, J. A. & Schultz, S. C. Crystal structure of the *Oxytricha nova* telomere end binding protein complexed with single strand DNA. *Cell* **95,** 963–974 (1998).
18. Lei, M., Podell, E. R. & Cech, T. R. Structure of human POT1 bound to telomeric single-stranded DNA provides a model for chromosome end-protection. *Nature Struct. Mol. Biol.* **11,** 1223–1229 (2004); published online 21 November 2004.
19. Yang, Q., Zheng, Y. L. & Harris, C. C. POT1 and TRF2 cooperate to maintain telomeric integrity. *Mol. Cell. Biol.* **25,** 1070–1080 (2005).
20. Takai, H., Smogorzewska, A. & de Lange, T. DNA damage foci at dysfunctional telomeres. *Curr. Biol.* **13,** 1549–1556 (2003).
21. d'Adda di Fagagna, F. *et al.* A DNA damage checkpoint response in telomere-initiated senescence. *Nature* **426,** 194–198 (2003); published online 13 November 2005.
22. Wu, L. *et al.* Pot1 deficiency initiates DNA damage checkpoint activation and aberrant homologous recombination at telomeres. *Cell* **126,** 49–62 (2006).
23. Hockemeyer, D., Daniels, J. P., Takai, H. & de Lange, T. Recent expansion of the telomeric complex in rodents: Two distinct POT1 proteins protect mouse telomeres. *Cell* **126,** 63–77 (2006).
24. O'Connor, M. S., Safari, A., Xin, H., Liu, D. & Songyang, Z. A critical role for TPP1 and TIN2 interaction in high-order telomeric complex assembly. *Proc. Natl Acad. Sci. USA* **103,** 11874–11879 (2006).
25. Houghtaling, B. R., Cuttonaro, L., Chang, W. & Smith, S. A dynamic molecular link between the telomere length regulator TRF1 and the chromosome end protector TRF2. *Curr. Biol.* **14,** 1621–1631 (2004).
26. Loayza, D. & De Lange, T. POT1 as a terminal transducer of TRF1 telomere length control. *Nature* **424,** 1013–1018 (2003).
27. Fang, G. & Cech, T. R. The β subunit of *Oxytricha* telomere-binding protein promotes G-quartet formation by telomeric DNA. *Cell* **74,** 875–885 (1993).
28. Verdun, R. E., Crabbe, L., Haggblom, C. & Karlseder, J. Functional human telomeres are recognized as DNA damage in G2 of the cell cycle. *Mol. Cell* **20,** 551–561 (2005).
29. Fang, G. & Cech, T. R. *Oxytricha* telomere-binding protein: DNA-dependent dimerization of the alpha and beta subunits. *Proc. Natl Acad. Sci. USA* **90,** 6056–6060 (1993).
30. Chen, J. L. & Greider, C. W. Determinants in mammalian telomerase RNA that mediate enzyme processivity and cross-species incompatibility. *EMBO J.* **22,** 304–314 (2003).

Supplementary Information is linked to the online version of the paper at www.nature.com/nature.

Acknowledgements We thank J. L. Chen for kindly providing the HA–TERT and hTR plasmids and we thank A. Laegeler, K. Huang and L.-Y. Chen for help. This work was supported by awards to Z.S. and D.L. from NIH, the Department of Defense, the American Cancer Society, and the American Heart Association. Z.S. is a Leukaemia and Lymphoma Society Scholar.

Author Information Reprints and permissions information is available at www.nature.com/reprints. The authors declare no competing financial interests. Correspondence and requests for materials should be addressed to Z.S. (songyang@bcm.tmc.edu).

©2007 Nature Publishing Group

[Frontiers in Bioscience 13, 5905-5915, May 1, 2008]

BRCT Domains: phosphopeptide binding and signaling modules

Maria C. Rodriguez, Zhou Songyang[1]

[1]*Verna and Marrs McLean Department of Biochemistry and Molecular Biology, Baylor College of Medicine, One Baylor Plaza, Houston, Texas 77030*

TABLE OF CONTENTS

1. Abstract
2. Introduction
3. BRCT domains as phosphopeptide interaction motifs
3.1. BRCA1
3.1.1. Phospho-dependent BRCA1 BRCT interacting proteins
3.1.1.1. BACH1
3.1.1.2. CtIP
3.1.1.3. Acetyl-CoA carboxylase
3.1.1.4. Abraxas/CCDC98 and RAP80
3.2. MDC1
3.3. PTIP
3.4. MCPH1
4. Cancer-associated BRCA1 mutations
5. Structural basis for phosphopeptide recognition
5.1. Structures of the BRCA1/BACH1 and MDC1/H2AX phosphopeptide complexes
6. Predictions for phosphopeptide recognition by BRCT domains
6.1. Candidate phosphopeptide binding BRCT domains in human cells
6.2. Potential in vivo sites for human BRCT domains
7. Conclusions and perspectives
8. Acknowledgements
9. References

1. ABSTRACT

The *BR*CA1 *C*-*t*erminus (BRCT) domains are essential for the tumor suppressor function of BRCA1, and have been found in a variety of proteins from bacteria to men. Recent studies demonstrate that the BRCT domain constitutes a novel phosphopeptide binding region. In this review we seek to discuss the recent biochemical and structural data that have helped elucidate the molecular basis of BRCT domain function and BRCT-mediated interactions, with special emphasis on the role of phospho-specific interactions in key networks that regulate DNA repair. Finally we offer predictions on additional phospho-interacting BRCT domains and potential *in vivo* binding sites for several BRCT domains.

2. INTRODUCTION

The cloning of BRCA1 and the subsequent genetic, biochemical, and cellular studies of this familial breast and ovarian cancer susceptibility gene have implicated BRCA1 in regulating important nuclear functions such as transcription, recombination, DNA repair, and checkpoint response (1-11). Mutations in the BRCA1 gene account for approximately 80-90% of all hereditary breast cancers (12). BRCA1 consists of an N-terminal RING domain and a C-terminal region comprised of two tandem BRCT domains (amino acids 1649-1859) (6,9). Most cancer-causing BRCA1 mutations result in truncated BRCA1 gene products that lack one or both BRCT domains. In addition, cancer-associated missense

mutations in the BRCA1 BRCT domains have been shown to sensitize cells to a variety of DNA damaging agents, and to specifically disrupt the G2/M cell cycle checkpoint (13,14). Furthermore, experimental data support an essential role for the BRCT domains in regulating DNA repair and binding, cell cycle, and gene expression (15-21). These findings, together with the observation that deletion of the BRCA1 BRCT repeats led to tumor development in mice (22), demonstrate that BRCT repeats play a central role in BRCA1-mediated tumor suppressor function.

Careful bioinformatic and biochemical studies have revealed the presence of BRCT repeats in a diverse array of proteins, particularly in those involved in DNA damage responses. Examples include DNA damage response or repair and cell cycle checkpoint proteins (e.g., BRCA1, MDC1, 53BP1, NBS1, and XRCC1), oncoprotein ECT2, BARD1, and the PAX transcription-activation domain-interacting protein PTIP (1,10,11). Individual BRCT repeats (~90-100 amino acids in length) are capable of folding independently, but often exist in tandem pairs separated by regions of various sizes.

It is particularly interesting to note the presence of BRCT domains in prokaryotes as well as viruses (1,23). For example, single BRCT domains have been found in bacterial DNA ligases, raising tantalizing possibilities about the evolutionary origin of BRCT domains. Perhaps the sequences and complexity of the BRCT domains have evolved over time to accommodate their increasingly complex and indispensable roles in higher organisms.

3. BRCT DOMAINS AS PHOSPHOPEPTIDE INTERACTION MOTIFS

While BRCT domains can interact with each other, as in the case of XRCC1 and DNA ligase III that interact through their respective BRCT domains (24), the most common type of BRCT-mediated interactions occurs between the BRCT domain and a non-BRCT partner (25,26). Besides BRCA1, the BRCT domains of several other proteins such as 53BP1, DNA ligase IV, and XRCC1 have also been shown to mediate phospho-independent protein-protein interactions (28-31). In addition, BRCT domains can also mediate protein-DNA interactions. For example, several of the ToPBP1 BRCT domains have been demonstrated to bind both single and double stranded DNA fragments in a sequence independent manner (32).

The activities of protein kinases and phosphatases are often modulated in response to cues such as cell cycle or DNA damage, which in turn controls the dynamics of protein complex formation. Phosphorylation and dephosphorylation are mediated through the opposing activities of these enzymes thereby regulating the signals that are relayed through phosphorylation-dependent protein-protein interactions. Recent work from several laboratories has indicated that BRCT repeats can also function as phosphopeptide-binding modules, shedding new light on how signals may be transduced from protein kinases through BRCT containing proteins (13,14,33). These findings provide a unique opportunity to understand how BRCT-containing proteins may be coupled to different downstream signaling pathways in a regulated manner. We will discuss in more detail phospho-specific interactions mediated through BRCT domains.

3.1. BRCA1

The first indication of BRCT domain involvement in phospho-dependent protein-protein interactions emerged from studies in *Saccharomyces cerevisiae* with the cell cycle protein RAD9. RAD9 was shown to homo-oligomerize preferentially with hyperphosphorylated RAD9 via its C-terminal BRCT domains (34). Recently, studies from three groups have demonstrated that BRCT domains can indeed function as phospho-interacting modules (13,14,33). Yu *et al* showed that BRCA1 BRCT could interact with phosphorylated BACH1 (BRCA1-Associated Carboxyl-terminal helicase) (33). The binding was mapped specifically to Ser990 on BACH1, and this interaction was required for DNA damage-induced checkpoint function during G2/M phase transition. Using an oriented peptide library analysis, Rodriguez *et al* arrived at similar conclusions and found that BRCA1 BRCT domains preferred a phosphoserine-aromatic-hydrophobic-Phe/Tyr motif (14). The selection for Phe was remarkably strong at the P+3 position (13,14). Notably, the region surrounding Ser990 in BACH1 matches very well with this predicted motif. Furthermore, substitution with amino acids other than Phe at the P+3 position abolished BRCA1 BRCT interaction and resulted in G2/M checkpoint defect (14,33). ATM/ATR activation in response to gamma-irradiation results in the phosphorylation of a variety of proteins including other kinases, transcription factors, scaffold and DNA repair proteins (35). Manke *et al* therefore constructed an oriented phosphopeptide library that resembled the Ser/Thr-Gln motif generated by ATM/ATR, to search for novel modular phosphoserine or phosphothreonine (pSer or pThr) binding domains involved in DNA damage response (13). The group found that the BRCT domains in BRCA1 and PTIP recognized ATM/ATR substrates such as p53 only after irradiation, indicating the requirement of phosphorylation for interaction and the role of BRCT domains as phospho-protein binding modules in DNA damage response pathways (13).

Additional BRCT domains from proteins such as MDC1 (mediator of DNA damage checkpoint 1), BARD1, DNA ligase IV, and *Saccharomyces cerevisiae* RAD9 have been examined by oriented peptide library analysis, revealing a phospho-dependent binding specificity that extends from the residues in position P+1 (with pSer/pThr as P0) to P+5, with particularly strong selections for aromatic/aliphatic residues at the P+3 position (14,33). In the study by *Rodriguez et al*, BRCT repeats from MDC1 were predicted to have a preference for pSer-X-X-Y (14). Based on this prediction, H2AX, a marker for sites of DNA breaks, may be a potential binding partner of MDC1. Indeed, these predictions have been confirmed by later studies (36,37). The recently solved crystal and NMR structures of several BRCT domains have further provided the molecular basis for recognition of specific phosphopeptides by BRCT domains (36,38-41). For

example, the residues that form the phospho-serine binding pocket in BRCA1 are conserved in several BRCT domains (Figure 2). Taken together, these observations indicate that phosphopeptide binding (with definable specificities) may be a common function of a set of BRCT repeats. For example, multiple proteins may interact with the BRCT region of BRCA1 in a phosphorylation-dependent manner and collaborate functionally with BRCA1 to participate in multiple cellular processes. The incorporation of enzymatic activities and post-translational modifications therefore afford the BRCA1 interaction networks more specificity and range in regulation.

3.1.1. Phospho-dependent BRCA1 BRCT interacting proteins

3.1.1.1. BACH1

BACH1 was originally identified in a screen for proteins that directly interact with the BRCT domain of BRCA1 (26). In fact, phosphorylation of BACH1 at Ser990 is a prerequisite for its association with BRCA1 (14,33). This interaction is cell cycle regulated and required for the G2/M checkpoint control in response to DNA damage. Mutant BRCA1 that either lacks one BRCT domain or contains missense mutations (P1749R and M1775R) fails to interact with BACH1. These data suggest that an intact BRCT domain structure is required for its interaction and function. As discussed above, Phe at position P+3 is also critical for phosphorylation-dependent interactions between BACH1 and BRCA1. These studies and the analyses of other BRCT-containing proteins indicate that phospho-dependent binding constitutes a crucial aspect of BRCT function, and demonstrate the versatility of this interaction module. The various modes of interaction (such as homodimerization and non-phospho dependent binding) should complement each other functionally and allow the BRCT-containing proteins to act in diverse pathways.

3.1.1.2. CtIP

The transcriptional suppressor CtBP binding partner CtIP was identified by two-hybrid screening as interacting with BRCA1 BRCT domains (25). Within the BRCA1-binding region of CtIP, the sequence surrounding Ser327 resembles the phosphorylation motif on BACH1 and undergoes transient phosphorylation during G2 (42). Furthermore, Ala mutation of Ser327 abolished the *in vitro* and *in vivo* interaction of CtIP with BRCT BRCA1 (42). The BRCA1/CtIP complex, which only exists during G2, is required for the G2/M transition checkpoint and DNA damage-induced Chk1 activation, suggesting that CtIP cooperates with BRCA1 in cell cycle checkpoint control (42). However, the BRCA1/CtIP complex is not required for prolonged G2 accumulation after DNA damage, a process controlled by a separate BRCA1/BACH1 complex (42). Notably, the *in vivo* interaction between BRCA1 and CtIP is completely ablated by the tumor-associated mutations of BRCA1 (A1708E and P1749R) as well as the nonsense mutation that eliminates the C-terminal 11 amino acids of BRCA1 (Y1853delta) (25). In fact, tumor derived-mutations on any BRCA1 BRCT repeats or its spacer region disrupt the BRCA1/CtIP interaction (43). Clearly, the BRCT domain assists BRCA1 function by its ability to interact with diverse partners at different cell cycle stages.

3.1.1.3. Acetyl-CoA carboxylase

Magnard *et al* identified ACCA (Acetyl Coenzyme A (CoA) Carboxylase alpha) as a BRCA1 BRCT interacting protein through a glutathione-S-transferase (GST) pull down assay with murine cells (44). ACCA is the rate-limiting step enzyme that catalyzes the carboxylation of Acetyl CoA to malonyl-CoA for the synthesis of long-chain fatty acids (45,46). A short-term regulatory mechanism for ACCA involves the phosphorylation and dephosphorylation of its Ser79 that result in its inactivation and activation. BRCA1 interacts only with the phosphorylated (i.e. inactive) form of ACCA. Sequences surrounding residue Ser1263 on ACCA strongly resemble those surrounding residue Ser990 of BACH1, and likely mediate the recognition by BRCT repeats of BRCA1. BRCA1 modulates lipid synthesis through its phospho-dependent binding to ACCA, thereby preventing ACCA from dephosphorylation and its subsequent activation (47). Importantly, this interaction is disrupted by germ-line BRCA1 BRCT mutations (e.g., A1708E, M1775R, P1749R, R1835X and Y1853X) (44). A number of studies have linked lipogenesis with cancer. For example, ACCA and another major enzyme in lipogenesis FAS (Fatty Acid Synthase), are highly expressed in several human malignancies including breast cancer (48). These observations have provided new mechanisms by which BRCA1 may exert its tumor suppressor function, and offered clues to how BRCT domains may signal in metabolic pathways.

3.1.1.4. Abraxas/CCDC98 and RAP80

Phosphopeptide affinity proteomic analysis of the BRCA1 complex revealed Abraxas/CCDC98 as directly binding to the BRCA1 BRCT domains through a pSer-X-X-Phe motif (49-51). In addition, Abraxas/CCDC98 mediates the formation of BRCA1 foci in response to DNA damage and BRCA1-dependent G2/M checkpoint activation. The binding of Abraxas/CCDC98 to BRCA1 requires phosphorylation, and is mutually exclusive with BACH1 or CtIP interaction with BRCA1. This is consistent with the observation that each of these proteins interacts with BRCA1 through the BRCT domains. Another ubiquitin-binding protein, RAP80, was found to associate with the Abraxas/CCDC98-BRCA1 complex (49,52,53). RAP80 and BRCA1 interact in a BRCA1 BRCT dependent manner, as two clinical missense mutations of BRCA1 BRCT domains (V1696L and P1749R) led to disrupted RAP80-BRCA1 binding (49,52). However, RAP80 does not contain a pSXXF motif, suggesting an indirect interaction between RAP80 and BRCA1. Indeed, several groups have shown that Abraxas/CCDC98 bridges the interaction between RAP80 and BRCA1 (49-51). After DNA damage, the Abraxas/CCDC98-RAP80 complex translocates to sites of damage, followed by the recruitment of BRCA1 via its binding to the phosphorylated C-terminus of Abraxas/CCDC98. Both Abraxas/CCDC98 and RAP80 are required for DNA damage resistance, DNA repair and

G2/M checkpoint control. The biochemical understanding of the interactions of these proteins with BRCA1 therefore not only helps to illustrate signaling pathways that recruit BRCA1 to sites of DNA damage, but also sheds light on the function and activity of other BRCT containing proteins.

3.2. MDC1

The recently identified mediator of DNA damage responses MDC1 contains tandem BRCT domains (54-56). Cells lacking MDC1 are sensitive to ionizing radiation, and fail to efficiently activate the intra S-phase and G2/M phase checkpoints. Upon treatment of cells with double-strand break inducing agents, MDC1 rapidly translocates to sites of DNA damage, where it mediates the accumulation of checkpoint and repair factors into nuclear foci together with proteins such as phosphorylated H2AX (54-56). Recent studies have shown that the BRCT domain of MDC1 directly interacts with the C-terminus of the phosphorylated H2AX that harbors the sequence SQEY (36,37). In the predicted MDC1 BRCT recognition motif (pSer-X-X-Y), tyrosine at position P+3 plays a critical role in mediating MDC1 binding (14). In the case of phospho-H2AX peptide, Ala substitution of Tyr completely abrogates its interaction with MDC1 (36). Furthermore, the addition of two extra Ala residues to the C-terminus of the peptide dramatically weakened the binding. Although the BRCT domains of MDC1 have a similar pattern of recognition compared to those of BRCA1 BRCT, biochemical and crystallographic data highlight the importance of a free carboxyl terminus for the overall sequence specificity (36,37). Since H2AX is the only MDC1 BRCT-interacting protein identified so far, the possibility that MDC1 BRCT may be able to recognize internal sequences cannot be ruled out.

The SQEY sequence on H2AX is also conserved in budding yeast and known to be phosphorylated by ATM-family kinases (57). Hammet *et al.* reported that the BRCT protein RAD9 binds to phosphorylated H2A in yeast and regulates the G1 check point (58), suggesting MDC1 may have evolved to function similarly in yeast and mammalian cells.

3.3. PTIP

The transcriptional regulatory protein PTIP appears to play an important role in regulating genome stability and mitosis (59-61). PTIP is required for the survival of cells exposed to ionizing radiation. Manke *et al* have shown that a pair of tandem BRCT repeats of PTIP has specific and high-affinity binding for peptides with the pS/T-Q-V-F sequence (13). It appears that BRCT-phosphopeptide interaction is responsible for PTIP localization to nuclear foci that contain 53BP1 and phospho-H2AX. Phosphorylated Ser25 on 53BP1 is bound by the BRCT repeats on PTIP after DNA damage, which requires ATM-dependent phosphorylation (61). Interestingly, this pair of tandem BRCT domains on PTIP can bind to ATM-phosphorylated epitopes other than the pS/T-Q-V-F sequence as well, highlighting the versatility of the BRCT domains in binding different phosphorylated targets.

3.4. MCPH1

MCPH1, also known as BRIT1 (78), contains 3 predicted BRCT domains, two of which are located at the C-terminus of MCPH1. MCPH1 was cloned as a gene that shows correlation with microcephely brains in animals (62). While its implication in controlling brain size is still controversial, recent evidence favors its role in DNA damage responses and mitosis (63-67, 79). MCPH1 appears to mediate early DNA damage responses, because RNAi knockdown of MCPH1 prevented the recruitment of BRCA1 and 53BP1 to damage foci. MCPH1 itself is known to localize to DNA damage foci through the interaction between its C-terminal BRCT repeats and the phosphorylated SQEY motif on H2AX (66). Mutations of MCPH1 BRCT repeats have been found in breast cancer (65), again underlining the importance of BRCT domains in protecting cells from genomic instability and cancer.

4. CANCER-ASSOCIATED BRCA1 MUTATIONS

Structural and sequence analysis of BRCA1 BRCT domains reveals that the residues that form or stabilize the binding pockets for phosphoserine and phenylalanine residues are among the most highly conserved among BRCA1 orthologs (68). And these regions strongly correlate with the location of cancer-associated mutations. Interestingly, clinically relevant missense mutations have been found within the two BRCT motifs of BRCA1 (27), implying a link between the function of BRCT domains and BRCA1-mediated tumor suppression (Table 1). Based on data from the Breast Cancer Information Database http://research.nhgri.nih.gov/bic/, the amino acids most frequently targeted for missense mutations in the BRCT repeats are Met1652, Arg1699, Ala17008, and Met1775. Interestingly, Arg1699 and Met1775 residues directly interact with residues in the BACH1 phosphopeptide, therefore these mutations may result in disrupted interactions between BRCT domains and their phosphorylated substrates.

Some cancer-associated mutations may destabilize the global BRCT fold whereas others are more likely to specifically interfere with ligand binding (3,27,69-71). Several mutations have been tested for binding to Ser-X-X-Phe and BACH1 peptides (summarized in Table 1) (40). Highly destabilizing truncation or missense mutations led to disrupted binding to phosphorylated peptides, demonstrating that correct folding is essential for the recognition of the phosphorylated target (39). In the instances where the missense mutations have little or no folding defects, the specificity or affinities of the interaction may be affected. For instance, the M1775R mutation that prevents BRCA1/BACH1 interaction, has exhibited not only decreased affinity for the BACH1 peptide, but also altered specificity, where a tyrosine residue at P+3 is preferred over Phe (40).

Clearly, examination of the effects of other missense mutations on the ability of BRCA1 BRCT to bind phosphorylated physiological targets will provide another

Table 1. Effect of BRCA1 BRCT missense mutations on BRCT folding and/or phosphopeptide binding

Missense mutations[1]	Position	pSer-X-X-Phe peptide binding[2]	BACH1 peptide binding[2]	Folding Defect[3]
M1652I	BRCT 1	+	?	-
F1695L	BRCT 1	+	?	-
R1699Q	BRCT 1	+/-	+/-	-
T1720A	BRCT 1	+	?	-
Y1853C	BRCT 2	+/-	-	++
C1697R	BRCT 1	+/-	?	++
A1708E	BRCT 1	+/-	?	++
S1715R	BRCT 1	+/-	?	++
W1718C	BRCT 1	+/-	?	++
P1749R	BRCT 2	+/-	-	++
G1738E	Linker	+/-	-	++
G1738R	Linker	+/-	?	++
V1809F	BRCT 2	+/-	?	+
D1692Y	BRCT 1	+/-	?	+
R1699W	BRCT 1	+/-	~ weak	+
R1751Q	BRCT 2	+	?	+
M1775R	BRCT 2	-	~ weak	+
M1783T	BRCT 2	+	?	+
S1655A	BRCT 1	?	-	?
S1655F	BRCT 1	-	-	?
K1702M	BRCT 1	?	-	?

[1]The mutants are grouped based on their effects solely on protein folding or peptide binding. [2]Ability to bind to phospho-peptide compared to non-phosphorylated counterpart: (+) bind specifically to phosphopeptide; (-) no binding; (+/-) no specific binding; (?) not determined (36,49,52,55). [3]Proteolytic sensitivity of the protein fold: (-) stability of the mutant indistinguishable from WT; (+) moderate destabilized; (++) severely destabilized; (?) not determined (70).

platform for studying the biochemical effects and clinical consequences of BRCT mutations in DNA damage proteins.

5. STRUCTURAL BASIS FOR PHOSPHOPEPTIDE INTERACTIONS

The first structural information for BRCT domains came from the crystal structure of the C-terminal BRCT domain of XRCC1 (72). In general, a single BRCT repeat forms a compact domain composed of a parallel four-stranded beta-sheet surrounded by a pair of alpha-helices (alpha1 and alpha3) on one side and a single alpha helix (alpha2) on the other (27,72) (Figure 1 and 2). Studies of the tandem BRCT domains of BRCA1 have shown that both repeats stack closely against each other through a large hydrophobic interface, giving rise to a deep surface cleft (27) (Figure 1). Sequence comparison and structural analysis revealed that this surface cleft is highly conserved among BRCA1 orthologs (68). In addition, the repeats are connected by a relatively flexible linker and packed in a head-to-tail manner that is conserved between human and rat BRCA1, as well as in the BRCT domain of p53BP1. To date, structural data have become available for the BRCT domains of BRCA1 (27,38-41), 53BP1 (29,30), DNA ligase III and IV (73,74), a NAD+-dependent DNA ligase (75), MDC1 (36,37), and BARD1 (76). To understand the molecular basis for phosphorylation-dependent interactions, we will focus on the BRCT structures that have been co-crystallized with phosphopeptides.

5.1. Structures of the BRCA1/BACH1 and MDC1/H2AX phosphopeptide complexes

The crystal and NMR structures of the BRCA1 tandem BRCT repeats in complex with the pSer BACH1 containing peptide have been solved, helping to illustrate the mechanism by which phosphopeptide recognition occurs (38-41). Overall, the structures of the unbound and BACH1-bound BRCT repeats are similar, with only a slight relative rotation of each BRCT domain and a translation of the N-terminal BRCT helix α1 toward the cleft between the domains in the presence of the peptide (40). The phosphorylated BACH1 peptide binds to this cleft, interacting with residues from both repeats, consistent with the requirement of both domains for efficient phosphopeptide binding (Figure 1 and 2). In addition, the structure illustrates the BRCT domain preference for pSer over pTyr, since the phospho recognition pocket appears too shallow to accept a bulky phenyl ring.

The structure also provides evidence for the observation that the binding of tandem BRCT domains to phosphorylated BACH1 requires both pSer and a Phe at the P+3 position (38-41). The N-terminal half of the BRCA1 interface has a basic pocket where pSer990 from BACH1 binds, through three hydrogen bonds involving the side chains of Ser1655 and Lys1702 and the backbone amide of Gly1656 located in the first BRCT repeat. Additionally, the C-terminal half of the interface has the aromatic side chain of Phe (at P+3) from BACH1 interacting with the hydrophobic pocket formed by the side chains of Phe1704, Met1775 and Leu1839. Additional hydrogen bonding with the main chain of Phe is supplied by main and side chain atoms from Arg1699.

Several residues (Ser1655, Lys1702, Phe1704, Met1775 and Leu1839) responsible for the recognition are conserved in BRCA1 orthologs, suggesting that phosphopeptide recognition may be an evolutionarily conserved function among BRCA1 proteins (Figure 2). In fact, Ala mutations of either Ser1655 or Lys1702 abolished the interaction with BACH1 and resulted in loss of function of BRCA1 in DNA damage-induced checkpoint control

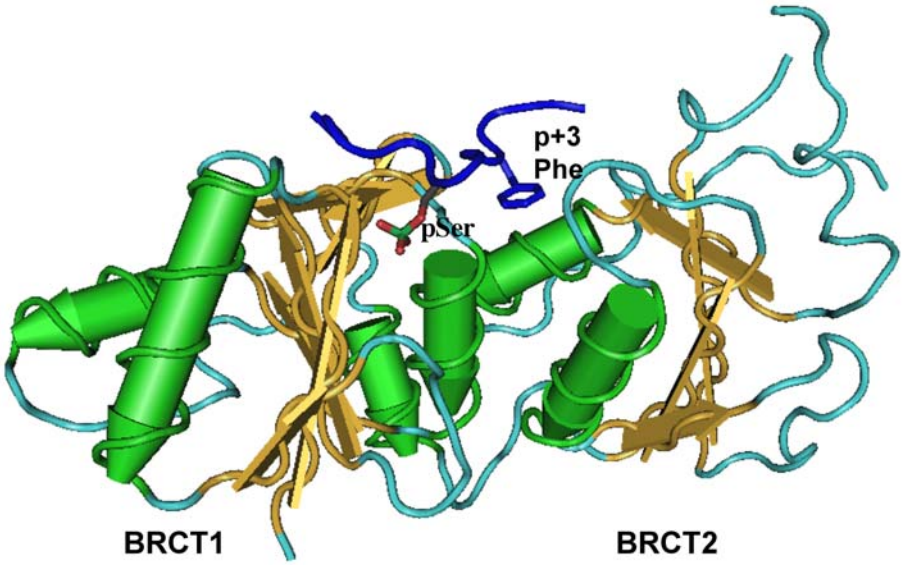

Figure 1. Structure of the BRCA1 tandem BRCT repeats bound to BACH1 phosphopeptide (38-41). The BRCT alpha helices are green, the beta strands are gold, and the phosphopeptide is blue (stick representation). The two BRCT repeats are connected by a linker region and arranged in tandem. The pSer-binding pocket is formed by residues on the BRCT1, whereas Phe at p+3 position sits into a hydrophobic groove formed by residues from both BRCT domains. Model was constructed using Cn3D4.1.1.

(38). However, the various members of this large family must be able to differentiate among the multitude of phosphorylated substrates in order to perform their distinct functions. A number of studies have examined the sequence conservation of several BRCT-motif containing proteins, including those from BARD1, BRCA1, and MDC1 (36-38,40,41,68,76). As expected, the residues in the BRCA1 BRCT domain that coordinate binding to pSer990 of BACH1 are highly conserved among these four proteins, whereas the residues that interact with Phe993 of BACH1 seem less well conserved (38-41) (Table 2). Such sequence variability may help to explain why different BRCT containing proteins were found to prefer different phosphopeptides, with the strongest selection at the P+3 position (13,14).

Notably, pSer990 of BACH1 exclusively interacts with the first BRCT domain, whereas Phe993 primarily interacts with the second BRCT through *van der Waals* contacts (38-41). It is therefore not surprising that tandem, rather than single, BRCA1 BRCT repeats are required for BACH1 phosphopeptide binding. For the few single BRCT domain containing proteins such as telomeric protein RAP1, the mechanism of how they achieve specificity remains unclear. On the other hand, single BRCT domains may form homo- or hetero-dimers (72,77). One possibility is that single BRCT containing proteins would homo- or hetero-dimerize to bind phosphorylated sequences in a manner similar to tandem BRCT repeats (38).

The recently solved crystal structure of MDC1 BRCT repeats bound to the H2AX phosphopeptide offers additional clues about phosphopeptide recognition by BRCT domains (36,37,41). The overall structure of MDC1-H2AX complex is similar to that of BRCA1-BACH1, where the BRCT-phosphate interaction interfaces are highly conserved. However, unlike BRCA1, MDC1 prefers Tyr residue at the P+3 position that is at the C-terminus of the H2AX peptide. The free carboxyl group of H2AX forms two salt bridges with Arg1933 on MDC1. Extension of the H2AX peptide by adding amino acids to the C-terminus of P+3 Tyr greatly reduced binding affinity, consistent with an essential role of the interaction between the free carboxyl group and MDC1 BRCT domains.

6. PREDICTIONS FOR PHOSPHOPEPTIDE RECOGNITION BY BRCT DOMAINS

6.1. Candidate phosphopeptide binding BRCT domains in human cells

While it remains unclear whether the BRCT domains as yet studied can mediate phosphorylation-dependent interactions as well, structural analyses of phosphopeptides-bound BRCT domains have provided us the opportunity to predict BRCT-phosphopeptide interactions. As discussed in detail in Sections 5, phosphopeptide recognition is achieved primarily through two key binding pockets formed by the tandem BRCT domains. The phosphoserine recognition pocket is formed by three residues on Lbeta1alpha1 and alpha2 from the first BRCT domain (Table 2). All the BRCT repeats known to bind phosphopeptides contain a (T/S)G motif and a K/N residue within Lbeta1alpha1 and alpha2 respectively. Based on these observations, we have predicted 5 additional putative phosphopeptide-binding BRCT repeats from human BRCTD1, TOPBP1, ECT2, and XRCC1. These BRCT repeats harbor either the (T/S)G or a closely related (T/S)S motif at the corresponding Lbeta1alpha1 positions (Table 2).

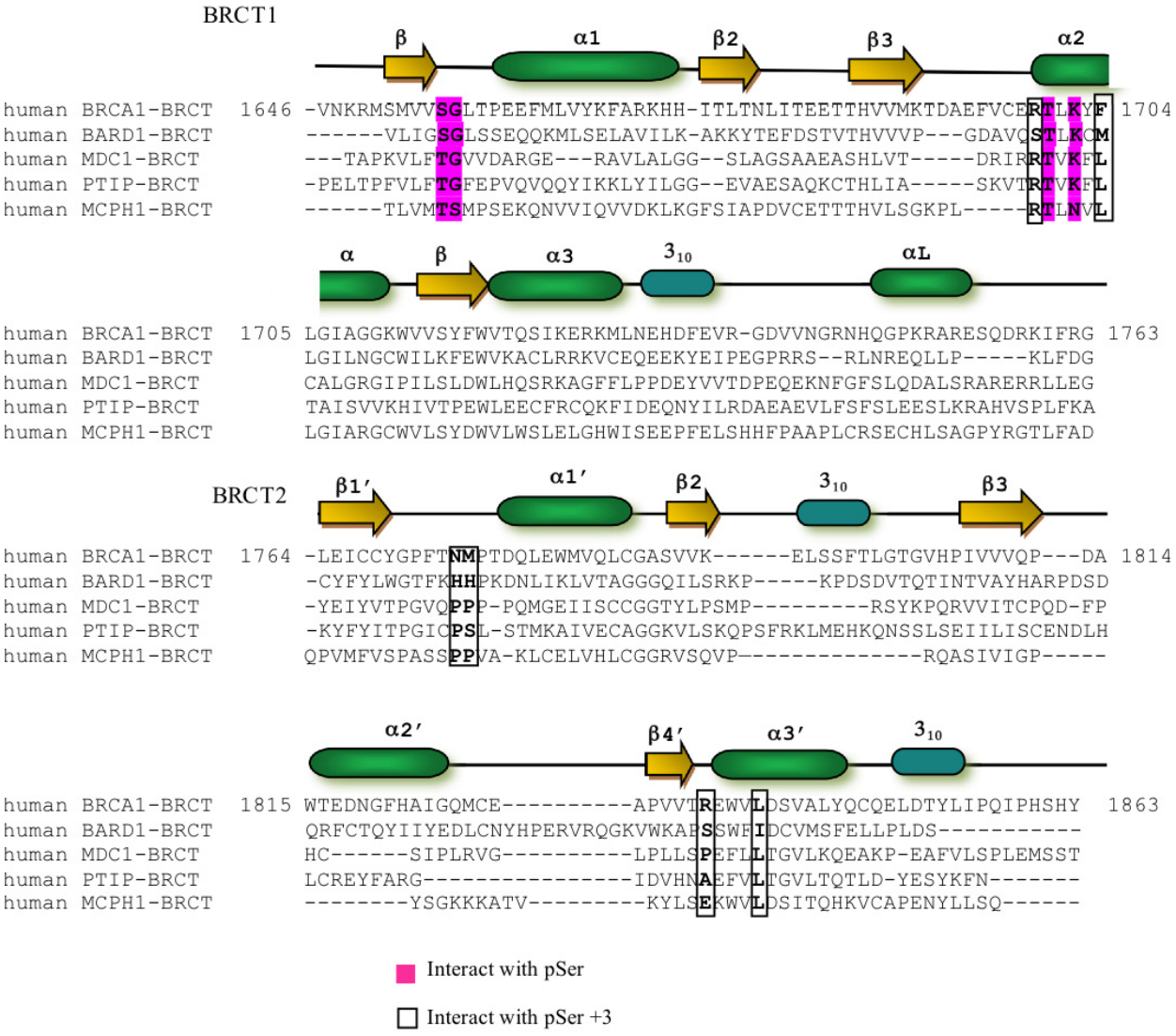

Figure 2. Amino acid sequence alignment of the BRCT repeats of BRCA1, BARD1, MDC1 PTIP, and MCPH1. The secondary structure and numbering are indicated for human BRCA1. Residues involved in binding to pSer are highly conserved among these proteins (pink shadow), whereas residues that interact with Phe at P+3 position seem less well conserved (black boxes) The positions of the BRCT BRCA1 missense mutations from Table1 are indicated here by asterisks. The alignment was generated using ClustalW from EMBL.

The other key binding pocket is involved in specificity determination of BRCT-phosphopeptide interaction. As revealed by the structures of phosphopeptides binding to BRCA1 or MDC1 BRCT domains, the P+3 residue (relative to pSer) plays an important role in governing the specificity of BRCT repeats (38-41). BRCA1 and MDC1 prefer Phe and Tyr respectively at this position (14). Unlike the phosphoserine-binding pocket that is mainly formed by residues from the first BRCT domain, the P+3 pocket is formed by residues from both the first and second BRCT domains (Table 2). In the BRCA1 BRCT structure, the Phe residue from alpha2, Met residue from Lbeta1'alpha1', and Leu residue from alpha3' contribute to Phe recognition at the pSer+3 position. In comparison, Leu of alpha2, Pro of Lbeta1'alpha1', and Leu of alpha3' help to coordinate the recognition of Tyr at the P+3 position in the MDC1-H2AX peptide structure. Interestingly, MCPH1 contains the same residues as MDC1 in the P+3 pocket and was shown recently to bind the phospho-H2AX peptide (66). These data lend support to utilizing the residues that make up the pSer+3 binding pocket for specificity prediction of BRCT domains. For example, the P+3 pocket residues from PTIP BRCT repeats (residues 560-757) are similar to those of MDC1. Accordingly, PTIP was shown to bind with high affinity peptides with Phe at the P+3 position (13). It is also possible that PTIP BRCT domains

Table 2. Predicted phosphopeptide-binding pockets for BRCT domains

BRCT domains	pSer pocket		P+3 pocket			Known Motif or peptides
	Lbeta1alpha1	alpha2	Lbeta1'alpha1'	alpha2	alpha3'	
BRCA1	SG	K	M	F	L	pSPTF
MDC1	TG	K	P	L	L	pSQEY
MCPH1	SG	N	P	L	L	pSQEY
BARD1	SG	K	H	M	I	pSEDE?
ECT2	TG	K	E	R	W	?
PTIP (560-757)	TG	K	P	L	L	pSQVF pSQEY?
TOPBP1 (22-207)	TS	K	L	L	F	?
TOPBP1 (1177-1401)	SS	K	E	L	A	?
XRCC1	SG	K	E	S	Y	?
BRCTD1	TG	K	K	L	G	?
DNL4	SG	K	T	I	T	pSYYI?

Table 3. Potential *in vivo* binding sites for human BRCA1, MDC1, and PTIP BRCT domains

Phosphorylation sites	Protein	Potential BRCT domains
SPVY	ABL1M1	PTIP, MDC1
SQSY	ATM	PTIP, MDC1
SQSY	CD19	PTIP, MDC1
SQDY	CHD5	PTIP, MDC1
SQRY	FLJ10726	PTIP, MDC1
SQSY	FLJ12949	PTIP, MDC1
SQGY	MSH2	PTIP, MDC1
SISY	RNF19	PTIP, MDC1
SQDY	USP28	PTIP, MDC1
SQDF	ATE1	PTIP, BRCA1
SQKF	CENTB2	PTIP, BRCA1
SQQF	DDX17	PTIP, BRCA1
SQAF	KIAA2018	PTIP, BRCA1
SQEF	BCORL1	PTIP, BRCA1
SQKF	KIAA1840	PTIP, BRCA1
SQAF	LRG6	PTIP, BRCA1
SQDF	PFS2	PTIP, BRCA1
SQRF	PNKD	PTIP, BRCA1
SQNF	RAD23	PTIP, BRCA1
SQDF	RAD50	PTIP, BRCA1
SQSF	RIC8	PTIP, BRCA1
SQDF	SCML2	PTIP, BRCA1
SQSF	53BP1	PTIP, BRCA1
SQRF	VPS26B	PTIP, BRCA1

may interact with the phosphorylated tail of H2AX (Table 2). This may explain the finding that PTIP is targeted to phospho-H2AX DNA damage foci (13).

6.2. Potential *in vivo* sites for human BRCT domains

Many of the BRCT-containing proteins have been implicated in DNA damage and repair pathways. Because ATM and ATR are major regulators of DNA damage and repair, it is likely that BRCT domains bind to phosphorylated Ser or Thr sites that are substrates of these two kinases. Recent advances in mapping endogenous phosphorylation sites by ATM and ATR kinases in human cells have provided a reservoir of potential binding sites for BRCT repeats (35). It would be of great interest in the near future to match these phosphorylation sites with different BRCT domains and assemble a phosphorylation-mediated interaction network, in order to better understand signal transduction initiated by DNA damages. In addition to bench work, one can start to predict such interactions based on known properties of different BRCT domains. In Table 3, we have listed potential interacting sites of BRCA1, MDC1, and PTIP BRCT domains based on the data set from Matsuoka *et al*. These known phosphorylation sites contain either Phe or Tyr at the P+3 position.

7. SUMMARY AND PERSPECTIVE

Among the majority of the proteins studied so far, tandem BRCT domains appear to be required for binding to phosphopeptides. However, single BRCT repeats as found in the DNA polymerase REV1, the phosphatase FCP1, NBS1 and DNA ligase III have also been proposed to interact with phosphopeptides based on *in vitro* binding experiments (33). Therefore the function of single BRCT domain and whether they (perhaps in conjunction with other domains) can bind phosphorylated sequences remain unknown. Here we have also listed a number of candidate BRCT domains including the tandem BRCT domains of XRCC1 that are predicted to interact with phosphopeptides. It will be of great interest to determine whether these predictions are correct and if so, the specificities of these interactions.

Due to the lack of space, we did not discuss at all the DNA-binding activities of BRCT domains. One important question to ask is how BRCT modules might function as a molecular sensor by direct or indirect recognition of particular DNA structures. As noted above, some cancer relevant mutations appear to affect the affinity as well as specificity of BRCT-mediated interactions. Are

these changes pertinent to cancer? Numerous studies have helped to map out the vast interaction networks mediated by BRCT domain containing proteins such as BRCA1 and MDC1. How do phospho-dependent interactions regulate the assembly/dis-assembly of the complexes as well as the ordered recruitment/translocation of signaling molecules to sites of responses? Many of the BRCT proteins were found at the DNA damage foci and known to bind phosphorylated H2AX tail. What is the order of recruitment of different BRCT domain proteins? Do they function as nucleating sites to initiate different signals or are they recruited at different times during the repair process? These questions and many more await for further biochemical and cellular studies.

8. ACKNOWLEDGEMENT

We thank Dr. Dan Liu for critical review of the manuscript. We apologize for not being able to include many of the published work related to the discussed topic due to lack of space. This work is supported by funds from NIH, DOD and a NRSA individual fellowship.

9. REFERENCES

1. Bork, P., K. Hofmann, P. Bucher, A. F. Neuwald, S. F. Altschul & E. V. Koonin: A superfamily of conserved domains in DNA damage-responsive cell cycle checkpoint proteins. *Faseb J*, 11, 68-76 (1997)
2. Wu, L. C., Z. W. Wang, J. T. Tsan, M. A. Spillman, A. Phung, X. L. Xu, M. C. Yang, L. Y. Hwang, A. M. Bowcock & R. Baer: Identification of a RING protein that can interact *in vivo* with the BRCA1 gene product. *Nat Genet*, 14, 430-40(1996)
3. Scully, R., S. Ganesan, K. Vlasakova, J. Chen, M. Socolovsky & D. M. Livingston: Genetic analysis of BRCA1 function in a defined tumor cell line. *Mol Cell*, 4, 1093-9 (1999)
4. Holt, J. T., M. E. Thompson, C. Szabo, C. Robinson-Benion, C. L. Arteaga, M. C. King & R. A. Jensen: Growth retardation and tumour inhibition by BRCA1. *Nat Genet*, 12, 298-302 (1996)
5. Rao, V. N., N. Shao, M. Ahmad & E. S. Reddy: Antisense RNA to the putative tumor suppressor gene BRCA1 transforms mouse fibroblasts. *Oncogene*, 12, 523-8 (1996)
6. Koonin, E. V., S. F. Altschul & P. Bork: BRCA1 protein products ... Functional motifs. *Nat Genet*, 13, 266-8 (1996)
7. Zhou, B. B. & S. J. Elledge: The DNA damage response: putting checkpoints in perspective. *Nature*, 408, 433-9 (2000)
8. Khanna, K. K. & S. P. Jackson: DNA double-strand breaks: signaling, repair and the cancer connection. *Nat Genet*, 27, 247-54 (2001)
9. Venkitaraman, A. R.: Cancer susceptibility and the functions of BRCA1 and BRCA2. *Cell*, 108, 171-82 (2002)
10. Callebaut, I. & J. P. Mornon: From BRCA1 to RAP1: a widespread BRCT module closely associated with DNA repair. *FEBS Lett*, 400, 25-30 (1997)
11. Glover, J. N., R. S. Williams & M. S. Lee: Interactions between BRCT repeats and phosphoproteins: tangled up in two. *Trends Biochem Sci*, 29, 579-85 (2004)
12. Gayther, S. A., W. Warren, S. Mazoyer, P. A. Russell, P. A. Harrington, M. Chiano, S. Seal, R. Hamoudi, E. J. van Rensburg, A. M. Dunning, R. Love, G. Evans, D. Easton, D. Clayton, M. R. Stratton & B. A. Ponder: Germline mutations of the BRCA1 gene in breast and ovarian cancer families provide evidence for a genotype-phenotype correlation. *Nat Genet*, 11, 428-33 (1995)
13. Manke, I. A., D. M. Lowery, A. Nguyen & M. B. Yaffe: BRCT repeats as phosphopeptide-binding modules involved in protein targeting. *Science*, 302, 636-9 (2003)
14. Rodriguez, M., X. Yu, J. Chen & Z. Songyang: Phosphopeptide binding specificities of BRCA1 COOH-terminal (BRCT) domains. *J Biol Chem*, 278, 52914-8 (2003)
15. Wu-Baer, F. & R. Baer: Effect of DNA damage on a BRCA1 complex. *Nature*, 414, 36 (2001)
16. Li, S., N. S. Ting, L. Zheng, P. L. Chen, Y. Ziv, Y. Shiloh, E. Y. Lee & W. H. Lee: Functional link of BRCA1 and ataxia telangiectasia gene product in DNA damage response. *Nature*, 406, 210-5 (2000)
17. Lee, J. S., K. M. Collins, A. L. Brown, C. H. Lee & J. H. Chung: hCds1-mediated phosphorylation of BRCA1 regulates the DNA damage response. *Nature*, 404, 201-4 (2000)
18. Cortez, D., Y. Wang, J. Qin & S. J. Elledge: Requirement of ATM-dependent phosphorylation of brca1 in the DNA damage response to double-strand breaks. *Science*, 286, 1162-6 (1999)
19. Hartman, A. R. & J. M. Ford: BRCA1 induces DNA damage recognition factors and enhances nucleotide excision repair. *Nat Genet*, 32, 180-4 (2002)
20. Welcsh, P. L., M. K. Lee, R. M. Gonzalez-Hernandez, D. J. Black, M. Mahadevappa, E. M. Swisher, J. A. Warrington & M. C. King: BRCA1 transcriptionally regulates genes involved in breast tumorigenesis. *Proc Natl Acad Sci U S A*, 99, 7560-5 (2002)
21. Xu, X., W. Qiao, S. P. Linke, L. Cao, W. M. Li, P. A. Furth, C. C. Harris & C. X. Deng: Genetic interactions between tumor suppressors Brca1 and p53 in apoptosis, cell cycle and tumorigenesis. *Nat Genet*, 28, 266-71 (2001)
22. Ludwig, T., P. Fisher, S. Ganesan & A. Efstratiadis: Tumorigenesis in mice carrying a truncating Brca1 mutation. *Genes Dev*, 15, 1188-93 (2001)
23. Benarroch, D. & S. Shuman: Characterization of mimivirus NAD+-dependent DNA ligase. *Virology*, 353, 133-43 (2006)
24. Taylor, R. M., B. Wickstead, S. Cronin & K. W. Caldecott: Role of a BRCT domain in the interaction of DNA ligase III-alpha with the DNA repair protein XRCC1. *Curr Biol*, 8, 877-80 (1998)
25. Yu, X., L. C. Wu, A. M. Bowcock, A. Aronheim & R. Baer: The C-terminal (BRCT) domains of BRCA1 interact *in vivo* with CtIP, a protein implicated in the CtBP pathway of transcriptional repression. *J Biol Chem*, 273, 25388-92 (1998)
26. Cantor, S. B., D. W. Bell, S. Ganesan, E. M. Kass, R. Drapkin, S. Grossman, D. C. Wahrer, D. C. Sgroi, W. S. Lane, D. A. Haber & D. M. Livingston: BACH1, a

novel helicase-like protein, interacts directly with BRCA1 and contributes to its DNA repair function. *Cell*, 105, 149-60 (2001)
27. Williams, R. S., R. Green & J. N. Glover: Crystal structure of the BRCT repeat region from the breast cancer-associated protein BRCA1. *Nat Struct Biol*, 8, 838-42 (2001)
28. Critchlow, S. E., R. P. Bowater & S. P. Jackson: Mammalian DNA double-strand break repair protein XRCC4 interacts with DNA ligase IV. *Curr Biol*, 7, 588-98 (1997)
29. Derbyshire, D. J., B. P. Basu, L. C. Serpell, W. S. Joo, T. Date, K. Iwabuchi & A. J. Doherty: Crystal structure of human 53BP1 BRCT domains bound to p53 tumour suppressor. *Embo J*, 21, 3863-72 (2002)
30. Joo, W. S., P. D. Jeffrey, S. B. Cantor, M. S. Finnin, D. M. Livingston & N. P. Pavletich: Structure of the 53BP1 BRCT region bound to p53 and its comparison to the Brca1 BRCT structure. *Genes Dev*, 16, 583-93 (2002)
31. Beernink, P. T., M. Hwang, M. Ramirez, M. B. Murphy, S. A. Doyle & M. P. Thelen: Specificity of protein interactions mediated by BRCT domains of the XRCC1 DNA repair protein. *J Biol Chem*, 280, 30206-13 (2005)
32. Yamane, K. & T. Tsuruo: Conserved BRCT regions of TopBP1 and of the tumor suppressor BRCA1 bind strand breaks and termini of DNA. *Oncogene*, 18, 5194-203 (1999)
33. Yu, X., C. C. Chini, M. He, G. Mer & J. Chen: The BRCT domain is a phospho-protein binding domain. *Science*, 302, 639-42 (2003)
34. Soulier, J. & N. F. Lowndes: The BRCT domain of the S. cerevisiae checkpoint protein Rad9 mediates a Rad9-Rad9 interaction after DNA damage. *Curr Biol*, 9, 551-4 (1999)
35. Matsuoka, S., B. A. Ballif, A. Smogorzewska, E. R. McDonald, 3rd, K. E. Hurov, J. Luo, C. E. Bakalarski, Z. Zhao, N. Solimini, Y. Lerenthal, Y. Shiloh, S. P. Gygi & S. J. Elledge: ATM and ATR substrate analysis reveals extensive protein networks responsive to DNA damage. *Science*, 316, 1160-6 (2007)
36. Stucki, M., J. A. Clapperton, D. Mohammad, M. B. Yaffe, S. J. Smerdon & S. P. Jackson: MDC1 directly binds phosphorylated histone H2AX to regulate cellular responses to DNA double-strand breaks. *Cell*, 123, 1213-26 (2005)
37. Lee, M. S., R. A. Edwards, G. L. Thede & J. N. Glover: Structure of the BRCT repeat domain of MDC1 and its specificity for the free COOH-terminal end of the gamma-H2AX histone tail. *J Biol Chem*, 280, 32053-6 (2005)
38. Botuyan, M. V., Y. Nomine, X. Yu, N. Juranic, S. Macura, J. Chen & G. Mer: Structural basis of BACH1 phosphopeptide recognition by BRCA1 tandem BRCT domains. *Structure*, 12, 1137-46 (2004)
39. Williams, R. S., M. S. Lee, D. D. Hau & J. N. Glover: Structural basis of phosphopeptide recognition by the BRCT domain of BRCA1. *Nat Struct Mol Biol*, 11, 519-25 (2004)
40. Clapperton, J. A., I. A. Manke, D. M. Lowery, T. Ho, L. F. Haire, M. B. Yaffe & S. J. Smerdon: Structure and mechanism of BRCA1 BRCT domain recognition of phosphorylated BACH1 with implications for cancer. *Nat Struct Mol Biol*, 11, 512-8 (2004)
41. Varma, A. K., R. S. Brown, G. Birrane & J. A. Ladias: Structural basis for cell cycle checkpoint control by the BRCA1-CtIP complex. *Biochemistry*, 44, 10941-6 (2005)
42. Yu, X. & J. Chen: DNA damage-induced cell cycle checkpoint control requires CtIP, a phosphorylation-dependent binding partner of BRCA1 C-terminal domains. *Mol Cell Biol*, 24, 9478-86 (2004)
43. Li, S., P. L. Chen, T. Subramanian, G. Chinnadurai, G. Tomlinson, C. K. Osborne, Z. D. Sharp & W. H. Lee: Binding of CtIP to the BRCT repeats of BRCA1 involved in the transcription regulation of p21 is disrupted upon DNA damage. *J Biol Chem*, 274, 11334-8 (1999)
44. Magnard, C., R. Bachelier, A. Vincent, M. Jaquinod, S. Kieffer, G. M. Lenoir & N. D. Venezia: BRCA1 interacts with acetyl-CoA carboxylase through its tandem of BRCT domains. *Oncogene*, 21, 6729-39 (2002)
45. Tong, L. & H. J. Harwood, Jr.: Acetyl-coenzyme A carboxylases: versatile targets for drug discovery. *J Cell Biochem*, 99, 1476-88 (2006)
46. Wakil, S. J.: The relationship between structure and function for and the regulation of the enzymes of fatty acid synthesis. *Ann N Y Acad Sci*, 478, 203-19 (1986)
47. Moreau, K., E. Dizin, H. Ray, C. Luquain, E. Lefai, F. Foufelle, M. Billaud, G. M. Lenoir & N. D. Venezia: BRCA1 affects lipid synthesis through its interaction with acetyl-CoA carboxylase. *J Biol Chem*, 281, 3172-81 (2006)
48. Milgraum, L. Z., L. A. Witters, G. R. Pasternack & F. P. Kuhajda: Enzymes of the fatty acid synthesis pathway are highly expressed in in situ breast carcinoma. Clin Cancer Res, 3, 2115-20 (1997)
49. Wang, B., S. Matsuoka, B. A. Ballif, D. Zhang, A. Smogorzewska, S. P. Gygi & S. J. Elledge: Abraxas and RAP80 form a BRCA1 protein complex required for the DNA damage response. Science, 316, 1194-8 (2007)
50. Kim, H., J. Huang & J. Chen: CCDC98 is a BRCA1-BRCT domain-binding protein involved in the DNA damage response. Nat Struct Mol Biol, 14, 710-5 (2007)
51. Liu, Z., J. Wu & X. Yu: CCDC98 targets BRCA1 to DNA damage sites. Nat Struct Mol Biol, 14, 716-20 (2007)
52. Sobhian, B., G. Shao, D. R. Lilli, A. C. Culhane, L. A. Moreau, B. Xia, D. M. Livingston & R. A. Greenberg: RAP80 targets BRCA1 to specific ubiquitin structures at DNA damage sites. *Science*, 316, 1198-202 (2007)
53. Kim, H., J. Chen & X. Yu: Ubiquitin-binding protein RAP80 mediates BRCA1-dependent DNA damage response. Science, 316, 1202-5 (2007)
54. Stewart, G. S., B. Wang, C. R. Bignell, A. M. Taylor & S. J. Elledge: MDC1 is a mediator of the mammalian DNA damage checkpoint. Nature, 421, 961-6 (2003)
55. Goldberg, M., M. Stucki, J. Falck, D. D'Amours, D. Rahman, D. Pappin, J. Bartek & S. P. Jackson: MDC1 is required for the intra-S-phase DNA damage checkpoint. Nature, 421, 952-6 (2003)
56. Lou, Z., K. Minter-Dykhouse, X. Wu & J. Chen: MDC1 is coupled to activated CHK2 in mammalian DNA damage response pathways. Nature, 421, 957-61(2003)
57. Downs, J. A., N. F. Lowndes & S. P. Jackson: A role for Saccharomyces cerevisiae histone H2A in DNA repair. *Nature*, 408, 1001-4 (2000)

58. Hammet, A., C. Magill, J. Heierhorst & S. P. Jackson: Rad9 BRCT domain interaction with phosphorylated H2AX regulates the G1 checkpoint in budding yeast. *EMBO Rep*, 8, 851-7 (2007)
59. Cho, E. A., M. J. Prindle & G. R. Dressler: BRCT domain-containing protein PTIP is essential for progression through mitosis. *Mol Cell Biol*, 23, 1666-73 (2003)
60. Jowsey, P. A., A. J. Doherty & J. Rouse: Human PTIP facilitates ATM-mediated activation of p53 and promotes cellular resistance to ionizing radiation. *J Biol Chem*, 279, 55562-9 (2004)
61. Munoz, I. M., P. A. Jowsey, R. Toth & J. Rouse: Phospho-epitope binding by the BRCT domains of hPTIP controls multiple aspects of the cellular response to DNA damage. *Nucleic Acids Res*, 35, 5312-22 (2007)
62. Jackson, A. P., H. Eastwood, S. M. Bell, J. Adu, C. Toomes, I. M. Carr, E. Roberts, D. J. Hampshire, Y. J. Crow, A. J. Mighell, G. Karbani, H. Jafri, Y. Rashid, R. F. Mueller, A. F. Markham & C. G. Woods: Identification of microcephalin, a protein implicated in determining the size of the human brain. *Am J Hum Genet*, 71, 136-42 (2002)
63. Xu, X., J. Lee & D. F. Stern: Microcephalin is a DNA damage response protein involved in regulation of CHK1 and BRCA1. *J Biol Chem*, 279, 34091-4 (2004)
64. O'Driscoll, M., A. P. Jackson & P. A. Jeggo: Microcephalin: a causal link between impaired damage response signalling and microcephaly. *Cell Cycle*, 5, 2339-44 (2006)
65. Lin, S. Y., R. Rai, K. Li, Z. X. Xu & S. J. Elledge: BRIT1/MCPH1 is a DNA damage responsive protein that regulates the Brca1-Chk1 pathway, implicating checkpoint dysfunction in microcephaly. *Proc Natl Acad Sci U S A*, 102, 15105-9 (2005)
66. Wood, J. L., N. Singh, G. Mer & J. Chen: MCPH1 Functions in an H2AX-dependent but MDC1-independent Pathway in Response to DNA Damage. *J Biol Chem*, 282, 35416-35423 (2007)
67. Brunk, K., B. Vernay, E. Griffith, N. L. Reynolds, D. Strutt, P. W. Ingham & A. P. Jackson: Microcephalin coordinates mitosis in the syncytial Drosophila embryo. *J Cell Sci*, 120, 3578-88 (2007)
68. Shiozaki, E. N., L. Gu, N. Yan & Y. Shi: Structure of the BRCT repeats of BRCA1 bound to a BACH1 phosphopeptide: implications for signaling. *Mol Cell*, 14, 405-12 (2004)
69. Vallon-Christersson, J., C. Cayanan, K. Haraldsson, N. Loman, J. T. Bergthorsson, K. Brondum-Nielsen, A. M. Gerdes, P. Moller, U. Kristoffersson, H. Olsson, A. Borg & A. N. Monteiro: Functional analysis of BRCA1 C-terminal missense mutations identified in breast and ovarian cancer families. *Hum Mol Genet*, 10, 353-60 (2001)
70. Williams, R. S. & J. N. Glover: Structural consequences of a cancer-causing BRCA1-BRCT missense mutation. *J Biol Chem*, 278, 2630-5 (2003)
71. Williams, R. S., D. I. Chasman, D. D. Hau, B. Hui, A. Y. Lau & J. N. Glover: Detection of protein folding defects caused by BRCA1-BRCT truncation and missense mutations. *J Biol Chem*, 278, 53007-16 (2003)
72. Zhang, X., S. Morera, P. A. Bates, P. C. Whitehead, A. I. Coffer, K. Hainbucher, R. A. Nash, M. J. Sternberg, T. Lindahl & P. S. Freemont: Structure of an XRCC1 BRCT domain: a new protein-protein interaction module. *Embo J*, 17, 6404-11 (1998)
73. Krishnan, V. V., K. H. Thornton, M. P. Thelen & M. Cosman: Solution structure and backbone dynamics of the human DNA ligase IIIalpha BRCT domain. *Biochemistry*, 40, 13158-66 (2001)
74. Sibanda, B. L., S. E. Critchlow, J. Begun, X. Y. Pei, S. P. Jackson, T. L. Blundell & L. Pellegrini: Crystal structure of an Xrcc4-DNA ligase IV complex. *Nat Struct Biol*, 8, 1015-9 (2001)
75. Jeon, H. J., H. J. Shin, J. J. Choi, H. S. Hoe, H. K. Kim, S. W. Suh & S. T. Kwon: Mutational analyses of the thermostable NAD+-dependent DNA ligase from Thermus filiformis. *FEMS Microbiol Lett*, 237, 111-8 (2004)
76. Birrane, G., A. K. Varma, A. Soni & J. A. Ladias: Crystal structure of the BARD1 BRCT domains. *Biochemistry*, 46, 7706-12 (2007)
77. Dulic, A., P. A. Bates, X. Zhang, S. R. Martin, P. S. Freemont, T. Lindahl & D. E. Barnes: BRCT domain interactions in the heterodimeric DNA repair protein XRCC1-DNA ligase III. *Biochemistry*, 40, 5906-13 (2001)
78. Lin, S. Y. & S. J. Elledge: Multiple tumor suppressor pathways negatively regulate telomerase. *Cell*, 113, 881-9(2003)
79. Rai, R., H. Dai, A. S. Multani, K. Li, K. Chin, J. Gray, J. P. Lahad, J. Liang, G. B. Mills, F. Meric-Bernstam & S. Y. Lin: BRIT1 regulates early DNA damage response, chromosomal integrity, and cancer. *Cancer Cell*, 10, 145-57(2006)

Key Words: BRCT domains, phosphopeptide binding, BRCA1, BACH1, protein-protein interactions, CtIP, Abraxas, RAP80, DNA damage, DNA repair, phosphoserine binding domain, cancer mutations, tumor suppressor, cell cycle, crystal structure, signal transduction, phosphorylation, protein folding, sequence homology, missense mutations, Review

Send correspondence to: Zhou Songyang, Department of Biochemistry and Molecular Biology, Baylor College of Medicine, One Baylor Plaza, Houston, TX 77030, USA, Tel: 713-798-5220, Fax: 713-798-9438, E-mail: songyang@bcm.tmc.edu

http://www.bioscience.org/current/vol13.htm

nature structural & molecular biology

TRF2 functions as a protein hub and regulates telomere maintenance by recognizing specific peptide motifs

Hyeung Kim[1,3], Ok-Hee Lee[1,3], Huawei Xin[1,3], Liuh-Yow Chen[1], Jun Qin[1], Heekyung Kate Chae[1], Shiaw-Yih Lin[2], Amin Safari[1], Dan Liu[1] & Zhou Songyang[1]

In mammalian cells, the telomeric repeat binding factor (TRF) homology (TRFH) domain–containing telomeric proteins TRF1 and TRF2 associate with a collection of molecules necessary for telomere maintenance and cell-cycle progression. However, the specificity and the mechanisms by which TRF2 communicates with different signaling pathways remain largely unknown. Using oriented peptide libraries, we demonstrate that the TRFH domain of human TRF2 recognizes [Y/F]XL peptides with the consensus motif YYHKYRLSPL. Disrupting the interactions between the TRF2 TRFH domain and its targets resulted in telomeric DNA-damage responses. Furthermore, our genome-wide target analysis revealed phosphatase nuclear targeting subunit (PNUTS) and microcephalin 1 (MCPH1) as previously unreported telomere-associated proteins that directly interact with TRF2 via the [Y/F]XL motif. PNUTS and MCPH1 can regulate telomere length and the telomeric DNA-damage response, respectively. Our findings indicate that an array of TRF2 molecules functions as a protein hub and regulates telomeres by recruiting different signaling molecules via a linear sequence code.

© 2009 Nature America, Inc. All rights reserved.

Telomere dysfunction has been implicated in cancer and aging[1–9]. Mammalian chromosomal ends contain long tracts of duplex telomere repeats with 3′ single-stranded G overhangs[10]. The telosome/shelterin complex, which includes TRF1, TRF2, TRF1-interacting nuclear factor 2 (TIN2), RAP1 (also known as TERF2IP), TPP1 (for TINT1/PIP1/PTOP) and protection of telomeres 1 (POT1), helps to maintain telomere integrity by protecting the telomeres from chromosomal abnormalities and DNA-damage responses due to telomere replication, recombination and erosion[11,12]. Both TRF1 and TRF2 contain a TRFH domain, which mediates homodimerization, and a myb domain, which directly binds the telomeric double-stranded DNA[13,14]. In addition to telomeric DNA, TRF1 and TRF2 also associate with various proteins involved in telosome assembly, telomere-length regulation, DNA replication, repair, end joining, recombination and cell-cycle control[11,12,15]. Consistent with the essential roles of TRF1 and TRF2, homozygous inactivation of either gene resulted in early embryonic lethality in mice[16,17]. In cultured cells, impairment of TRF2 function (for example, dominant negative expression of TRF2ΔBΔM, which lacks the basic and myb domains) led to DNA-damage responses[18,19], telomere loop deletion[20] or anaphase bridging[21]. However, the mechanisms of TRF2-mediated interaction and the direct targets of TRF2 remain elusive.

One known target of TRF2 in telomere maintenance is the exonuclease Apollo[22,23]. Indeed, biochemical and structural analyses revealed a direct interaction between the TRFH domain of TRF2 ($TRF2_{TRFH}$) and a short Apollo peptide sequence (500-LALK YLLTPVNFFQA-514)[24]. Notably, $TRF1_{TRFH}$ and $TRF2_{TRFH}$ seem to harbor distinct binding specificities, suggesting differential recruitment of distinct proteins by different TRFH domains. However, the specific determinant for $TRF2_{TRFH}$ recognition and the identities of other TRF2 targets remain unknown. Here we investigated the specificity of $TRF2_{TRFH}$ and demonstrated that $TRF2_{TRFH}$ is a protein domain that recognizes specific peptides with the [Y/F]XL motif. Through proteomic analyses, we identified several [Y/F]XL motif–containing proteins that can directly interact with TRF2 and mediate telomere-length control and end protection. Our results indicate that an array of TRF2 molecules at the telomeres serves as a protein hub for telomeric signaling.

RESULTS

Determining the binding specificity of $TRF2_{TRFH}$

We reasoned that $TRF2_{TRFH}$ might represent a modular protein-protein interaction domain whose specificity could be studied using the oriented peptide library technique[25]. We therefore synthesized an oriented peptide library with the sequence KGXXXX[FYWH]X[ILV]XPXN (where X is any amino acid other than cysteine). Because Tyr504, Leu506 and Pro508 of Apollo are essential for its interaction with TRFH[24], we partially fixed the corresponding positions (P0, P+2 and P+4) in the library (as indicated by square brackets) (**Fig. 1a**). Peptide mixtures that specifically associated with glutathione *S*-transferase (GST)-$TRF2_{TRFH}$ fusion proteins were isolated and sequenced. Among the four aromatic residues partially fixed

[1]Verna and Marrs McLean Department of Biochemistry and Molecular Biology, Baylor College of Medicine, Houston, Texas 77030, USA. [2]Department of System Biology, The University of Texas M.D. Anderson Cancer Center, Houston, Texas 77054, USA. [3]These authors contributed equally to this work. Correspondence should be addressed to Z.S. (songyang@bcm.tmc.edu).

Received 10 September 2008; accepted 10 February 2009; published online 15 March 2009; doi:10.1038/nsmb.1575

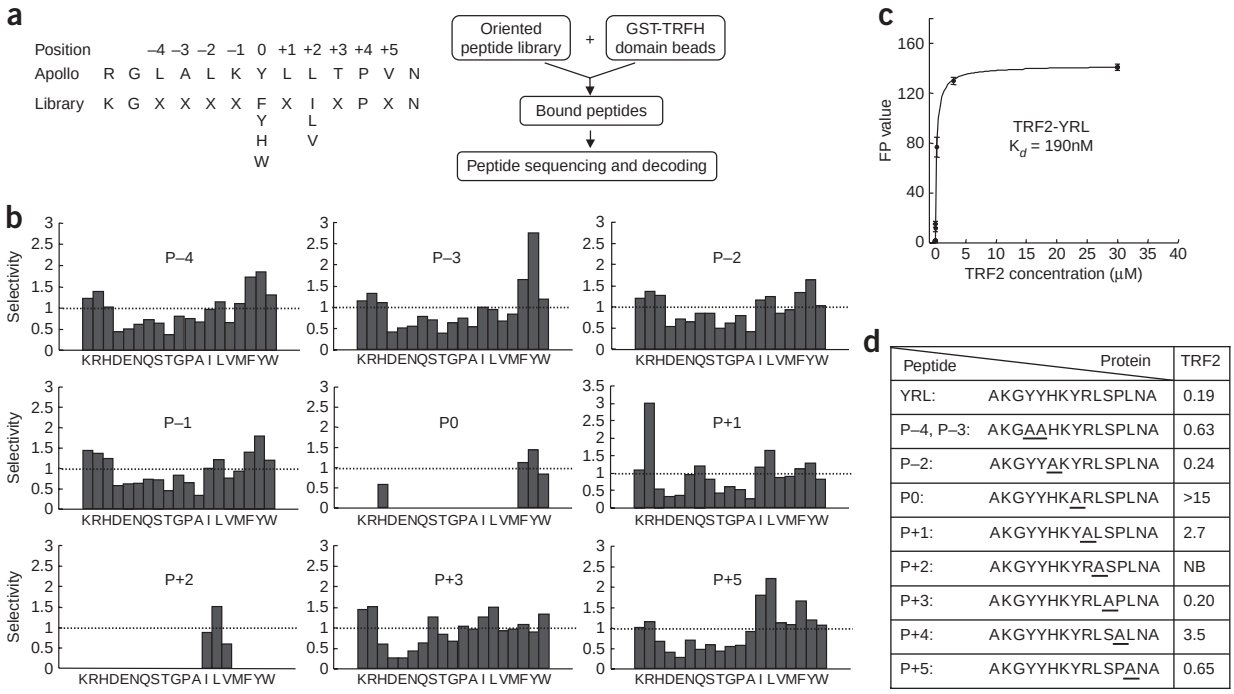

d

Peptide	Protein	TRF2
YRL:	AKGYYHKYRLSPLNA	0.19
P–4, P–3:	AKGAAHKYRLSPLNA	0.63
P–2:	AKGYYAKYRLSPLNA	0.24
P0:	AKGYYHKARLSPLNA	>15
P+1:	AKGYYHKYALSPLNA	2.7
P+2:	AKGYYHKYRASPLNA	NB
P+3:	AKGYYHKYRLAPLNA	0.20
P+4:	AKGYYHKYRLSALNA	3.5
P+5:	AKGYYHKYRLSPANA	0.65

Figure 1 The TRFH domain of TRF2 recognizes short peptide sequences. (**a**) A schematic representation of the oriented peptide library design. X indicates any amino acids except for cysteine. (**b**) The specificity of $TRF2_{TRFH}$ as revealed by oriented peptide library analyses. A selectivity value of ≥ 1 indicates preference for a particular amino acid. (**c**) The consensus TRF2 peptide YRL (AKGYYHKYRLSPLNA) binds $TRF2_{TRFH}$ with high affinity as measured by fluorescence polarization (FP). Error bars indicate s.e.m. ($n = 3$). (**d**) The YXL motif on the consensus peptide is crucial for $TRF2_{TRFH}$ interaction. The affinities (μM) of alanine-substituted peptides for $TRF2_{TRFH}$ were measured by FP. NB, not bound.

at position P0, $TRF2_{TRFH}$ preferred tyrosine and phenylalanine to a lesser extent) for binding (**Fig. 1b**). At the P+2 position, leucine (but not isoleucine or valine) was selected. Additional selections at other positions were also evident, including tyrosine at P−3, lysine at P−1 and arginine at P+1. Indeed, a synthesized consensus peptide YRL (KGYYHKYRLSPLN) bound the TRFH domain of TRF2 with high affinity (190 nM) (**Fig. 1c**). Furthermore, alanine substitution of the YXL motif in the YRL peptide resulted in its loss of TRF2 interaction, whereas alanine substitution of the P+1 residue arginine or the P+4 residue proline reduced its affinity by more than ten-fold (**Fig. 1d**). These results indicate that $TRF2_{TRFH}$ recognizes specific peptide sequences with the core motif of [Y/F]XL.

TRF2–[Y/F]XL interaction is crucial for telomere maintenance

These findings suggest that TRFH domains may recruit different signaling molecules via a linear sequence code, in a manner similar to other protein-protein interaction modules such as the SH3 and WW domains[26,27]. In addition, disruption of $TRF2_{TRFH}$ interaction with its cellular targets may trigger telomere dysfunction. To further investigate the biological importance of the TRFH–[Y/F]XL motif interaction, we expressed the TRF2 consensus peptide in tandem repeats (2×YRL) in human HTC75 cells. We reasoned that this tandem repeat peptide should occupy the two [Y/F]XL binding sites on a TRFH dimer and act as dominant negatives to inhibit endogenous TRF2 activity by competing for $TRF2_{TRFH}$ binding. Indeed, whereas the chromatin association of either TRF1 or TRF2 remained intact (**Supplementary Fig. 1** online), expression of this peptide did elicit DNA-damage responses, as measured by p53 binding protein 1 (53BP1)-containing telomere dysfunction–induced foci (TIF)[18,28] (**Fig. 2a**,**b**). In contrast, expression of the control peptide (2×YRA) that does not bind TRF2 had no effect, underlining the important role of the TRFH–YXL motif interaction in telomere maintenance.

On the basis of the TRF2–Apollo crystal structure, TRF2 Phe120, sandwiched between the P+4 proline of the Apollo peptide and TRF2 Arg109, is essential for the $TRF2_{TRFH}$–YRL interaction[24]. We therefore generated the F120A mutant form of TRF2 (TRF2 FA, **Fig. 2c**) and found that it expressed at a level comparable to wild-type TRF2 expression (**Fig. 2d**). Consistent with our biochemical and structural analyses, the F120A mutation led to a dramatic reduction in YRL peptide binding (**Fig. 2d**). Furthermore, although TRF2 FA still retained its ability to interact with wild-type TRF2 (**Fig. 2e**), its expression in HTC75 cells increased the percentage of TIF-containing cells compared to that of cells expressing wild-type TRF2 (8% versus 2%; **Fig. 2f–h**). Notably, the percentage of TRF2 FA–expressing cells that contained TIF was similar to that of TRF2ΔBΔM-expressing cells (**Fig. 2g**).

The mechanism of how TRF2ΔBΔM expression triggers telomeric DNA-damage responses has remained poorly understood[18,29]. Vastly overexpressed TRF2ΔBΔM can lead to the displacement of endogenous TRF2 from telomeres[21]. In our experiments, modestly overexpressed TRF2ΔBΔM could associate with telomeres and did not drastically alter the chromatin association of endogenous TRF2 (**Supplementary Fig. 2a**,**b** online). We reasoned that the intact TRFH domain on TRF2ΔBΔM allowed it to act in a dominant negative manner, preventing multiple [Y/F]XL motif–containing proteins from binding to endogenous TRF2. Indeed, alanine mutation of Phe120 on TRF2ΔBΔM abolished the effect of TRF2ΔBΔM expression in TIF assays (**Fig. 2f**,**g**). Collectively, these experiments indicate that the association of TRFH with different [Y/F]XL motif–containing targets is crucial for TRF2-mediated telomere protection in human cells.

© 2009 Nature America, Inc. All rights reserved.

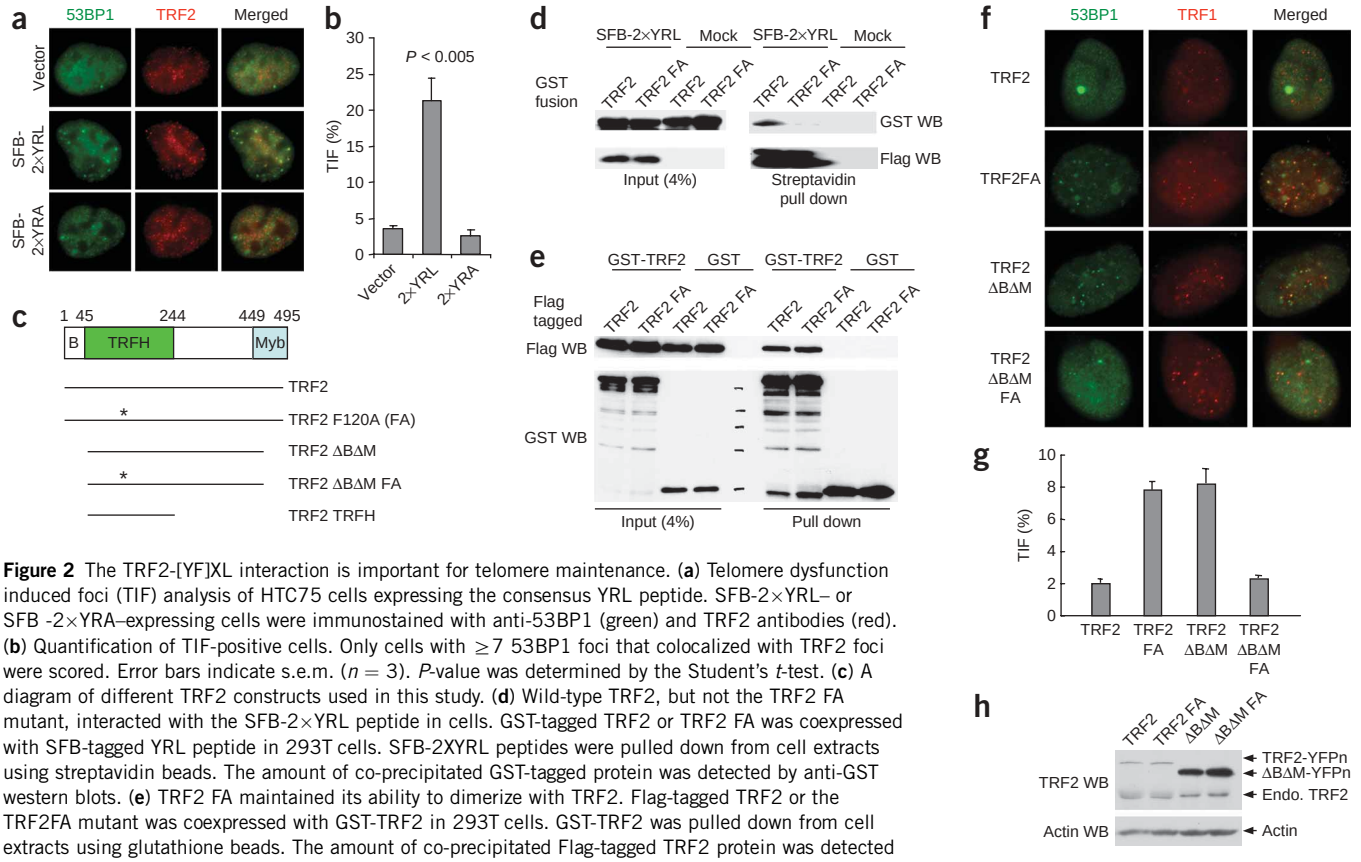

Figure 2 The TRF2-[YF]XL interaction is important for telomere maintenance. (**a**) Telomere dysfunction induced foci (TIF) analysis of HTC75 cells expressing the consensus YRL peptide. SFB-2×YRL– or SFB -2×YRA–expressing cells were immunostained with anti-53BP1 (green) and TRF2 antibodies (red). (**b**) Quantification of TIF-positive cells. Only cells with ≥7 53BP1 foci that colocalized with TRF2 foci were scored. Error bars indicate s.e.m. ($n = 3$). *P*-value was determined by the Student's *t*-test. (**c**) A diagram of different TRF2 constructs used in this study. (**d**) Wild-type TRF2, but not the TRF2 FA mutant, interacted with the SFB-2×YRL peptide in cells. GST-tagged TRF2 or TRF2 FA was coexpressed with SFB-tagged YRL peptide in 293T cells. SFB-2XYRL peptides were pulled down from cell extracts using streptavidin beads. The amount of co-precipitated GST-tagged protein was detected by anti-GST western blots. (**e**) TRF2 FA maintained its ability to dimerize with TRF2. Flag-tagged TRF2 or the TRF2FA mutant was coexpressed with GST-TRF2 in 293T cells. GST-TRF2 was pulled down from cell extracts using glutathione beads. The amount of co-precipitated Flag-tagged TRF2 protein was detected by anti-Flag western blotting (WB). (**f**) TIF analysis of HTC75 cells expressing wild-type or mutant TRF2 proteins. Cells expressing vector alone, or YFPn-tagged TRF2, TRF2 FA (F120A), TRF2ΔBΔM or TRF2ΔBΔM-FA were stained with anti-53BP1 (green) and TRF1 (red) antibodies. YFPn, N-terminal fragment of YFP. (**g**) Quantification of data from **f**. Only cells with ≥7 53BP1 foci that colocalized with TRF1 foci were scored. Error bars indicate s.e.m. ($n = 3$). (**h**) Western blotting analysis of the expression levels of endogenous TRF2 and different TRF2 constructs used in **f** and **g**.

© 2009 Nature America, Inc. All rights reserved.

Identification of TIN2, PNUTS and MCPH1 as TRF2$_{TRFH}$ targets

The identification and analysis of specific TRFH binding partners should greatly facilitate the understanding of TRF2 function and telomere maintenance. To this end, we performed a genome-wide search of potential TRF2-interacting partners based on our peptide library data of TRF2$_{TRFH}$ (**Supplementary Fig. 3** online). From this list, we selected several human proteins that have been implicated in signal transduction and RNA or DNA regulation for further analysis (**Fig. 3a** and **Supplementary Fig. 4** online). On the basis of their sequences, we synthesized [Y/F]XL peptides and measured their affinities to TRF2$_{TRFH}$. Three of the peptides (from TIN2, PNUTS and MCPH1, respectively) bound TRF2$_{TRFH}$ with affinities in the low micromolar range (**Supplementary Fig. 4**), and we followed up further on these interactions. Notably, TIN2 and PNUTS were also identified in our large-scale immunoprecipitation and MS analysis of TRF2 (**Fig. 3b**) and RAP1 protein complexes[30,31]. As in Apollo, TIN2 (known to associate with TRF2) also harbors a TRFH domain binding motif (FNL) (**Supplementary Fig. 4**). Indeed, TRF2$_{TRFH}$ can interact with the TIN2 FNL peptide with a modest affinity that is dependent on the FXL motif (**Supplementary Fig. 5a–c** online).

It has been suggested that TIN2 may bind TRF2 through two distinct regions, the high-affinity TIN2 N-terminal region and the low-affinity region containing the TRFH binding motif[24]. The TRFH–TIN2 interaction was not stable enough to survive co-immunoprecipitation[24]. To further explore the association of the TIN2 FNL motif with TRF2 *in vivo*, we studied the TRF2–TIN2 interaction in live cells through the bimolecular fluorescence complementation (BiFC) assay[32,33]. Here we tagged TRF2 and TIN2, respectively, with the N-terminal half of Venus yellow fluorescent protein (YFP) (YFPn-TRF2) and the C-terminal domain of YFP (YC-TIN2). These proteins were stably expressed in HTC75 cells for fluorescence complementation analysis. Consistent with the notion of multiple domains mediating the TRF2–TIN2 interaction, the FNL motif mutant TIN2AA showed reduced association with TRF2 (**Supplementary Fig. 5d**). The TRF2–TIN2 interaction is unlikely to be mediated through TRF1, because the TRF1 binding mutant TIN2AA can still interact with TRF2 and TRF1 does not interact directly with TRF2. In addition, interaction of TRF2 FA to endogenous TIN2 was decreased (**Fig. 4**), indicating that the FNL motif contributes to the TRF2–TIN2 interaction *in vivo*.

Other TRF2-associated proteins identified include PNUTS, a nuclear targeting subunit of the protein phosphatase PP1 (ref. 34), and the microcephaly syndrome protein MCPH1 (also known as BRIT1), a BRCT domain–containing protein that functions in DNA-damage responses[35–38]. Neither protein has been shown previously to interact with telomere proteins. To confirm the TRF2–PNUTS and TRF2–MCPH1 interactions, we first carried out co-immunoprecipitation experiments using antibodies against the endogenous TRF2 and RAP1 complexes. Anti-RAP1 immunoprecipitation brought down endogenous TRF2 and endogenous PNUTS and MCPH1 (**Fig. 3c**,**d**). In addition, both PNUTS and MCPH1 could be targeted to telomeres (**Fig. 3e**). Flag-tagged PNUTS co-stained with about 10% of the TRF2 foci, whereas Flag-MCHP1 co-localized with endogenous TRF2.

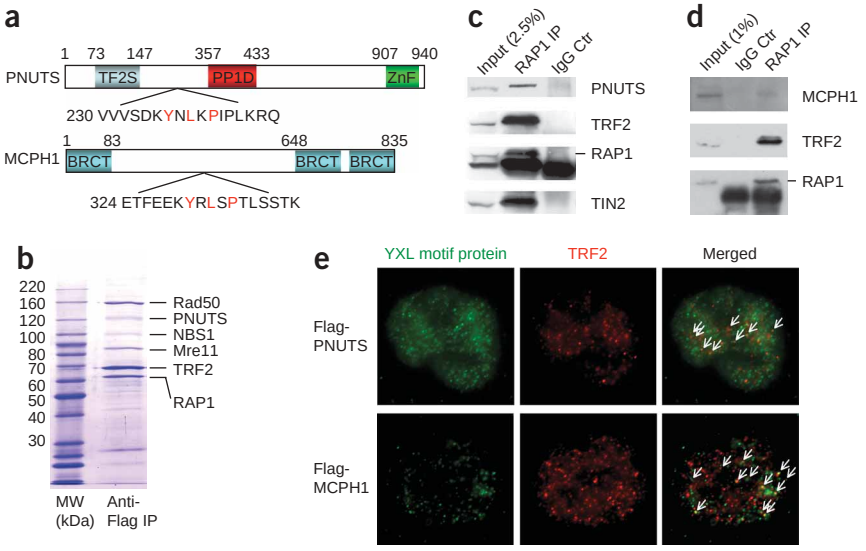

Figure 3 TRF2 specifically interacts with YXL-containing proteins PNUTS and MCPH1. (**a**) Domain structures of PNUTS and MCPH1. TF2S, transcription elongation factor S-II like domain; PP1D, phosphatase PP1 binding domain; ZnF, zinc finger; BRCT, BRCA1 C-terminal domain. (**b**) Co-immunoprecipitation (IP) and MS identified PNUTS as a Flag-TRF2–associating protein in Flag-TRF2–expressing Hela cells. (**c**,**d**) Endogenous TRF2–RAP1 complex associates with endogenous PNUTS (**c**) and MCPH1 (**d**). The TRF2–RAP1 complex was immunoprecipitated from Hela nuclear extracts using anti-RAP1 antibodies, followed by western blotting analyses with the indicated antibodies. (**e**) PNUTS and MCPH1 foci colocalized with endogenous TRF2. Cells expressing Flag-tagged PNUTS or MCPH1 were co-immunostained with anti-TRF2 (red) and anti-Flag (green) antibodies. Arrows indicate colocalized spots.

© 2009 Nature America, Inc. All rights reserved.

YXL-dependent interaction between PNUTS/MCPH1 and TRF2

Next, we synthesized YXL motif–containing peptides based on PNUTS and MCPH1 sequences. The two peptides bound $TRF2_{TRFH}$ (but not $TRF1_{TRFH}$) *in vitro* with K_d values of 1.1 μM and 0.42 μM, respectively (**Fig. 4a**), demonstrating the specificity of the interaction. Moreover, alanine scanning analysis of the PNUTS or MCPH1 peptide confirmed the importance of the YXLXP motif in mediating TRF2 binding (**Fig. 4a**).

To determine whether TRF2–PNUTS or TRF2–MCPH1 association is dependent on the YXL motif *in vivo*, we generated alanine substitution mutants of PNUTS (PNUTS-AA) and MCPH1 (MCPH1-AA). Flag-tagged wild-type and mutant PNUTS or MCPH1 was then coexpressed with TRF2 in 293T cells for co-precipitation experiments. GST-TRF2 was able to specifically pull down wild-type

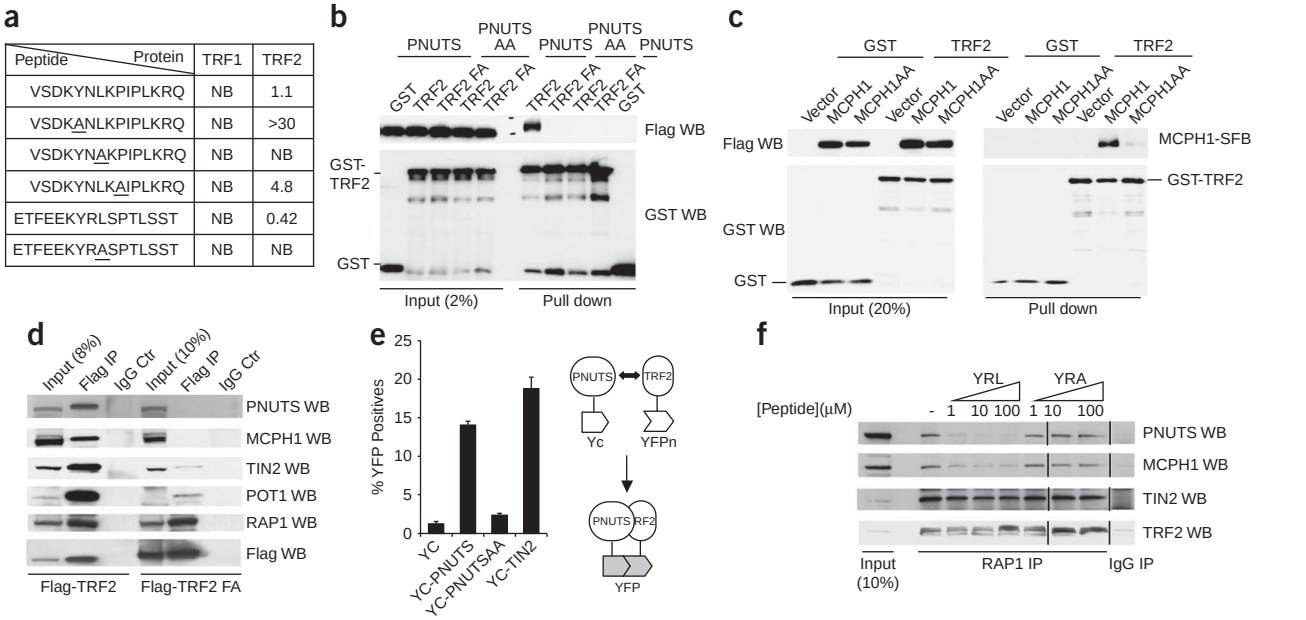

Figure 4 TRF2 interacts with PNUTS and MCPH1 through the YXL motif. (**a**) YXL peptides derived from PNUTS or MCPH1 bind the TRFH domain of TRF2 (but not TRF1). NB, not bound. Affinities are measured in micromoles. (**b**) TRF2 interacts with PNUTS through its YXL motif. GST and GST-tagged TRF2 or TRF2 FA (F120A) proteins were coexpressed with Flag-tagged PNUTS or PNUTS-AA (Y236A L238A) in 293T cells. GST fusion proteins were pulled down using glutathione beads. The amounts of co-precipitated Flag-tagged PNUTS proteins were detected by western blotting. (**c**) TRF2 interacts with MCPH1 through its YXL motif. GST alone and GST-tagged TRF2 were coexpressed with SFB-tagged MCPH1 or MCPH1AA in 293T cells. Co-immunoprecipitation (IP) was performed as described in **b**. (**d**) The TRF2 FA mutant showed reduced interaction with endogenous PNUTS, MCPH1 and TIN2. Cells expressing Flag-tagged TRF2 or TRF2 FA were immunoprecipitated with anti-Flag antibodies and blotted with different antibodies as indicated. (**e**) TRF2 interacts with PNUTS in live cells. Venus YFP N-terminal fragment tagged TRF2 (TRF2-YFPn) was coexpressed with YFP C-terminal fragment (YC) alone or YC-tagged TIN2, PNUTS or PNUTSAA in 293T cells. The percentages of YFP-positive cells were measured by flow cytometry. Error bars indicate s.e.m. ($n = 3$). (**f**) Differential binding of PNUTS and MCPH1 to TRF2. Hela cell nuclear extracts were first incubated with increasing concentrations of the YRL peptides, and then the TRF2 complex was immunoprecipitated with anti-RAP1 antibodies. IgG was used as a control. The amounts of co-precipitated PNUTS and MCPH1 proteins were detected by western blotting. Western blotting data were rearranged from the same gel.

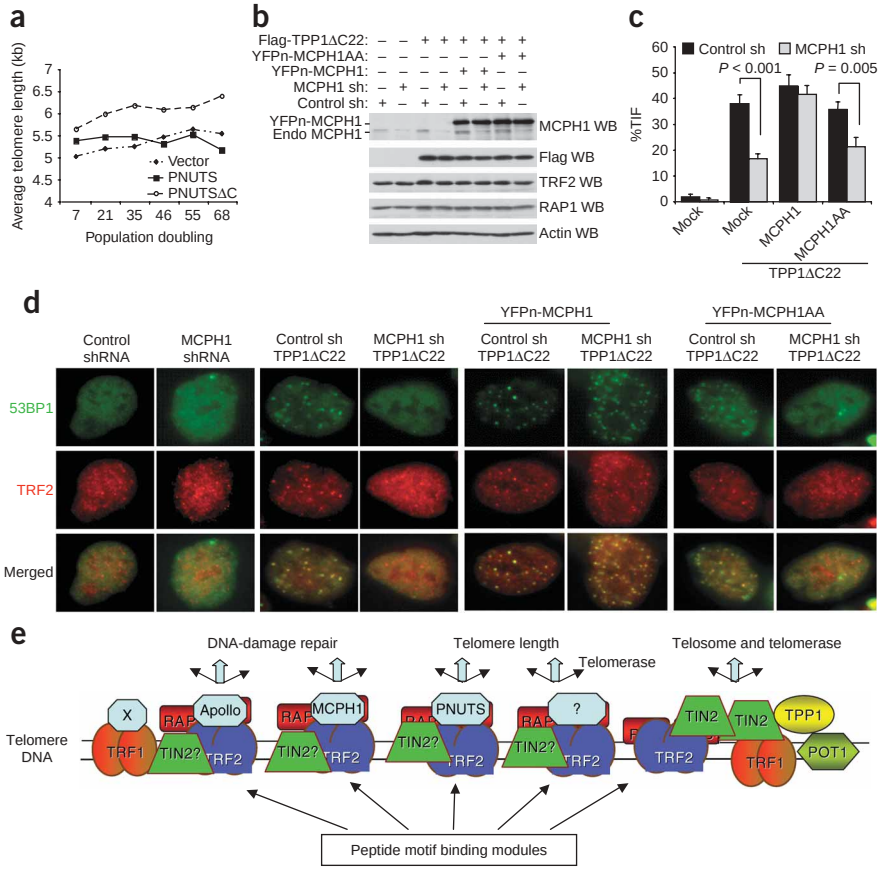

Figure 5 MCPH1 and PNUTS regulate DNA-damage response and telomere length, respectively, at the telomeres. (**a**) A comparison of the average telomere length in cells expressing vector alone, full-length PNUTS and the PNUTS C-terminal deletion mutant (PNUTSΔC, residues 1–337). (**b**) Stable shRNA knockdown of endogenous MCPH1 in the indicated cells. Flag-TPP1ΔC22–expressing HTC75 cells that also stably coexpressed different combinations of shRNA constructs and RNAi-resistant MCPH1 proteins were generated. Whole-cell extracts were prepared from these cells for western blotting. Anti-actin antibodies were used for loading controls. (**c**) Wild-type MCPH1 but not MCPH1-AA mutants rescued the effects of MCPH1 knockdown on TIF formation. Error bars indicate s.e.m. ($n = 10$). *P*-value was determined by the Student's *t*-test. (**d**) Immunostaining pictures of the data in **c**. Mock, TPP1ΔC22-expressing cells or TPP1ΔC22- and RNAi-resistant MCPH1 coexpressing cells were infected with retroviruses expressing either a control or MCPH1 shRNA1. The cells were fixed and immunostained using anti-TRF2 and anti-53BP1 antibodies. (**e**) A model of TRF2 signaling via different [Y/F]XL motif–containing proteins.

PNUTS but not PNUTS-AA (**Fig. 4b**). Similarly, TRF2 interaction with MCPH1-AA was considerably impaired compared to its interaction with wild-type MCPH1 (**Fig. 4c**), strongly supporting the notion that both PNUTS and MCPH1 bind TRF2 through the YXL motif. To confirm whether the TRF2–PNUTS interaction is mediated through $TRF2_{TRFH}$, we coexpressed Flag-tagged PNUTS with GST-tagged wild-type TRF2 or TRF2 FA. In these cells, TRF2, but not TRF2 FA, could bring down PNUTS, even though the F120A mutation did not affect TRF2 dimerization (**Figs. 2e** and **4b**). Moreover, the ability of Flag–TRF2 FA to precipitate endogenous PNUTS and MCPH1 was greatly reduced (**Fig. 4d**). These observations indicate that the TRF2–PNUTS and the TRF2–MCPH1 interactions are indeed mediated through the TRFH domain.

We then went on to investigate the TRF2–PNUTS and TRF2–MCPH1 interactions in live cells through the BiFC assay, using the YFPn-TRF2 constrcut described above and PNUTS or MCPH1 tagged with with the C-terminal domain of YFP (YC-PNUTS and YC-MCPH1, respectively). Whereas YFP-positive cells were virtually absent in control cells, about 14% of the cells coexpressing YFPn-TRF2 and YC-PNUTS were YFP positive (**Fig. 4e**), indicating an interaction between TRF2 and PNUTS *in vivo*. This number is comparable to the percentage of YFP-positive cells in cells coexpressing YFPn-TRF2 and YC-TIN2 (20%), which served as a positive control[33]. However, coexpression of YFPn-TRF2 and the YC-PNUTS-AA mutant did not result in increased fluorescence complementation over background (**Fig. 4e**). Similarly, MCPH1, but not MCPH1-AA, complemented YFPn-TRF2 in BiFC assays (**Supplementary Fig. 6** online). These data provide further support that the YXL motif is crucial for the TRF2–PNUTS and TRF2–MCPH1 interactions in cells.

The identification of multiple $TRF2_{TRFH}$ targets raises the possibility that these proteins may compete for TRF2 binding in cells. To test this, we investigated whether the YRL peptide could cause differential displacement of endogenous PNUTS and MCPH1 from TRF2. Indeed, increasing the concentration of the YRL peptide reduced the association of both PNUTS and MCPH1 with TRF2 in the anti-RAP1 immunoprecipitates (**Fig. 4f**). Notably, the PNUTS–TRF2 interaction seemed to be more sensitive than the MCPH1–TRF2 interaction in this peptide-titration experiment. This difference in sensitivity can be correlated with the affinities of their corresponding YXL peptides for the TRFH domain (that is, the PNUTS peptide binds more weakly than the MCPH1 peptide). These observations open up the possibility that the affinity of the YXL motif may affect the outcome of competition between different TRFH binding proteins.

PNUTS and MCPH1 regulate telomere length and end protection

We next studied the telomeric function of PNUTS and MCPH1. Expression of a C-terminal truncation mutant of PNUTS (PNUTSΔC, residues 1–337, without its phosphatase-interacting domain) in telomerase-positive HTC75 cells resulted in modest telomere elongation (**Fig. 5a** and **Supplementary Fig. 7** online) but had little effect on TIF formation (data not shown), indicating a role for PNUTS in telomere-length maintenance but not DNA-damage responses. It should be noted that PNUTSΔC may not act as an ideal dominant negative protein, so that the telomeric activity of PNUTS may have been underestimated in these assays.

Because MCPH1 has been implicated in DNA damage–response pathways[35–38], we hypothesized that the TRF2–MCPH1 interaction might regulate DNA-damage responses at the telomeres. To test this, we used a mutant form of TPP1 (TPP1ΔC22), whose expression results in elevated TIF formation[33]. Consistent with our hypothesis, knocking down MCPH1 by two different short hairpin RNA (shRNA) sequences inhibited the TPP1ΔC22-induced TIF response (**Fig. 5b–d**

© 2009 Nature America, Inc. All rights reserved.

and **Supplementary Fig. 8** online), indicating a requirement of MCPH1 for foci formation in response to DNA damage at the telomeres. Furthermore, an RNA interference (RNAi)-resistant form of wild-type MCPH1, but not MCPH1-AA, rescued the effect of MCPH1 knockdown (**Fig. 5b–d**), suggesting that the TRF2–MCPH1 interaction modulates the function of MCPH1 at the telomeres. These data collectively demonstrate that PNUTS and MCPH1 are physiological targets of TRF2 and are likely to function in distinct pathways.

DISCUSSION

The ability of TRF1 and TRF2 to bind telomeric sequences and thereby help to organize telomere chromatin structure and recruit other proteins to the telomeres has long been appreciated. Recent studies have further hypothesized that TRF1 and TRF2 may serve as molecular platforms for the recruitment and assembly of the telomere interaction network ('telomere interactome')[12]. However, the mechanisms by which this ever-expanding list of TRF1- and TRF2-interacting proteins contribute to TRF protein function remain unclear. The data presented here support the model that TRFH domains represent telomere-specific domains that recognize linear peptide sequence motifs, in a manner similar to that of many known protein modules such as the SH3 and WW domains. These sequences would effectively serve as molecular glue, allowing for the telomeric association of various signaling molecules and enabling TRF1 and TRF2 to function as hubs at the telomeres.

The long, repetitive DNA sequences at the telomere end enable its association with arrays of TRF1 and TRF2 molecules to accommodate temporal, combinatorial and perhaps developmental regulation of diverse signaling cascades (**Fig. 5e**). For example, our data indicate that TRF2 arrays can function as a telomeric hub via $TRF2_{TRFH}$ and recruit at least four [Y/F]XL motif proteins: TIN2, Apollo, MCPH1 and PNUTS. The TRF2–TIN2 interaction regulates telosome formation and telomerase recruitment[39,40], whereas the TRF2–Apollo and TRF2–MCPH1 interactions regulate DNA damage–repair responses[22,23] (**Fig. 5e**). In addition, the TRF2–PNUTS association modulates telomere length. Because each TRF2 homodimer contains two [Y/F]XL motif binding sites, it is possible that two different TRFH targets can be recruited to the same TRF2 homodimer, promoting communication between two distinct signaling branches. In this sense, TRF2 arrays serve not merely as a hub but as a structural platform. It will be important to identify other proteins that directly interact with TRF2 and to dissect the function of and cross-talk between the TRF2 targets. To this end, the specificity of TRFH domains for particular linear sequences as determined by our peptide library experiments should prove highly valuable in predicting possible targets. In this study, we have successfully identified MCPH1 and PNUTS as new targets of the TRF2 TRFH domain.

It has been proposed that telomeres are protected by a single large protein complex formed by the six core telomere proteins: TRF1, TRF2, RAP1, TIN2, TPP1 and POT1 (ref. 11). The TIN2–TRF1 and TIN2–TRF2 interactions are required to build such a complex. However, TIN2 contains a [Y/F]XL motif, and the TIN2 binding pockets on TRF1 and TRF2 overlap with the binding pockets of other [Y/F]XL targets of TRF1 and TRF2, such as PINX1, Apollo and PNUTS (data not shown). As a result, we suggest that the telosome/shelterin complex may be one of several complexes (possibly competing with each other) at the telomeres at any given time. Consistent with this notion, we found that TRF2 complexes are heterogeneous[30]. A large fraction of TRF2 and RAP1 was detected in distinct peaks from the telosome. In addition, a distinct TRF2–RAP1 complex has been implicated in telomere nonhomologous end joining[41,42]. Furthermore, interactions of the TRFH mutant TRF2 FA with [Y/F]XL proteins MCPH1, PNUTS and TIN2 were compromised, but its interaction with RAP1 was not (**Fig. 4d**). The ability of a TRFH domain to recruit different targets indicates a much more 'proactive' role for TRF2 in determining the assortment of complexes at the telomeres. Our findings point to new avenues into which the function of TRFH-containing proteins can be probed and offer new clues regarding the mechanisms of telomere dysfunction relevant to cancer and aging.

METHODS

Protein expression and purification. We expressed human $TRF2_{TRFH}$ (residues 42–245) and $TRF1_{TRFH}$ (residues 65–267) as GST fusion proteins in *E. coli* BL21(DE3) using the pGEX vector. The GST-fusion proteins were purified with glutathione agarose beads and eluted with elution buffer (20 mM glutathione, 20 mM Tris-HCl pH 7.3, 100 mM NaCl, 0.2 mM EDTA and 20% (v/v) glycerol).

Vectors and antibodies. We cloned cDNAs encoding human wild-type and mutant TRF2 and TIN2, and mouse wild-type and mutant PNUTS and MCPH1, into a pBabe-based or pcl-based retroviral vector (Flag or YFP-fragment tagged) for generating stable cell lines or for expression in 293T cells. For expression of GST fusion proteins in human cells, we cloned wild-type and mutant TRF2 into pDEST-27 (Invitrogen). MCPH1 and sequences encoding tandem repeats of the YRL (2×YRL) or YRA (2×YRA) peptides were cloned into SFB-tagged pBabe-based vectors[43], where SFB stands for S-, Flag- and streptavidin binding tag[43]. TRF2 mutants included TRF2 FA (F120A), TRF2 ΔBΔM (residues 45–454)[21] and TRF2 ΔBΔM FA. YXL mutants included TIN2 AA (F258A and L260A), PNUTS AA (Y236A and L238A) and MCPH1 AA (Y330A and L332A). PNUTS ΔC contains residues 1–337.

The antibodies used were monoclonal and polyclonal anti-Flag (Sigma), anti-Flag-HRP (Sigma), anti-GST-HRP (Amersham), anti-hTRF2 (CalBiochem), polyclonal antibodies from Bethyl laboratories against RAP1, TIN2 (ref. 33), POT1N[40] and PNUTS, anti-53BP1 (ref. 40), anti-MCPH1 (ref. 35) and monoclonal anti-TRF1 (Genetex).

Oriented peptide library screening. We synthesized the oriented peptide library (KGXXXX[HFYW]X[ILV]XPXN, where X is any amino acid other than cysteine) as described[44]. The peptide libraries (0.5–1.0 mg) were incubated with saturated GST-TRFH beads (150 μl) for 15–30 min at room temperature (25°C), and washed with 1× PBS (10 ml). The bound peptides were then eluted by acetic acid, dried and resuspended in double-distilled H_2O for Edman peptide sequencing (Tufts University Proteomic Core). We calculated the selectivity value in **Figure 1** by two steps. First, the amount of each amino acid at a given degenerate position was divided by its amount from the control 'GST alone' experiment. Second, the ratio from the first step was normalized such that the sum of the ratios at a given degenerate position was equal to 19 (the number of total amino acids included at each degenerate position). The resulting number from step 2 became the selectivity value. If no an amino acid was selected, the ratio in step 2 would be 1. Therefore, a selectivity value of ≥ 1 indicates preference.

Peptide synthesis, fluorescence polarization and affinity measurements. We synthesized the peptides by solid-phase synthesis using an automated multiple peptide synthesizer (INTAVIS Bioanalytical Instruments AG) and standard 9H-flouren-9-ylmethoxycarbonyl chemistry. The synthesized peptides were incubated overnight with 2 equivalent of fluorescein isothiocyanate (FITC) in pyridine/dimethylformamide/dichloromethane (50:29:21, v/v). The FITC-labeled peptides were then cleaved overnight from the resin with trifluoroacetic acid (TFA)/tri-isopropyl silane/water (95:2.5:2.5, v/v/v). The final peptides were precipitated with cold diethyl ether, washed twice with cold diethyl ether and stored at −20 °C.

The purified GST-tagged TRFH domain proteins were serially diluted in binding buffer (50 mM Tris-HCl, pH 8.0, 50 mM NaCl or 50 mM KCl plus 15mM NaCl, 5% (v/v) glycerol, and 1 mM DTT) and incubated with FITC-labeled peptides (50 nM) at room temperature for 5–30 min. Fluorescence

© 2009 Nature America, Inc. All rights reserved.

polarization was subsequently measured in a 384-well plate using a Victor V plate reader (Perkin Elmer).

Immunoprecipitation, western blotting and immunofluorescence. For large-scale immunoprecipitations, we prepared nuclear extracts from HelaS cells stably expressing Flag-tagged human TRF2. We purified the TRF2 complex using anti-Flag M2 agarose beads (Sigma) and analyzed the sample by MS sequencing as reported[45].

We carried out co-immunoprecipitation studies as described[45]. Glutathione agarose beads (Molecular Probes) and streptavidin-agarose beads (Fluka) were used to pull down GST fusion proteins and SFB-tagged proteins, respectively. We detected tagged proteins by western blotting using anti-Flag horseradish peroxidase (HRP) or anti-GST HRP antibodies. We also detected Flag-tagged proteins and endogenous TRF2 with anti-Flag polyclonal and anti-TRF2 monoclonal antibodies.

We carried out indirect immunofluorescence studies on a Deltavision deconvolution microscope and a Nikon TE200 microscope[45]. We performed TIF assays using anti-53BP1 antibodies together with anti-TRF2 (ref. 18) or anti-TRF1 antibodies[40].

Subcellular fractionation. We performed subcellular fractionation as described[46]. Briefly, HTC75 cells were trypsinized, washed with PBS and resuspended in hypotonic buffer with protease inhibitors. We then lysed the cells by adding Trition X-100 to a final concentration of 0.1% (v/v) on ice. After a 5-min incubation, we collected the nuclei by low-speed centrifugation (1,300*g*, 4 min). The supernatant was clarified by high-speed centrifugation (10,000*g*, 10 min) and collected as the cytoplasmic fraction, S1. Isolated nuclei were washed once with buffer A, and lysed with buffer A (3mM EDTA, 0.2mM EGTA, 1mM DTT and protease inhibitors) on ice for 10 min. Soluble nuclear fractions (S2) were separated from chromatin (P) by centrifugation at 1,700*g* for 4 min. The chromatin pellet (P) was washed once with buffer A and collected under the same centrifugation conditions.

Bimolecular fluorescence complementation. We performed BiFC as described[33]. Briefly, The Venus YFP N-terminal domain (residues 1–155) was fused to TRF2 to construct TRF2-YFPn. The YFP C-terminal domain (Yc, residues 156–239) was fused to MCPH1, TIN2 or PNUTS. These vectors were either introduced into HTC75 cells by retroviral infection or co-transfected into 293T cells. We then collected the cells for flow cytometry analysis on a Guava PCA cytometer.

Short hairpin RNA knockdown and rescue. We used two different shRNA sequences (shRNA1 and shRNA2) to knockdown MCPH1 in human cells. shRNA1 (5′-GGATACAGTGGAAGTGTTAAA-3′) was cloned into the lentiviral vector pGIPZ (Openbiosystems) and shRNA2 (5′-AGGAAGTTG GAAGGATCCA-3′) was cloned into a retroviral vector[36]. We infected human cells with shRNA-expressing retroviruses, selected with puromycin, and used them for different experiments described here. To construct a MCPH1 retroviral vector that was resistant to shRNA1, were replaced the corresponding nucleotides sequences on MCPH1 with 5′-GGATACAGCGG GAGCGTTAAA-3′. For rescue experiments, cells that expressed RNAi-resistant MCPH1 were established first and subsequently infected with retroviruses expressing MCPH1 shRNA1.

TRF assay. As previously described[40], we used retroviruses encoding the pBabe vector, Flag-PNUTS or Flag–PNUTSΔC to establish stable HTC75 cells. The cells were selected in puromycin and passaged for genomic DNA extraction for the telomere restriction fragment assay[40].

Note: Supplementary information is available on the Nature Structural & Molecular Biology website.

ACKNOWLEDGMENTS

We thank S.Y. Jung and Q. He for technical help and M. Lei (University of Michigan) for the GST-TRF2$_{TRFH}$ fusion proteins. We thank J. Pennington and T. Palzkill for peptide synthesis. Work in the laboratories of Z.S. and D.L. is supported by awards from the US National Institutes of Health, the US Department of Defense, American Heart Association, the Welch foundation and the American Cancer Society. Z.S. is funded by the Leukemia and Lymphoma Society.

AUTHOR CONTRIBUTIONS

H.K., O.-H.L., H.X. and L.-Y.C. designed and performed most of the experiments; D.L. and J.Q. did the telomere length and MS experiment, respectively; A.S. and H.K.C. provided technical support. S.-Y.L. provided the MCHP1 reagents; D.L. and Z.S. wrote the paper.

Published online at http://www.nature.com/nsmb/
Reprints and permissions information is available online at http://npg.nature.com/reprintsandpermissions/

© 2009 Nature America, Inc. All rights reserved.

1. Blackburn, E.H. Switching and signaling at the telomere. *Cell* **106**, 661–673 (2001).
2. Hackett, J.A. & Greider, C.W. Balancing instability: dual roles for telomerase and telomere dysfunction in tumorigenesis. *Oncogene* **21**, 619–626 (2002).
3. Granger, M.P., Wright, W.E. & Shay, J.W. Telomerase in cancer and aging. *Crit. Rev. Oncol. Hematol.* **41**, 29–40 (2002).
4. Harrington, L. & Robinson, M.O. Telomere dysfunction: multiple paths to the same end. *Oncogene* **21**, 592–597 (2002).
5. Collins, K. & Mitchell, J.R. Telomerase in the human organism. *Oncogene* **21**, 564–579 (2002).
6. Maser, R.S. & DePinho, R.A. Connecting chromosomes, crisis, and cancer. *Science* **297**, 565–569 (2002).
7. Hahn, W.C. & Weinberg, R.A. Modelling the molecular circuitry of cancer. *Nat. Rev. Cancer* **2**, 331–341 (2002).
8. Blasco, M.A. Mammalian telomeres and telomerase: why they matter for cancer and aging. *Eur. J. Cell Biol.* **82**, 441–446 (2003).
9. Cech, T.R. Beginning to understand the end of the chromosome. *Cell* **116**, 273–279 (2004).
10. Henderson, E., Hardin, C.C., Walk, S.K., Tinoco Jr, I. & Blackburn, E.H. Telomeric DNA oligonucleotides form novel intramolecular structures containing guanine-guanine base pairs. *Cell* **51**, 899–908 (1987).
11. de Lange, T. Shelterin: the protein complex that shapes and safeguards human telomeres. *Genes Dev.* **19**, 2100–2110 (2005).
12. Songyang, Z. & Liu, D. Inside the mammalian telomere interactome: regulation and regulatory activities of telomeres. *Crit. Rev. Eukaryot. Gene Expr.* **16**, 103–118 (2006).
13. Broccoli, D., Smogorzewska, A., Chong, L. & de Lange, T. Human telomeres contain two distinct Myb-related proteins, TRF1 and TRF2. *Nat. Genet.* **17**, 231–235 (1997).
14. Bilaud, T. *et al.* Telomeric localization of TRF2, a novel human telobox protein. *Nat. Genet.* **17**, 236–239 (1997).
15. Verdun, R.E. & Karlseder, J. Replication and protection of telomeres. *Nature* **447**, 924–931 (2007).
16. Iwano, T., Tachibana, M., Reth, M. & Shinkai, Y. Importance of TRF1 for functional telomere structure. *J. Biol. Chem.* **279**, 1442–1448 (2004).
17. Celli, G.B. & de Lange, T. DNA processing is not required for ATM-mediated telomere damage response after TRF2 deletion. *Nat. Cell Biol.* **7**, 712–718 (2005).
18. Takai, H., Smogorzewska, A. & de Lange, T. DNA damage foci at dysfunctional telomeres. *Curr. Biol.* **13**, 1549–1556 (2003).
19. Denchi, E.L. & de Lange, T. Protection of telomeres through independent control of ATM and ATR by TRF2 and POT1. *Nature* **448**, 1068–1071 (2007).
20. Wang, R.C., Smogorzewska, A. & de Lange, T. Homologous recombination generates T-loop-sized deletions at human telomeres. *Cell* **119**, 355–368 (2004).
21. van Steensel, B., Smogorzewska, A. & de Lange, T. TRF2 protects human telomeres from end-to-end fusions. *Cell* **92**, 401–413 (1998).
22. van Overbeek, M. & de Lange, T. Apollo, an Artemis-related nuclease, interacts with TRF2 and protects human telomeres in S phase. *Curr. Biol.* **16**, 1295–1302 (2006).
23. Lenain, C. *et al.* The Apollo 5′ exonuclease functions together with TRF2 to protect telomeres from DNA repair. *Curr. Biol.* **16**, 1303–1310 (2006).
24. Chen, Y. *et al.* A shared docking motif in TRF1 and TRF2 used for differential recruitment of telomeric proteins. *Science* **319**, 1092–1096 (2008).
25. Songyang, Z. *et al.* SH2 domains recognize specific phosphopeptide sequences. *Cell* **72**, 767–778 (1993).
26. Songyang, Z. Recognition and regulation of primary-sequence motifs by signaling modular domains. *Prog. Biophys. Mol. Biol.* **71**, 359–372 (1999).
27. Yaffe, M.B. *et al.* A motif-based profile scanning approach for genome-wide prediction of signaling pathways. *Nat. Biotechnol.* **19**, 348–353 (2001).
28. d'Adda di Fagagna, F. *et al.* A DNA damage checkpoint response in telomere-initiated senescence. *Nature* **426**, 194–198 (2003).
29. Karlseder, J., Broccoli, D., Dai, Y., Hardy, S. & de Lange, T. p53- and ATM-dependent apoptosis induced by telomeres lacking TRF2. *Science* **283**, 1321–1325 (1999).
30. Liu, D., O'Connor, M.S., Qin, J. & Songyang, Z. Telosome, a mammalian telomere-associated complex formed by multiple telomeric proteins. *J. Biol. Chem.* **279**, 51338–51342 (2004).
31. O'Connor, M.S., Safari, A., Liu, D., Qin, J. & Songyang, Z. The human Rap1 protein complex and modulation of telomere length. *J. Biol. Chem.* **279**, 28585–28591 (2004).
32. Hu, C.D. & Kerppola, T.K. Simultaneous visualization of multiple protein interactions in living cells using multicolor fluorescence complementation analysis. *Nat. Biotechnol.* **21**, 539–545 (2003).
33. Chen, L.Y., Liu, D. & Songyang, Z. Telomere maintenance through spatial control of telomeric proteins. *Mol. Cell. Biol.* **27**, 5898–5909 (2007).

34. Allen, P.B., Kwon, Y.G., Nairn, A.C. & Greengard, P. Isolation and characterization of PNUTS, a putative protein phosphatase 1 nuclear targeting subunit. *J. Biol. Chem.* **273**, 4089–4095 (1998).
35. Lin, S.Y., Rai, R., Li, K., Xu, Z.X. & Elledge, S.J. BRIT1/MCPH1 is a DNA damage responsive protein that regulates the Brca1-Chk1 pathway, implicating checkpoint dysfunction in microcephaly. *Proc. Natl. Acad. Sci. USA* **102**, 15105–15109 (2005).
36. Rai, R. *et al.* BRIT1 regulates early DNA damage response, chromosomal integrity, and cancer. *Cancer Cell* **10**, 145–157 (2006).
37. Alderton, G.K. *et al.* Regulation of mitotic entry by microcephalin and its overlap with ATR signalling. *Nat. Cell Biol.* **8**, 725–733 (2006).
38. Wood, J.L., Singh, N., Mer, G. & Chen, J. MCPH1 functions in an H2AX-dependent but MDC1-independent pathway in response to DNA damage. *J. Biol. Chem.* **282**, 35416–35423 (2007).
39. O'Connor, M.S., Safari, A., Xin, H., Liu, D. & Songyang, Z. A critical role for TPP1 and TIN2 interaction in high-order telomeric complex assembly. *Proc. Natl. Acad. Sci. USA* **103**, 11874–11879 (2006).
40. Xin, H. *et al.* TPP1 is a homologue of ciliate TEBP-β and interacts with POT1 to recruit telomerase. *Nature* **445**, 559–562 (2007).
41. Bae, N.S. & Baumann, P.A. RAP1/TRF2 complex inhibits nonhomologous end-joining at human telomeric DNA ends. *Mol. Cell* **26**, 323–334 (2007).
42. Price, C.M. wRAPing up the end to prevent telomere fusions. *Mol. Cell* **26**, 463–464 (2007).
43. Kim, H., Chen, J. & Yu, X. Ubiquitin-binding protein RAP80 mediates BRCA1-dependent DNA damage response. *Science* **316**, 1202–1205 (2007).
44. Songyang, Z. & Cantley, L.C. The use of peptide library for the determination of kinase peptide substrates. *Methods Mol. Biol.* **87**, 87–98 (1998).
45. Liu, D. *et al.* PTOP interacts with POT1 and regulates its localization to telomeres. *Nat. Cell Biol.* **6**, 673–680 (2004).
46. Mendez, J. & Stillman, B. Chromatin association of human origin recognition complex, Cdc6, and minichromosome maintenance proteins during the cell cycle: assembly of prereplication complexes in late mitosis. *Mol. Cell. Biol.* **20**, 8602–8612 (2000).

© 2009 Nature America, Inc. All rights reserved.